

INFORMATION TO USERS

This was produced from a copy of a document sent to us for microfilming. While the most advanced technological means to photograph and reproduce this document have been used, the quality is heavily dependent upon the quality of the material submitted.

The following explanation of techniques is provided to help you understand markings or notations which may appear on this reproduction.

1. The sign or "target" for pages apparently lacking from the document photographed is "Missing Page(s)". If it was possible to obtain the missing page(s) or section, they are spliced into the film along with adjacent pages. This may have necessitated cutting through an image and duplicating adjacent pages to assure you of complete continuity.
2. When an image on the film is obliterated with a round black mark it is an indication that the film inspector noticed either blurred copy because of movement during exposure, or duplicate copy. Unless we meant to delete copyrighted materials that should not have been filmed, you will find a good image of the page in the adjacent frame.
3. When a map, drawing or chart, etc., is part of the material being photographed the photographer has followed a definite method in "sectioning" the material. It is customary to begin filming at the upper left hand corner of a large sheet and to continue from left to right in equal sections with small overlaps. If necessary, sectioning is continued again—beginning below the first row and continuing on until complete.
4. For any illustrations that cannot be reproduced satisfactorily by xerography, photographic prints can be purchased at additional cost and tipped into your xerographic copy. Requests can be made to our Dissertations Customer Services Department.
5. Some pages in any document may have indistinct print. In all cases we have filmed the best available copy.

**University
Microfilms
International**

300 N. ZEEB ROAD, ANN ARBOR, MI 48106
18 BEDFORD ROW, LONDON WC1R 4EJ, ENGLAND

8022661

SCHWARTZ, ROBERT EUGENE

ORGANIC CONSTITUENTS OF THE DEEP-SEA PRECIOUS CORALS
GERARDIA AND CORALLIUM SPP.

University of Hawaii

PH.D.

1980

**University
Microfilms
International**

300 N. Zeeb Road, Ann Arbor, MI 48106

18 Bedford Row, London WC1R 4EJ, England

ORGANIC CONSTITUENTS OF
THE DEEP-SEA PRECIOUS CORALS
GERARDIA AND CORALLIUM SPP.

A DISSERTATION SUBMITTED TO THE GRADUATE DIVISION OF THE
UNIVERSITY OF HAWAII IN PARTIAL FULFILLMENT
OF THE REQUIREMENTS FOR THE DEGREE OF

DOCTOR OF PHILOSOPHY

IN CHEMISTRY

MAY 1980

By

Robert Eugene Schwartz

Dissertation Committee:

Paul J. Scheuer, Chairman
Richard W. Grigg
Edgar F. Keefer
Ray L. McDonald
Hisashi Yamamoto

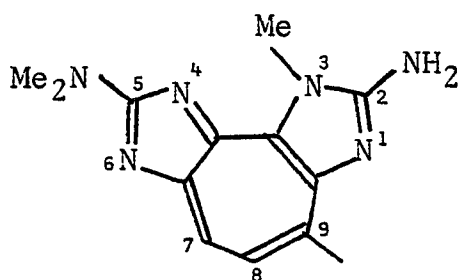
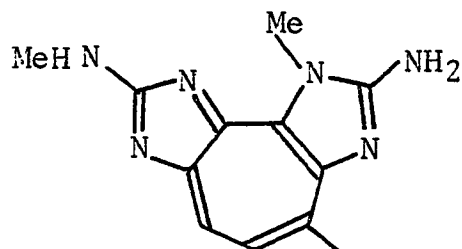
ACKNOWLEDGEMENTS

I would like to thank the following people for assistance with the completion of this research. Mark Yunker originally noted the unusual fluorescence of extracts of Gerardia sp. and got me interested in this organism. Frank Gerard also helped me with this project. Melissa Loui assisted me with the feeding experiments. Tor Ottersen did the single-crystal X-ray structure of the major constituent from Gerardia sp. Kazuo Tachibana obtained 360 MHz ^1H NMR spectra of some of the constituents of Corallium sp. Chris Ireland procured 220 MHz ^1H NMR spectra of some of the other constituents of Corallium sp., and provided valuable advice throughout the work on this project. Gary Schulte provided many helpful suggestions concerning HPLC separations and interpretation of spectral data. Professor Yamamoto discussed many of the synthetic aspects of this work with me. The X-ray structure of the major constituent of Corallium sp. was elucidated by Volker Zabel. Katherine Muzik and Richard Grigg identified all organisms examined in my research and discussed many of the biological aspects of these organisms with me. I should especially like to thank Maui Divers, Inc. and Boh Bartko for providing me with the organisms for this research. Without their help this research would not have been possible. Lastly, I would like to thank Professor Scheuer for his patience and guidance in helping me to become a chemist.

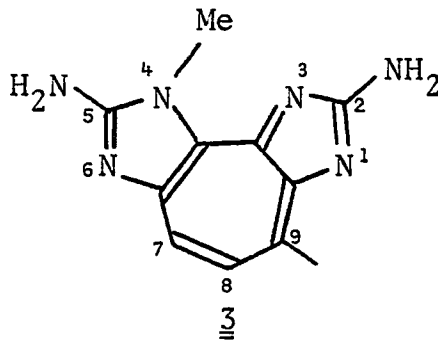
ABSTRACT

In Hawaii deep-sea (-350 m) corals are collected commercially for the production of jewelry. Maui Divers, Inc. operates the manned minisubmersible Star II in the Makapuu beds found in the Molokai Channel off the island of Oahu. Although a large number of deep-sea corals are found in Hawaii, gold coral (Gerardia sp.) and pink coral (Corallium sp.) are commercially two of the most important in the production of gems.

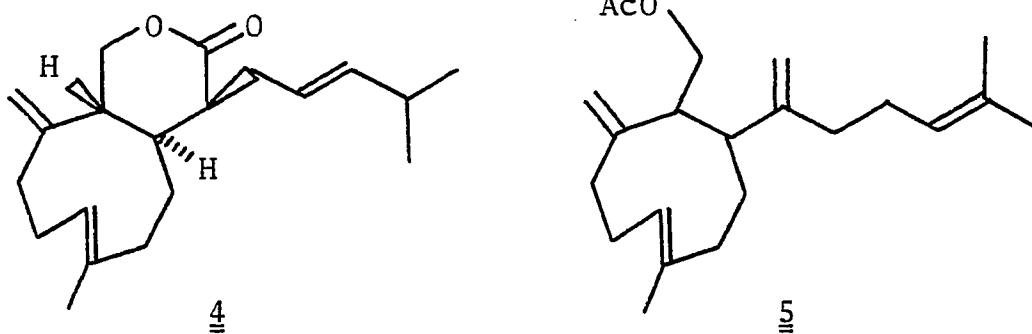
Gerardia sp. (Family Parazoanthidae, Order Zoanthidea, Subclass Zoantharia, Class Anthozoa, Phylum Cnidaria) is a yellow-colored animal with a hard, golden endoskeleton, and is bioluminescent in its deep-sea environment.¹ Two new fluorescent nitrogenous pigments, derivatives of tetraazacyclopentazulene, have been isolated from this organism. The major constituent, 2-amino-3-methyl-5-dimethylamino-3H-pseudozoanthoxanthin (1), is a yellow solid whose structure was established by spectral and chemical means, as well as by X-ray diffraction.^{2,3}

12

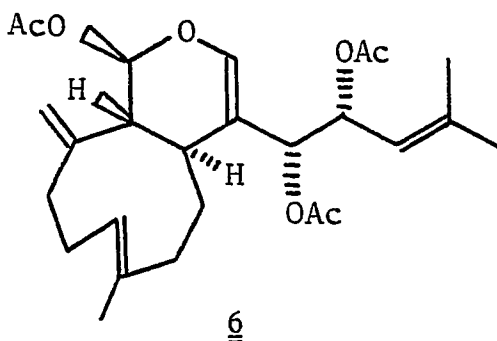
The minor constituent of Gerardia sp., 2-amino-3-methyl-5-methylamino-3H-pseudozoanthoxanthin (2), differs from 1 by the absence of a methyl group according to the ^1H NMR spectrum and mass spectrum. The structure of 2 was proven by transformation of 2 to 1 via methylation.³ Norpseudozoanthoxanthin (3), isolated from Parazoanthus axinellae by Prota and coworkers,^{4,5} is typical of previously isolated pseudozoanthoxanthins which differ from 1 and 2 in the relationship between the nuclear N-methyl and the ring C-methyl.



Pink coral (Corallium sp., Family Coralliidae, Order Gorgonacea, Subclass Alcyonaria, Class Anthozoa, Phylum Cnidaria) has yellow and orange polyps, and a hard pink endoskeleton. Four new diterpenoids containing a nine-membered carbocyclic ring fused to a δ -lactone were isolated from this organism. The structure of the major metabolite, coraxeniolide-A (4), was established by chemical and spectral means and confirmed by X-ray diffraction. The structures of the remaining lactones were obtained by correlation with 4. Corbohcin (5), a minor constituent of Corallium sp.,



contains a nine-membered ring and a single acetate; its structure was elucidated by spectral means. Paragorgia sp., another deep-sea gorgonian, appears to contain the identical five diterpenoids found in Corallium sp. Schmitz and co-workers⁶ suggested the name xeniane for the carbon skeleton found in the coraxeniolides and corbohcin, upon isolation of xenicin (6) from the soft coral Xenia elongata. Related



diterpenoids have been isolated from other species of soft corals belonging to the genus Xenia, as well as from the brown algal family Dictyotaceae.

Literature Cited

1. Bartko, B., personal communication, 1977.
2. Schwartz, R. E.; Yunker, M. B.; Scheuer, P. J.; Ottersen, T. Tetrahedron Lett. 1978, 2235-2238.
3. Schwartz, R. E.; Yunker, M. B.; Scheuer, P. J.; Ottersen, T. Can. J. Chem. 1979, 57, 1701-1711.
4. Cariello, L.; Crescenzi, S.; Prota, G.; Zanetti, L. Tetrahedron 1974, 30, 4191-4196.
5. Cariello, L.; Crescenzi, S.; Prota, G. Comp. Biochem. Physiol. 1979, 63B, 77-82.
6. Vanderah, D. J.; Steudler, P. A.; Ciereszko, L. S.; Schmitz, F. J.; Ekstrand, J. J.; van der Helm, D. J. Am. Chem. Soc. 1977, 99, 5870-5874.

TABLE OF CONTENTS

	Page
ACKNOWLEDGEMENTS	iii
ABSTRACT	iv
LIST OF TABLES	xii
LIST OF ILLUSTRATIONS	xiii
PREFACE	xviii
PART ONE CONSTITUENTS OF <u>GERARDIA</u> SP.	1
I. INTRODUCTION	2
II. EXPERIMENTAL	6
A. APPARATUS, METHODS, AND MATERIALS	6
B. ISOLATION	6
C. 2-AMINO-3-METHYL-5-DIMETHYLAMINO-3 <u>H</u> - PSEUDOZOANTHOXANTHIN (<u>2</u>)	7
D. 2-ACETAMINO-3-METHYL-5-DIMETHYLAMINO- 3 <u>H</u> -PSEUDOZOANTHOXANTHIN (<u>4</u>)	8
E. 2-AMINO-3-METHYL-5-METHYLAMINO-3 <u>H</u> - PSEUDOZOANTHOXANTHIN (<u>6</u>)	9
F. METHYLATION OF 2-AMINO-3-METHYL-5-METHYL- AMINO-3 <u>H</u> -PSEUDOZOANTHOXANTHIN (<u>6</u>)	9
G. 2-AMINO-3-METHYL-5-DIMETHYLAMINO-3 <u>H</u> - PSEUDOZOANTHOXANTHIN (<u>2</u> from <u>6</u>)	10
H. 2,5-BISDIMETHYLAMINO-3-METHYL-3 <u>H</u> - PSEUDOZOANTHOXANTHIN (<u>7</u> from <u>6</u>)	10
I. FEEDING EXPERIMENTS WITH 2-AMINO-3-METHYL- 5-DIMETHYLAMINO-3 <u>H</u> -PSEUDOZOANTHOXANTHIN (<u>2</u>).	10

III.	RESULTS AND DISCUSSION	12
A.	STRUCTURAL DETERMINATION OF 2-AMINO-3-METHYL-5-DIMETHYLAMINO-3 <u>H</u> -PSEUDOZOANTHOXANTHIN (<u>2</u>)	12
B.	STRUCTURAL DETERMINATION OF 2-AMINO-3-METHYL-5-METHYLAMINO-3 <u>H</u> -PSEUDOZOANTHOXANTHIN (<u>6</u>)	23
C.	FEEDING EXPERIMENTS WITH 2-AMINO-3-METHYL-5-DIMETHYLAMINO-3 <u>H</u> -PSEUDOZOANTHOXANTHIN (<u>2</u>)	36
IV.	RELATED RESEARCH BY OTHERS	37
A.	PREVIOUSLY ISOLATED ZOANTHOXANTHINS AND THEIR NOMENCLATURE	37
B.	BIOGENESIS OF ZOANTHOXANTHINS	41
C.	SYNTHESIS OF ZOANTHOXANTHINS	43
D.	BIOLOGICAL ACTIVITY OF ZOANTHOXANTHINS	46
V.	CONCLUSION	47
	PART TWO CONSTITUENTS OF <u>CORALLIUM</u> SP.	48
I.	INTRODUCTION	49
II.	EXPERIMENTAL	52
A.	APPARATUS, METHODS, AND MATERIALS	52
B.	ISOLATION	53
C.	CORAXENIOLIDE-A (<u>22</u>)	54
D.	HEXACORAXENIOLIDE-A (<u>23</u>) AND HEXACORAXENIOLIDE-A' (<u>24</u>) (FROM <u>22</u>).	55

	Page
E. CORAXENDIOL-A (<u>25</u> FROM <u>22</u>)	55
F. CORAXENIOLIDE-B (<u>26</u>)	56
G. CORAXENIOLIDE-C (<u>34</u>)	57
H. CORAXENIOLIDE-D (<u>36</u> from <u>34</u>)	58
I. HEXACORAXENIOLIDE-A (<u>23</u>) AND HEXA- CORAXENIOLIDE-A' (<u>24</u>) (FROM <u>36</u>)	59
J. CORAXENIOLIDE-D' (<u>37</u> FROM <u>34</u>)	60
K. CORAXENIOLIDE-C' (<u>38</u>)	61
L. CORAXENIOLIDE-D (<u>36</u> FROM <u>38</u>)	62
M. CORAXENIOLIDE-D' (<u>37</u> FROM <u>38</u>)	63
N. CORBOHCIN (<u>47</u>)	63
III. RESULTS AND DISCUSSION	65
A. STRUCTURAL DETERMINATION OF CORAXENIOLIDE-A (<u>22</u>)	65
B. STRUCTURAL DETERMINATION OF CORAXENIOLIDE-B (<u>26</u>)	82
C. STRUCTURAL DETERMINATION OF CORAXENIOLIDE-C (<u>34</u>)	94
D. STRUCTURAL DETERMINATION OF CORAXENIOLIDE-C' (<u>38</u>)	121
E. STRUCTURAL DETERMINATION OF CORBOHCIN (<u>47</u>)	132
F. CONSTITUENTS OF <u>PARAGORGIA</u> SP.	145

IV. RELATED RESEARCH BY OTHERS	148
A. PREVIOUSLY ISOLATED XENIANES	148
B. BIOGENESIS OF CORAXENIOLIDES	152
V. CONCLUSION	160
LITERATURE CITED	162

LIST OF TABLES

Table		Page
1	UV Spectral Data of Zoanthoxanthins	16
2	^1H NMR Spectral Data of Zoanthoxanthins	17
3	^1H NMR Spectral Data of Coraxeniolide-B (<u>26</u>), Xeniolide-A (<u>32</u>), and Isoxeniolide-A (<u>33</u>)	93
4	100 MHz ^1H NMR Spectral Data of Coraxeniolides -C (<u>34</u>), D (<u>36</u>), D' (<u>37</u>), and C' (<u>38</u>)	128

LIST OF ILLUSTRATIONS

Figure		Page
1	Mass spectrum of 2-amino-3-methyl-5-dimethyl- amino-3 <u>H</u> -pseudozoanthoxanthin (<u>2</u>)	13
2	UV spectrum of 2-amino-3-methyl-5-dimethylamino- 3 <u>H</u> -pseudozoanthoxanthin (<u>2</u>) in MeOH	14
3	UV spectrum of 2-amino-3-methyl-5-dimethylamino- 3 <u>H</u> -pseudozoanthoxanthin (<u>2</u>) in MeOH ₂ ⁺	15
4	¹ H NMR spectrum of 2-amino-3-methyl-5-dimethyl- amino-3 <u>H</u> -pseudozoanthoxanthin (<u>2</u>) in CF ₃ CO ₂ D	18
5	¹ H NMR spectrum of 2-amino-3-methyl-5-dimethyl- amino-3 <u>H</u> -pseudozoanthoxanthin (<u>2</u>) in Me ₂ SO-d ₆	19
6	Single-crystal X-ray structure of 2-amino-3- methyl-5-dimethylamino-3 <u>H</u> - pseudozoanthoxanthin (<u>2</u>)	22
7	Mass spectrum of 2-acetamino-3-methyl-5- dimethylamino-3 <u>H</u> -pseudozoanthoxanthin (<u>4</u>)	24
8	¹ H NMR spectrum of 2-acetamino-3-methyl-5- dimethylamino-3 <u>H</u> -pseudozoanthoxanthin (<u>4</u>) in Me ₂ SO-d ₆	25
9	UV spectrum of 2-acetamino-3-methyl-5- dimethylamino-3 <u>H</u> -pseudozoanthoxanthin (<u>4</u>) in MeOH	26
10	UV spectrum of 2-acetamino-3-methyl-5- dimethylamino-3 <u>H</u> -pseudozoanthoxanthin (<u>4</u>) in MeOH ₂ ⁺	27

Figure	Page
11	UV spectrum of 2-amino-3-methyl-5-methylamino-3H-pseudozoanthoxanthin (<u>6</u>) in MeOH 28
12	UV spectrum of 2-amino-3-methyl-5-methylamino-3H-pseudozoanthoxanthin (<u>6</u>) in MeOH ₂ ⁺ 29
13	Mass spectrum of 2-amino-3-methyl-5-methyl-amino-3H-pseudozoanthoxanthin (<u>6</u>) 30
14	¹ H NMR spectrum of 2-amino-3-methyl-5-methyl-amino-3H-pseudozoanthoxanthin (<u>6</u>) in CF ₃ CO ₂ D 31
15	Mass spectrum of 2,5-bisdimethylamino-3-methyl-3H-pseudozoanthoxanthin (<u>7</u>) 33
16	¹ H NMR spectrum of 2,5-bisdimethylamino-3-methyl-3H-pseudozoanthoxanthin (<u>7</u>) in CF ₃ CO ₂ D 34
17	UV spectrum of 2,5-bisdimethylamino-3-methyl-3H-pseudozoanthoxanthin (<u>7</u>) in MeOH 35
18	IR spectrum of coraxeniolide-A (<u>22</u>) 66
19	220 MHz ¹ H NMR spectrum of coraxeniolide-A (<u>22</u>) in CDCl ₃ 67
20	Mass spectrum of coraxeniolide-A (<u>22</u>) 69
21	¹³ C NMR spectrum of hexacoraxeniolide-A (<u>23</u>) and hexacoraxeniolide-A' (<u>24</u>) in CDCl ₃ 70
22	Mass spectrum of hexacoraxeniolide-A (<u>23</u>) and hexacoraxeniolide-A' (<u>24</u>) 71
23	360 MHz ¹ H NMR spectrum of hexacoraxeniolide-A (<u>23</u>) and hexacoraxeniolide-A' (<u>24</u>) in CDCl ₃ 73

Figure		Page
24	Expansion of the methyl region of the 360 MHz ^1H NMR spectrum of hexacoraxeniolide-A (<u>23</u>) and hexacoraxeniolide-A' (<u>24</u>) in CDCl_3	74
25	IR spectrum of hexacoraxeniolide-A (<u>23</u>) and hexacoraxeniolide-A' (<u>24</u>)	75
26	Mass spectrum of coraxendiol-A (<u>25</u>)	76
27	360 MHz ^1H NMR spectrum of coraxendiol-A (<u>25</u>) in C_6D_6	77
28	Single-crystal X-ray structure of coraxeniolide-A (<u>22</u>)	79
29	Expansion of the 71.07 ppm signal in the off-resonance ^{13}C NMR spectrum of coraxeniolide-B (<u>26</u>)	83
30	IR spectrum of coraxeniolide-B (<u>26</u>)	84
31	UV spectrum of coraxeniolide-B (<u>26</u>)	85
32	100 MHz ^1H NMR spectrum of coraxeniolide-B (<u>26</u>) in C_6D_6	86
33	100 MHz ^1H NMR spectrum of coraxeniolide-B (<u>26</u>) in CDCl_3	87
34	Mass spectrum of coraxeniolide-B (<u>26</u>)	89
35	Mass spectrum of coraxeniolide-C (<u>34</u>)	95
36	IR spectrum of coraxeniolide-C (<u>34</u>)	97
37	Expansion of the 71.66 ppm signal in the off-resonance ^{13}C NMR spectrum of coraxeniolide-C (<u>34</u>)	98

Figure	Page
38	UV spectrum of coraxeniolide-C (<u>34</u>) 99
39	100 MHz ^1H NMR spectrum of coraxeniolide-C (<u>34</u>) in CDCl_3 100
40	100 MHz ^1H NMR spectrum of coraxeniolide-C (<u>34</u>) in C_6D_6 101
41	IR spectrum of coraxeniolide-D (<u>36</u>) 104
42	UV spectrum of coraxeniolide-D (<u>36</u>) 106
43	Mass spectrum of coraxeniolide-D (<u>36</u>) 107
44	100 MHz ^1H NMR spectrum of coraxeniolide-D (<u>36</u>) in CDCl_3 109
45	Comparison of the C-1 proton signals in the 100 MHz ^1H NMR spectrum (CDCl_3) of hexa- coraxeniolide-A (<u>23</u>) and hexacoraxeniolide-A' (<u>24</u>) from coraxeniolide-A (<u>22</u>) and from coraxeniolide-D (<u>36</u>) 111
46	Mass spectrum of coraxeniolide-D' (<u>37</u>) 113
47	UV spectrum of coraxeniolide-D' (<u>37</u>) 114
48	100 MHz ^1H NMR spectrum of coraxeniolide-D' (<u>37</u>) in CDCl_3 115
49	360 MHz ^1H NMR spectrum of coraxeniolide-D' (<u>37</u>) in CDCl_3 117
50	IR spectrum of coraxeniolide-D' (<u>37</u>) 118
51	Conformation of coraxeniolide-D (<u>36</u>) and coraxeniolide-D' (<u>37</u>) 119

Figure	Page
52	Mass spectrum of coraxeniolide-C' (<u>38</u>) 122
53	IR spectrum of coraxeniolide-C' (<u>38</u>) 123
54	UV spectrum of coraxeniolide-C' (<u>38</u>) 124
55	100 MHz ¹ H NMR spectrum of coraxeniolide-C' (<u>38</u>) in C ₆ D ₆ 126
56	Mass spectrum of corbohcin (<u>47</u>) 133
57	IR spectrum of corbohcin (<u>47</u>) 134
58	220 MHz ¹ H NMR spectrum of corbohcin (<u>47</u>) in CDCl ₃ 136
59	TLC comparison of the CH ₂ Cl ₂ extracts from <u>Corallium</u> sp. and <u>Paragorgia</u> sp. 146

PREFACE

Few places on earth are less accessible and more hostile to human life than the deep ocean (<-100 m). It is a dark, cold, high pressure environment, where normal air becomes toxic for humans. A number of other organisms, on the other hand, have adapted to, and proliferated in, the deep-sea environment.

For a long time man ignored the deep ocean mainly because it was accessible only via nets, trawls, and dredges. There is today, however, a renewed interest in exploring the ocean floor. The most important reason for this interest is the development of deep-sea submersibles in which direct observation of this environment is possible. Commercial interests, especially the oil and mineral industries and, in Hawaii, the precious coral industry, are also supporting deep-sea exploration. And finally, scientists are becoming increasingly concerned with the oceans, which represent so large a proportion of the earth's surface.

Nevertheless, relatively little is known about the biology or chemistry of deep-sea organisms, largely because of the previous inaccessibility of this ecosystem. Even now that the depths have become more accessible, it is difficult to justify the immense expense of obtaining samples from this region when such a large body of work remains to be done on shallow-water organisms.

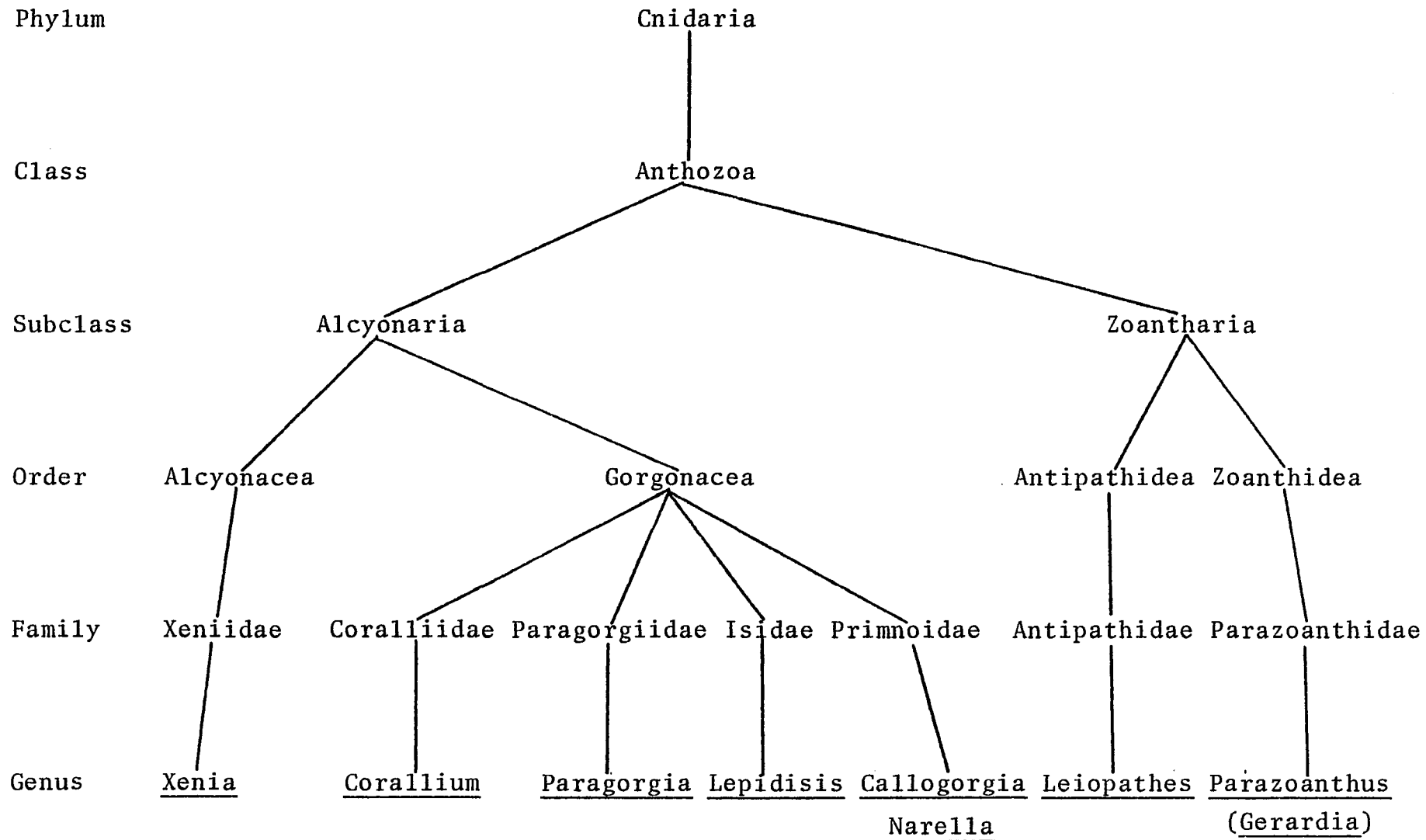
In Hawaii, however, the situation is different. Maui Divers, Inc. has for a number of years supported the collection of deep-sea corals for the production of jewelry. Boh Bartko, pilot of the minisubmersible Star II, collects the corals at depths up to 350 m in the Makapuu beds off the island of Oahu. Because of the generosity of Maui Divers Inc. and in particular Boh Bartko, I had a unique opportunity to examine the chemistry of organisms from this unusual environment.

One of the deep-sea organisms I examined was an unidentified, siliceous sponge which grows on dead pink coral (Corallium sp.). Testing of the aqueous extract from this sponge suggested that it contained a heart stimulant; this activity, however, could never be confirmed.

I also examined a number of corals from deep water. One of these was bamboo coral, Lepidisis olapa, a strongly bioluminescent, long, spiralling organism.¹ Its endoskeleton is made up of hard, hollow segments connected by flexible joints--hence the name bamboo. Another organism was Leiopathes glaberrima, a deep-sea coral with a black endoskeleton and blood-red polyps.² Smoky gold coral (tentatively identified as Callogorgia sp.) and Narella sp., two corals with hard, golden endoskeletons, were also investigated.³ Examination of extracts of these corals indicated that they contained no new or interesting natural products.

In my Dissertation I will present the structural determination of natural products isolated from two other deep-sea corals. Part One will be concerned with the constituents of a zoanthid trivially called gold coral (Gerardia sp.), while in Part Two I will discuss secondary metabolites isolated from a gorgonian known as pink coral (Corallium sp.).⁴ A preliminary investigation of the constituents of Paragorgia sp., another gorgonian,³ will also be presented in Part Two of this Dissertation.

The taxonomic relationships of these corals are outlined in the phyletic tree on the next page. .



Partial Systematics of the Cnidarian Class Anthozoa

PART ONE

CONSTITUENTS OF
GERARDIA SP.

I. INTRODUCTION

Very few corals have endoskeletons which are suitable for the production of jewelry. The precious corals usually have endoskeletons which are brightly colored. More importantly, they must be hard so that they can be cut, polished, and fashioned into durable gems. Calcium carbonate, the major constituent of coral endoskeletons, is white, soft, and porous. Consequently, for a coral to be useful in jewelry production its endoskeleton must contain organic polymers to provide a lattice for calcium carbonate, as well as to give the coral its characteristic color. The solubility of calcium carbonate in seawater increases with decreasing temperature and increasing pressure,⁵ thus making these polymers especially important in the endoskeletons of deep-sea corals. Although little work has been done on the structure of these organic polymers, the polymer in the endoskeleton of Pocillopora damicornis, a shallow-water coral, has been characterized as chitin, a polysaccharide made up of glucosamine.⁶

While most precious corals belong to the subclass Alcyonaria (see Preface), gold coral is a zoantharian which is collected commercially for the production of gems.² Alcyonarians have octomeroous symmetry, with eight pinnate (feathery) tentacles and eight septa attached to the pharynx. Zoantharians, on the other hand, are simply anthozoans with

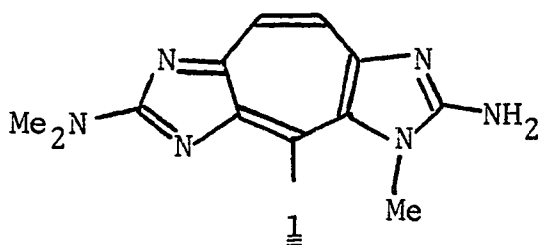
other than octomeros symmetry. In many cases zoantharians have hexamerous symmetry, and hence are referred to as hexacorals.⁷

Gold coral is a hexacoral belonging to the order Zoanthidea, and genus Gerardia (Parazoanthus).^{*} This organism has yellow polyps and a hard, golden endoskeleton, which acquires a deep luster when cut and polished. Also esthetically pleasing is the bioluminescence of the living animal, which is observed in its dark, deep-sea environment.⁸

The genera Epizoanthus, Parazoanthus, Isozoanthus, and Zoanthus of the order Zoanthidea are epizoic, i.e., they grow on other organisms. Members of this order have been reported to grow on sponges, hydroids, corals, gorgonians, bryozoans, and tubeworms. Certain species of the genus Epizoanthus even grow on the shells of hermit crabs and eventually cover and dissolve the shell. A crab that is covered with a zoanthid is referred to as a carcinoecium.⁷ Gerardia sp., which is also known to be epizoic, grows on and apparently kills its host Acanella sp.⁹

* Katherine Muzik, at the United States National Museum, has examined this species of gold coral and, in light of a precedent, feels that the correct generic name is Gerardia rather than Parazoanthus. This implies that the whole genus may have been named incorrectly. To avoid confusion, I will refer to this gold coral as Gerardia sp. and use the term Parazoanthus only when referring to previous literature.

Organic extracts of many species belonging to the genus Parazoanthus display an unusual purple fluorescence.¹⁰ The constituents responsible for this fluorescence are the zoanthoxanthin pigments (tetrazacyclopentazulenes), which were first isolated by Prota and coworkers,¹¹ and of which zoanthoxanthin (1) is a typical representative.



Zoanthoxanthins are extremely stable, amorphous or crystalline, yellow solids which strongly absorb ultra-violet and visible light in the range 200-500 nm. The reemission of this absorbed energy is responsible for the purple fluorescence of these compounds in organic solutions. Chemically, zoanthoxanthins are planar aromatic ring systems, and are strongly basic due to the presence of two guanidine units. Because of their polar nature, they are relatively insoluble in organic solvents. As they are basic, they are soluble in aqueous acid; however, they are rather insoluble in water. In the single-crystal X-ray structure determination of a chloro-derivative of zoanthoxanthin, Prota and coworkers found that water molecules were binding zoanthoxanthin molecules via hydrogen bonding to the nitrogens of the guanidine units.¹² Presumably in water zoanthoxanthins

form similar aggregates, which may explain their insolubility in this solvent.

I originally became interested in Gerardia sp. because of an oral report⁸ that contact with this coral caused severe irritation to the skin of workers who had handled it. Although I was never able to isolate the responsible agent, I did isolate two previously unknown zoanthoxanthins from this organism. In Part One of this Dissertation I will present the isolation and structural elucidation of these compounds.

II. EXPERIMENTAL

A. Apparatus, Methods, and Materials

Natural abundance ^{13}C NMR spectra were recorded on a Varian XL-100 Fourier transform spectrometer at 25.2 MHz. Field/frequency locking was provided by the deuterium signals of $\text{CF}_3\text{CO}_2\text{D}$ and D_2O . Proton NMR spectra were recorded on a Varian XL-100 NMR spectrometer at 100 MHz; TMS was used as an internal reference.

Mass spectra were determined on a Varian MAT 311 high resolution mass spectrometer at an ionizing voltage of 70 eV. To eliminate impurity peaks from H_2O (m/z 18) and N_2 (m/z 28), fragments with masses less than m/z 30 were not included in the mass spectral reproductions.

A Beckman ACTA III spectrophotometer was used for the UV spectra. Emission spectra were obtained on an Amico-Bowman spectrophotofluorometer. Melting points were taken on a Fisher-Johns apparatus. New England Nuclear silica gel OF 250 μ plates were used for all TLC's.

B. Isolation

Freshly collected animals (320 g) were soaked in 90% EtOH overnight and concentrated to a water layer of about 100 mL, which was diluted with water to approximately 350 mL, acidified to pH 1 with aqueous HCl, and continuously extracted with CH_2Cl_2 overnight. This CH_2Cl_2 extract, which contained mainly fats, was discarded.

The resulting aqueous acidic layer was again diluted to 1.5 L and passed through a Dowex 50W-4X cation exchange column. The column was washed with 7 L of 1 N HCl, then with water until the eluant had reached pH 6. This eluant was also discarded.

The top quarter of the column was removed and slurried with aqueous NH₃ to about 2 N. This suspension was then extracted 2X with n-BuOH and 4X with CHCl₃/MeOH (4:3). All six extracts were combined and concentrated to yield 1.2 g of a yellow residue.

This solid was chromatographed on Bio-Sil A with CHCl₃/MeOH/25% aq NH₃ (80:20:2), which was followed by chromatography on Sephadex LH-20 with CHCl₃/MeOH (4:3) and CHCl₃/MeOH (2:3), yielding about 900 mg of 2 and 60 mg of 6.

C. 2-Amino-3-methyl-5-dimethylamino-3H-pseudozoantho-xanthin (2)

Compound 2 was isolated as an amorphous yellow powder, R_f 0.61, CHCl₃/MeOH/25% aq NH₃ (80:20:2), dec ≈ 200°C; C₁₃H₁₆N₂ (calcd 256.143 647; found 256.143 53) m/z 256 (67%, M⁺), 241 (100, M⁺-CH₃), 227 (70, M⁺-NCH₃), 212 (17, M⁺-NMe₂) (Fig. 1). ¹³C NMR: (CF₃CO₂D) 153.67 (s), 150.68 (s), 149.09 (s), 139.06 (s), 137.47 (d), 136.85 (s), 130.16 (s), 121.88 (s), 39.37 (2q), 35.14 (q), and 23.51 (q) ppm. A ninth sp² carbon, which was obscured by the solvent absorbances in the CF₃CO₂D spectrum, was found at 160.57 (s)

ppm in the D₂O spectrum of the dihydrochloride salt of 2.
¹H NMR: (CF₃CO₂D, Fig. 4, Table 2) 8.29 1H d (J = 10 Hz), 4.63 3H s, 3.55 6H bs, 2.96 3H s ppm; (Me₂SO-d₆, Fig. 5, Table 2) 7.74 1H d (J = 11 Hz), 7.36 1H d (J = 11 Hz), 7.29 2H bs (D₂O exchangeable), 4.30 3H s, 3.27 6H s, 2.69 3H s ppm. UV λ_{max} nm (log ε): (MeOH, Fig. 2, Table 1) 416 (4.18), 377 (4.00), 317 sh (4.49), 306 (4.59), 261 (4.02), 226 (4.02); (MeOH₂⁺, Fig. 3) 414 (4.32), 359 (3.74), 298 (4.61), 249 (4.07), 241 (4.02). A 1.95x10⁻⁵ M solution of 2 showed a strong emission maximum at 440 nm upon excitation at 330 nm. Compound 2 was crystallized from EtOH/H₂O (80:20) by adding a minimum amount of hot solvent and allowing the solution to stand overnight. Crystalline 2 also dec ≈ 200°C.

D. 2-Acetamino-3-methyl-5-dimethylamino-3H-pseudozoanthoxanthin (4)

Acetylation of 20 mg of 2 with Ac₂O/pyridine yielded 10 mg of 4 as an orange, amorphous solid, R_f 0.81, CHCl₃/MeOH/25% aq NH₃ (80:20:2), mp 125-129°C, isolated from Sephadex LH-20 CHCl₃/MeOH (4:3); C₁₅H₁₈N₆O (calcd 298.154 213; found 298.152 13) m/z 298 (58%, M⁺), 283 (39, M⁺-CH₃), 269 (36, M⁺-NCH₃), 255 (22, M⁺-COCH₃), 241 (100), 227 (44) (Fig. 7). ¹H NMR: (Me₂SO-d₆, Fig. 8, Table 2) 7.62 2H bs, 4.26 3H s, 3.32 6H s, 2.82 3H s, 2.26 3H s ppm. UV λ_{max} nm (log ε): (MeOH, Fig. 9) 425 (4.12), 306 (4.22), 289 (4.22), 259 (4.31), 224 (4.21); (MeOH₂⁺, Fig. 10) 419 (4.23), 291 (4.35), 257 (4.18), 226 (4.18).

E. 2-Amino-3-methyl-5-methylamino-3H-pseudozoanthoxanthin
(6)

Compound 6 was isolated as an amorphous, yellow solid, R_f 0.30, $\text{CHCl}_3/\text{MeOH}/25\% \text{ aq NH}_3$ (80:20:2), dec $\approx 180^\circ\text{C}$;
 $\text{C}_{12}\text{H}_{14}\text{N}_6$ (calcd 242.127 997; found 242.127 70) m/z 242
 (100%, M^+), 214 (43, $\text{M}^+ - \text{CNH}_2$), 186 (36) (Fig. 13). $^1\text{H NMR}$:
 ($\text{CF}_3\text{CO}_2\text{D}$, Fig. 14, Table 2) 8.30 1H d ($J = 11$ Hz), 8.03 1H d
 ($J = 11$ Hz), 4.62 3H s, 3.42 3H s, 2.99 3H s ppm. UV λ_{max} nm
 ($\log \epsilon$); (MeOH, Fig. 11, Table 1) 409 (4.07), 371 (4.00),
 310 sh (4.59), 300 (4.65), 256 (4.03), 224 (4.12); (MeOH_2^+ ,
 Fig. 12) 407 (4.24), 363 (3.85), 302 (4.72), 247 (3.96),
 221 (4.09). A 1.95×10^{-5} M solution of 6 in MeOH showed a
 strong emission maximum at 431 nm upon excitation at 328 nm.

F. Methylation of 2-Amino-3-methyl-5-methylamino-3H-
pseudozoanthoxanthin (6)

In 20 mL of liquid NH_3 and 45 mg of Na (NaNH_2),
 15.4 mg of 6 was reacted with 1.5 mL of MeI to give a
 mixture of three compounds separated on Bio-Sil A
 $\text{CHCl}_3/\text{MeOH}/25\% \text{ aq NH}_3$ (80:20:2) and Sephadex LH-20
 $\text{CHCl}_3/\text{MeOH}$ (4:3). After separation this mixture yielded
 4.8 mg of a compound identical to 2 (UV, MS, NMR), 4.0 mg
 of 7, and 2.6 mg of a compound not further characterized.

G. 2-Amino-3-methyl-5-dimethylamino-3H-pseudozoantho-
xanthin (2 from 6)

Compound 2, from the methylation of 6, is an amorphous, yellow solid, R_f 0.61, $\text{CHCl}_3/\text{MeOH}/25\% \text{ aq NH}_3$ (80:20:2), dec $\approx 200^\circ\text{C}$; $\text{C}_{13}\text{H}_{16}\text{N}_6$ (calcd 256.143 647; found 256.143 57) m/z 256 (75%, M^+), 241 (100, M^+-CH_3), 227 (74, M^+-NCH_3), 212 (22, M^+-NMe_2). $^1\text{H NMR}$: ($\text{CF}_3\text{CO}_2\text{D}$) 8.28 1H d ($J = 10$ Hz), 8.03 1H d ($J = 10$ Hz), 4.62 3H s, 3.54 3H s, 2.95 3H s ppm. UV λ_{max} nm ($\log \epsilon$): (MeOH) 416 (4.15), 377 (4.00), 317 sh (4.42), 306 (4.59), 261 (4.00), 226 (4.02).

H. 2,5-Bisdimethylamino-3-methyl-3H-pseudozoanthoxanthin
(7 from 6)

Compound 7 was isolated as an oily, yellow solid, R_f 0.71, $\text{CHCl}_3/\text{MeOH}/25\% \text{ aq NH}_3$ (80:20:2), dec $\approx 115^\circ\text{C}$; $\text{C}_{15}\text{H}_{20}\text{N}_6$ (calcd 284.174 948; found 284.174 69) m/z 284 (100%, M^+), 269 (78, M^+-CH_3), 255 (42, M^+-NCH_3) (Fig. 15). $^1\text{H NMR}$: ($\text{CF}_3\text{CO}_2\text{D}$, Fig. 16, Table 2) 8.22 1H d ($J = 11$ Hz), 8.02 1H d ($J = 11$ Hz), 4.60 3H s, 3.62 6H s, 3.54 6H s, 2.96 3H s ppm. UV λ_{max} nm ($\log \epsilon$): (MeOH, Fig. 17) 420 (3.75), 373 (3.45), 314 (4.07), 262 (3.48), 218 (3.82).

I. Feeding Experiments with 2-Amino-3-methyl-5-dimethyl-
amino-3H-pseudozoanthoxanthin (2)

A stock solution was prepared by dissolving 50 mg of 2 in 100 mL of $\text{CHCl}_3/\text{MeOH}$ (1:1). Aliquots of the stock solution

were diluted to 50 mL and placed in flasks with 10 g dry bread crumbs in each. The solvent was then removed by rotary evaporation followed by 2 h exposure to direct vacuum, at which time the coated bread crumbs were free of solvent.

Sample A was a control, containing bread crumbs exposed only to $\text{CHCl}_3/\text{MeOH}$ (1:1). Sample B was prepared using a 10 mL aliquot of the stock solution. Samples C, D, and E were prepared using 20 mL, 30 mL, and 50 mL of the stock solution, respectively.

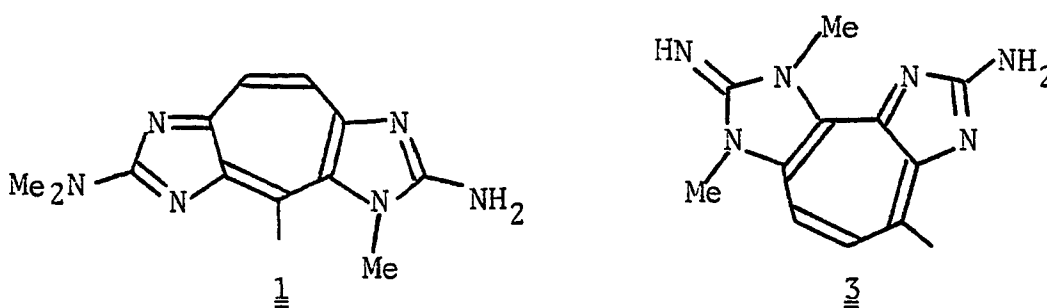
In the feeding experiment I snorkeled into the shallow water of a coral reef and hand-fed the bread crumbs to a variety of fish, mostly parrotfishes and wrasses. Sample A (the control) was fed to the fish first to determine if this method of preparation would affect their feeding behavior. Samples B through E were presented to the fish in a similar manner and their behavior was noted.

III. RESULTS AND DISCUSSION

A. Structural Determination of 2-Amino-3-methyl-5-dimethylamino-3H-pseudozoanthoxanthin (2)*

The major constituent of Gerardia sp. is the 3H-pseudozoanthoxanthin (2). It is a yellow solid which strongly absorbs ultraviolet radiation and displays a purple fluorescence in organic solvents. The mass spectrum of 2 (Fig. 1) shows a molecular ion at m/z 256 with composition $C_{13}H_{16}H_6$, indicating a highly unsaturated system ($u = 9$) with a large number of nitrogens. This initial characterization, in combination with the insolubility of 2 in organic solvents and solubility in aqueous acid, led me to believe that I was dealing with a zoanthoxanthin.

Zoanthoxanthins can be of two structural types, the linear zoanthoxanthin ring system (1), or the angular pseudozoanthoxanthin ring system (3). Comparison of the



UV spectrum of compound 2 (Fig. 2) with the relatively simple spectrum of a typical zoanthoxanthin (1)¹² and the more complex spectrum of a pseudozoanthoxanthin (3)¹³, indicated

* For a detailed discussion of the trivial nomenclature see p. 39.

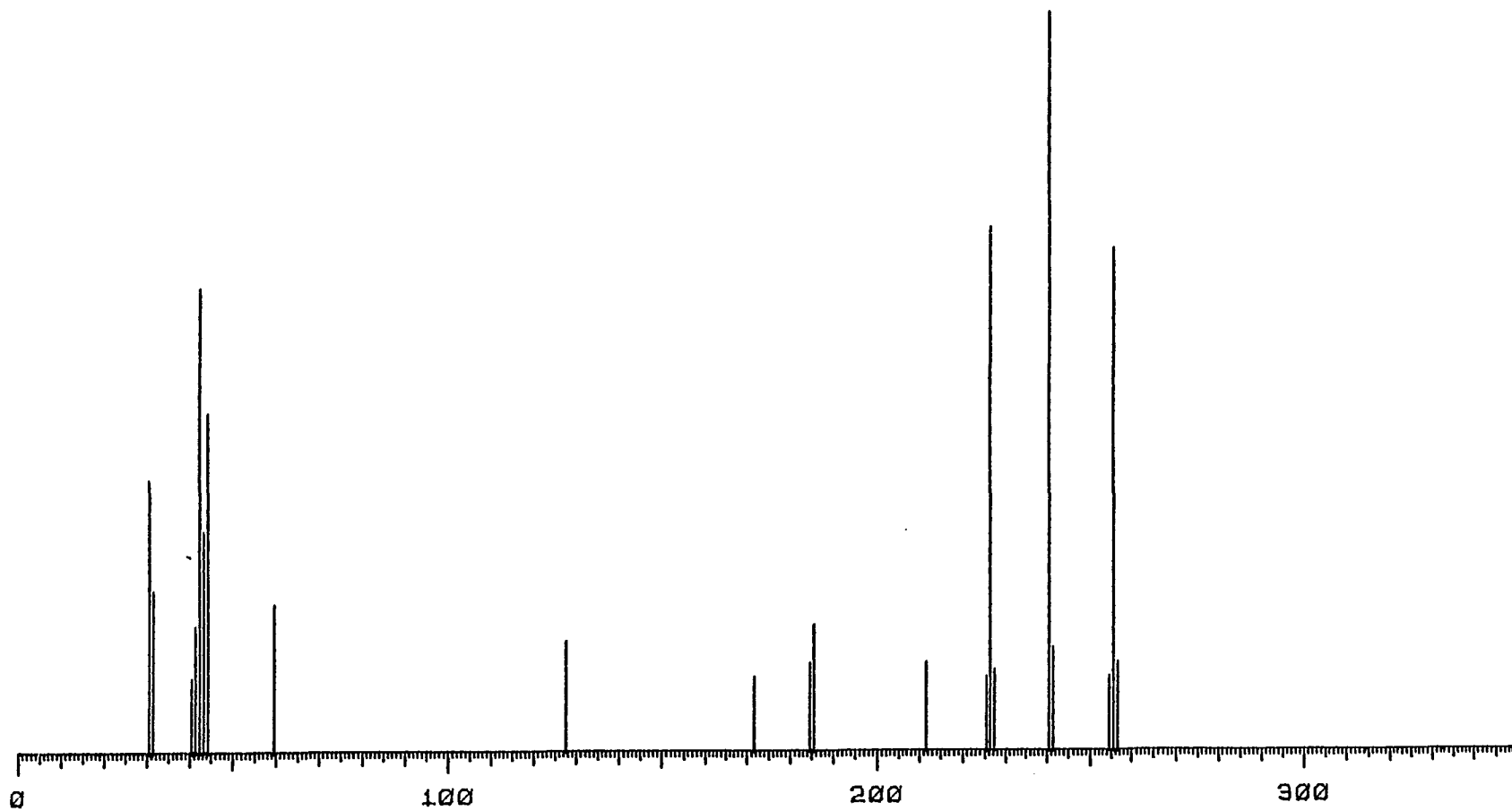


Figure 1. Mass spectrum of
2-amino-3-methyl-5-dimethylamino-3H-pseudoanthoxanthin (2).

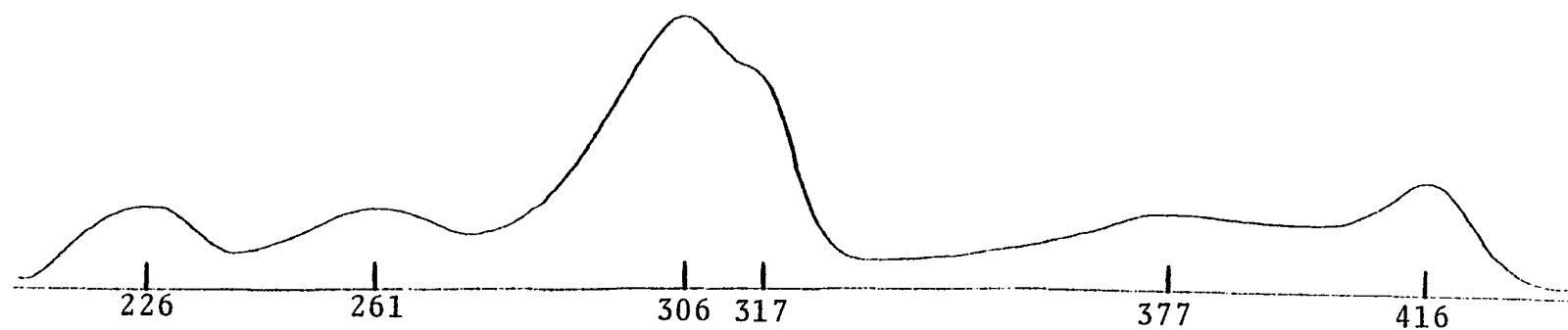


Figure 2. UV spectrum of
2-amino-3-methyl-5-dimethylamino-3H-pseudoanthoxanthin (2) in MeOH.

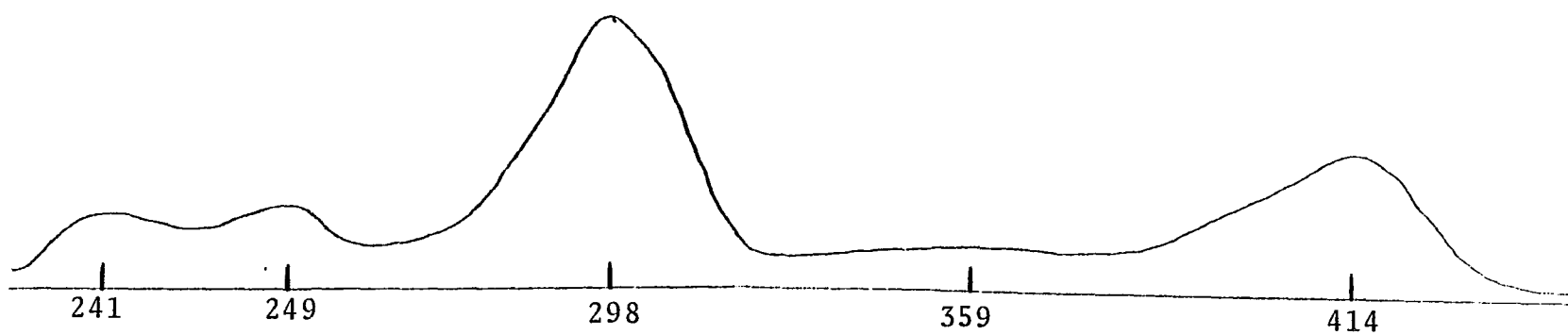


Figure 3. UV spectrum of
2-amino-3-methyl-5-dimethylamino-3H-pseudozoanthoxanthin (2) in MeOH₂⁺.

that 2 probably possessed a pseudozoanthoxanthin skeleton (Table 1). The UV spectrum of 2, however, differed from that of any pseudozoanthoxanthin known at the time.

Table 1.

UV Spectral Data of Zoanthoxanthins (MeOH)

 λ_{\max} nm (log ϵ)

<u>2</u>	416(4.18), 377(4.00), 317sh(4.49), 306(4.59), 261(4.02), 226(4.02)
<u>1</u>	427(4.35), 293(4.52)
<u>3</u>	421(3.93), 367(4.07), 307(4.67), 281(4.48)
<u>4</u>	425(4.12), 306(4.22), 289(4.22), 224(4.21) 259(4.31)
<u>6</u>	409(4.07), 371(4.00), 310sh(4.59), 300(4.65), 256(4.03), 224(4.12)

The emission spectrum of 2 also favors a pseudozoanthoxanthin skeleton. Compound 1 exhibits an emission maximum at 479 nm upon excitation at 348 nm,¹² while excitation of 3 at 340 nm produces an emission maximum at 446 nm.¹³ The emission spectrum of 2 reveals a maximum at 440 nm upon excitation at 330 nm, which suggests a structural similarity to pseudozoanthoxanthin (3).

Assignments in the ¹H NMR spectrum of 2 (CF₃CO₂D, Fig. 4) were made by comparison with known pseudozoanthoxanthins, as seen in Table 2. The two aromatic protons in 2, at δ 8.29 and δ 8.04, are coupled to each other and are, therefore, vicinal. Assuming a pseudozoanthoxanthin ring system, the C-methyl at δ 2.99 must also be adjacent to one of these

Table 2.

 ^1H NMR Spectral Data of Zoanthoxanthins in $\text{CF}_3\text{CO}_2\text{D}^{\text{a}}$ or $\text{Me}_2\text{SO}-\text{d}_6^{\text{b}}$ ($\delta = 0$ ppm)

Aromatic protons	$-\text{NH}_2$	Nuclear $-\text{NMe}$	$-\text{NHMe}$	$-\text{NMe}_2$	$-\text{CMe}$	$\begin{array}{c} \text{O} \\ \\ -\text{CMe} \end{array}$
$\underline{2}^{\text{a}}$ 8.29 1H d 8.04 1H d J = 10 Hz		4.63 3H s		3.55 6H bs	2.99 3H s	
$\underline{2}^{\text{b}}$ 7.74 1H d 7.36 1H d J = 11 Hz	7.29 2H bs ^c	4.30 3H s		3.27 6H s	2.69 3H s	
$\underline{3}^{\text{a}}$ 8.21 2H s		4.05 3H s 4.61 3H s			3.03 3H s	
$\underline{4}^{\text{b}}$ 7.62 2H bs		4.26 3H s		3.32 6H s	2.82 3H s	2.26 3H s
$\underline{5}^{\text{a}}$ 8.29 1H d 8.15 1H d J = 11 Hz		4.56 3H s			3.01 3H s	
$\underline{6}^{\text{a}}$ 8.30 1H d 8.03 1H d J = 11 Hz		4.62 3H s	3.42 3H s		2.99 3H s	
$\underline{7}^{\text{a}}$ 8.22 1H d 8.02 1H d J = 11 Hz		4.60 3H s		3.62 6H s ^d 3.54 6H bs ^d	2.96 3H s	

^c D_2O exchangeable.^dOverlapping singlets.

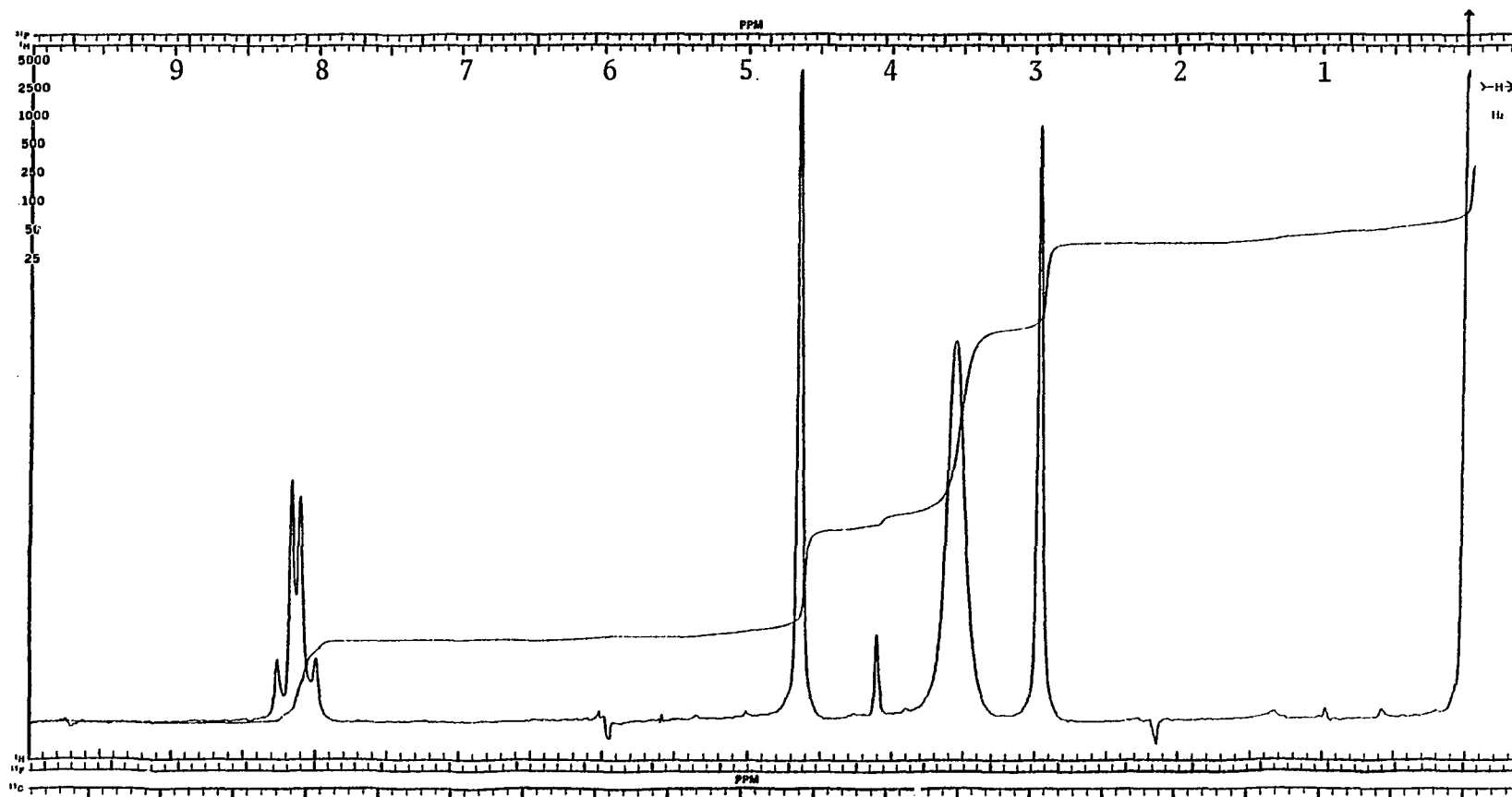


Figure 4. ^1H NMR spectrum of
2-amino-3-methyl-5-dimethylamino-3H-pseudoanthoxanthin (2) in $\text{CF}_3\text{CO}_2\text{D}$.

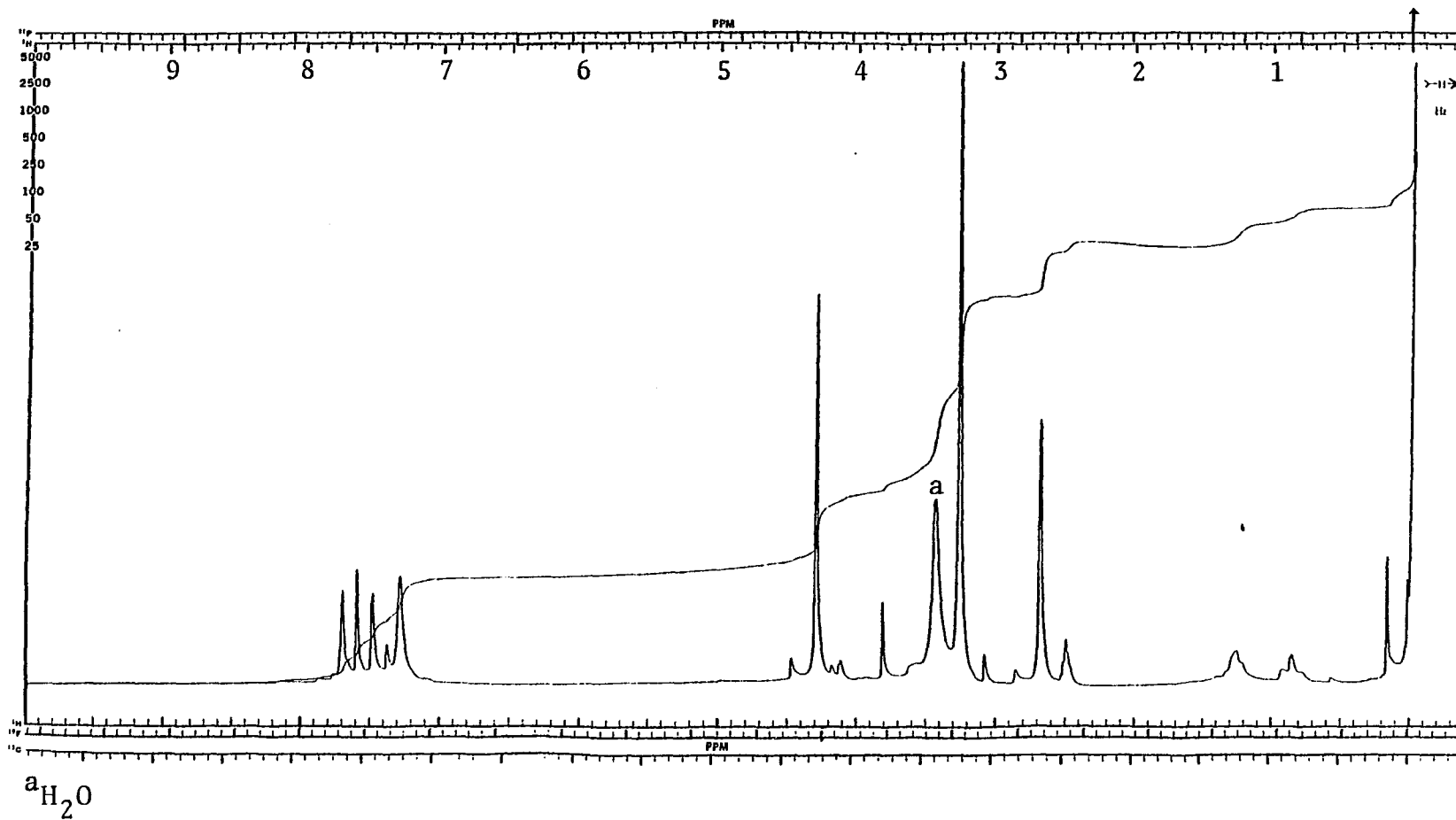
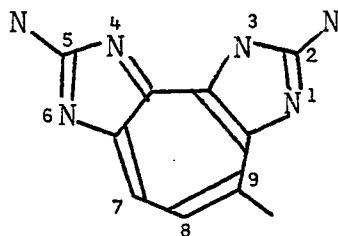


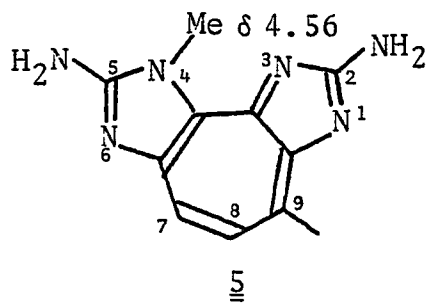
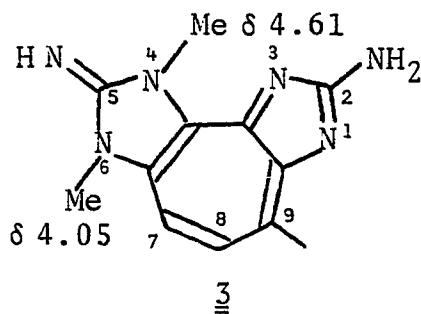
Figure 5. ^1H NMR spectrum of
 2-amino-3-methyl-5-dimethylamino-3H-pseudoanthoxanthin (2) in $\text{Me}_2\text{SO}-d_6$.



aromatic protons and has been arbitrarily placed at C-9 rather than C-7.

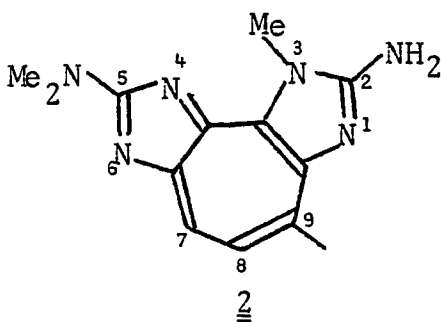
There was originally a question as to whether the broad, six-proton singlet at δ 3.55 was due to an N,N-dimethyl or two N-methyls. Inspection of the $\text{Me}_2\text{SO}-d_6$ ^1H NMR spectrum (Fig. 5), however, shows that the six-proton singlet has sharpened considerably, which supports an N,N-dimethyl assignment. Also, the isolation of a single monoacetate (4) of 2 suggests the presence of a primary amine and an N,N-dimethyl, rather than two N-methyls. This N,N-dimethyl group may be placed at C-2 or C-5.

Comparing the ^1H NMR spectra (Table 2) of pseudozoanthoxanthin (3) and norpseudozoanthoxanthin (5), one can see that the "inside" nuclear N-methyls (N-3 and N-4) absorb at approximately δ 4.5, while the "outside" nuclear N-methyls (N-1 and N-6) are found closer to δ 4.0. This means that the nuclear N-methyl in 2, found at δ 4.63, can be positioned at N-3 or N-4.

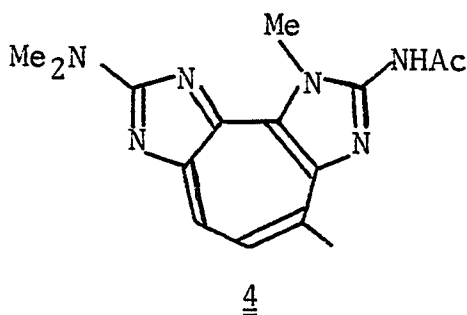


As a result of the lack of symmetry of the molecule, placing of the methyls at various positions generates different compounds. Since the lack of symmetry is subtle, however, I was unable to detect the differences by spectral or chemical means. Therefore, X-ray crystallography was used to determine the positions of the methyls in 2.

Crystals were obtained by dissolving 2 in a minimum amount of hot EtOH/H₂O (80:20) and allowing the solution to stand overnight. Single-crystal X-ray analysis showed that the structure of 2 is 2-amino-3,9-dimethyl-5-dimethylamino-3H-1,3,4,6-tetrazacyclopent[e]azulene monohydrate as seen in Figure 6; these results have been published.^{14,15}



The monoacetate of 2 is 2-acetamino-3-methyl-5-dimethylamino-3H-pseudozoanthoxanthin (4) seen below.



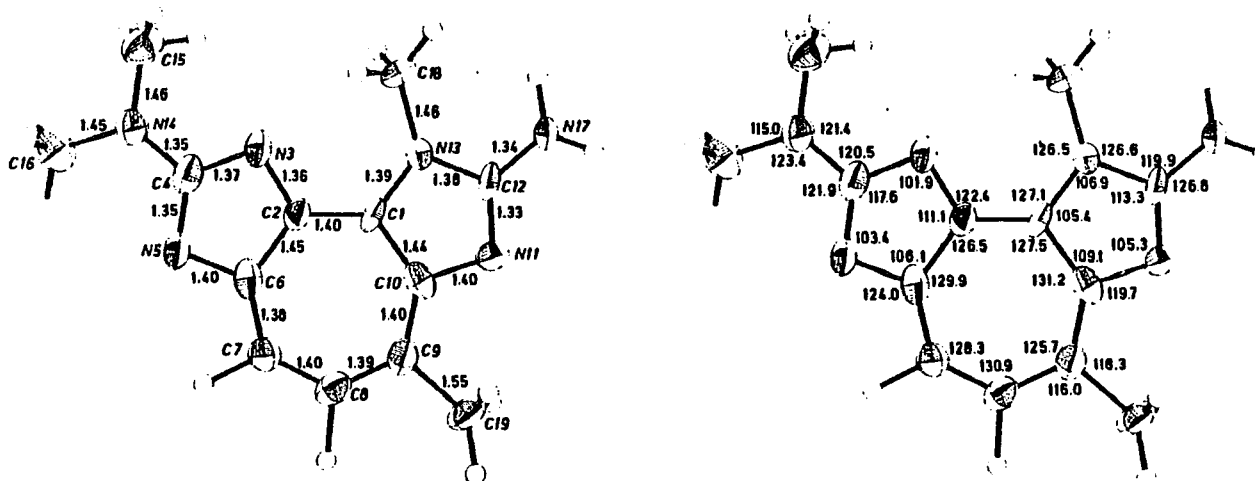


Figure 6. Single-crystal X-ray structure of
2-amino-3-methyl-5-dimethylamino-3H-pseudozoanthoxanthin (2).

Compound 4 is an orange, amorphous solid which, unlike 2, has a relatively sharp melting point in the range of 125-129°C. The molecular ion at m/z 298 in the mass spectrum of 4 (Fig. 7), as well as one additional methyl singlet in the ^1H NMR spectrum ($\text{Me}_2\text{SO-d}_6$, Fig. 8, Table 2) at δ 2.26, confirm that 4 is the monoacetate of 2.

B. Structural Determination of 2-Amino-3-methyl-5-methylamino-3H-pseudozoanthoxanthin (6)

The minor constituent of Gerardia sp. (6) is also a yellow, amorphous solid. While it is relatively insoluble in organic solvents, it is soluble in aqueous acid. The complexity of its UV spectrum (Fig. 11, Table 1), as well as its emission maximum at 431 nm, again suggest a pseudo-zoanthoxanthin ring system. The mass spectrum of 6 (Fig. 13) shows a molecular ion at m/z 242 with composition $\text{C}_{12}\text{H}_{14}\text{N}_6$, which differs from that of 2 by the absence of one methyl group.

The ^1H NMR spectrum of 6 ($\text{CF}_3\text{CO}_2\text{D}$, Fig. 14, Table 2) is virtually identical to that of 2, except that the six-proton broad singlet at δ 3.55 in 2, is a three-proton singlet at δ 3.42 in 6. Assuming that 6 was simply the C-5 mono N-methyl form of 2, I attempted to transform 6 to 2 by methylation (Scheme 1). With MeI and NaNH_2 in liquid ammonia I was able to monomethylate 6 to give, as the major product (29% yield), a compound identical with 2 (UV, NMR, MS).

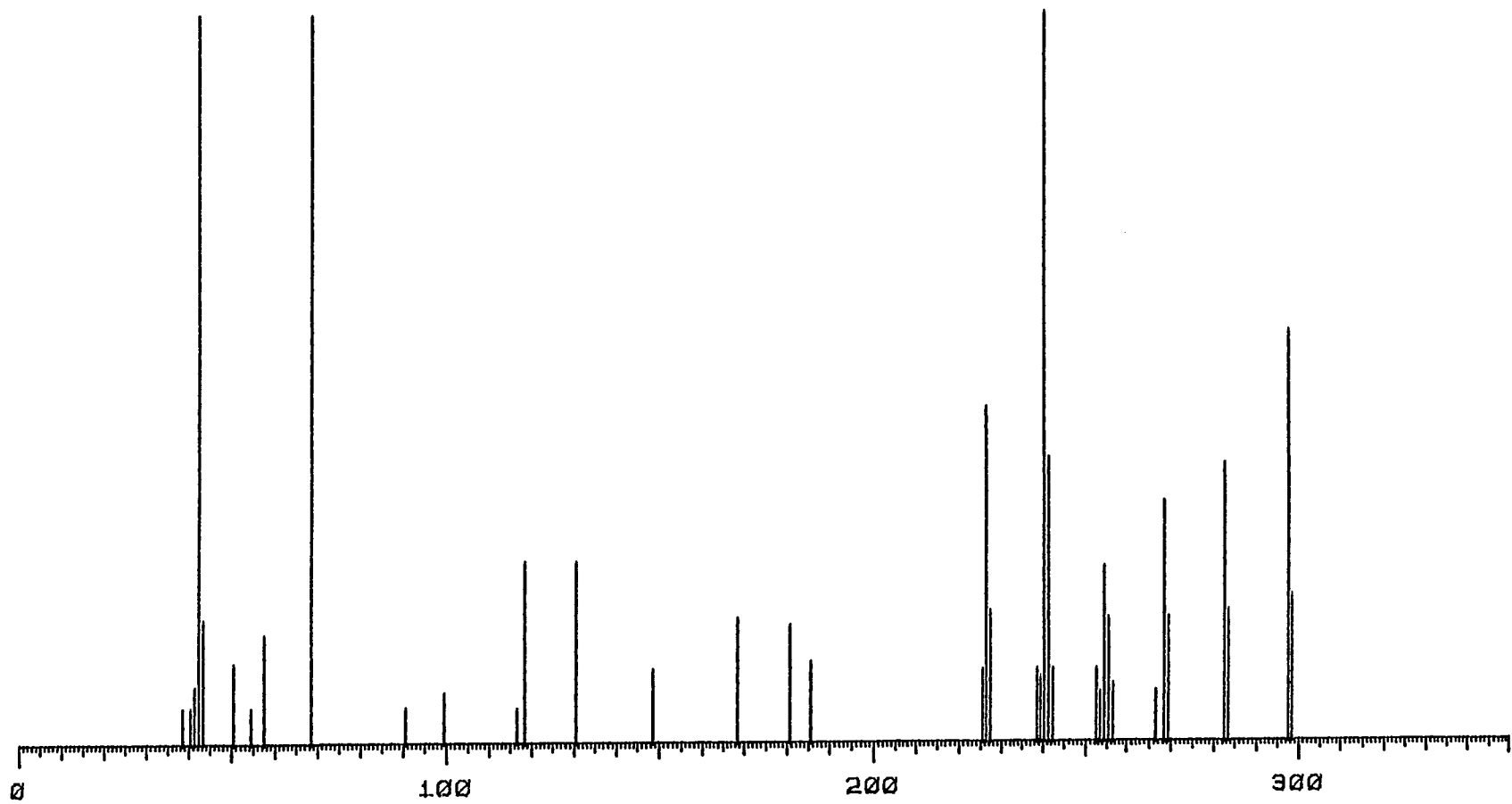
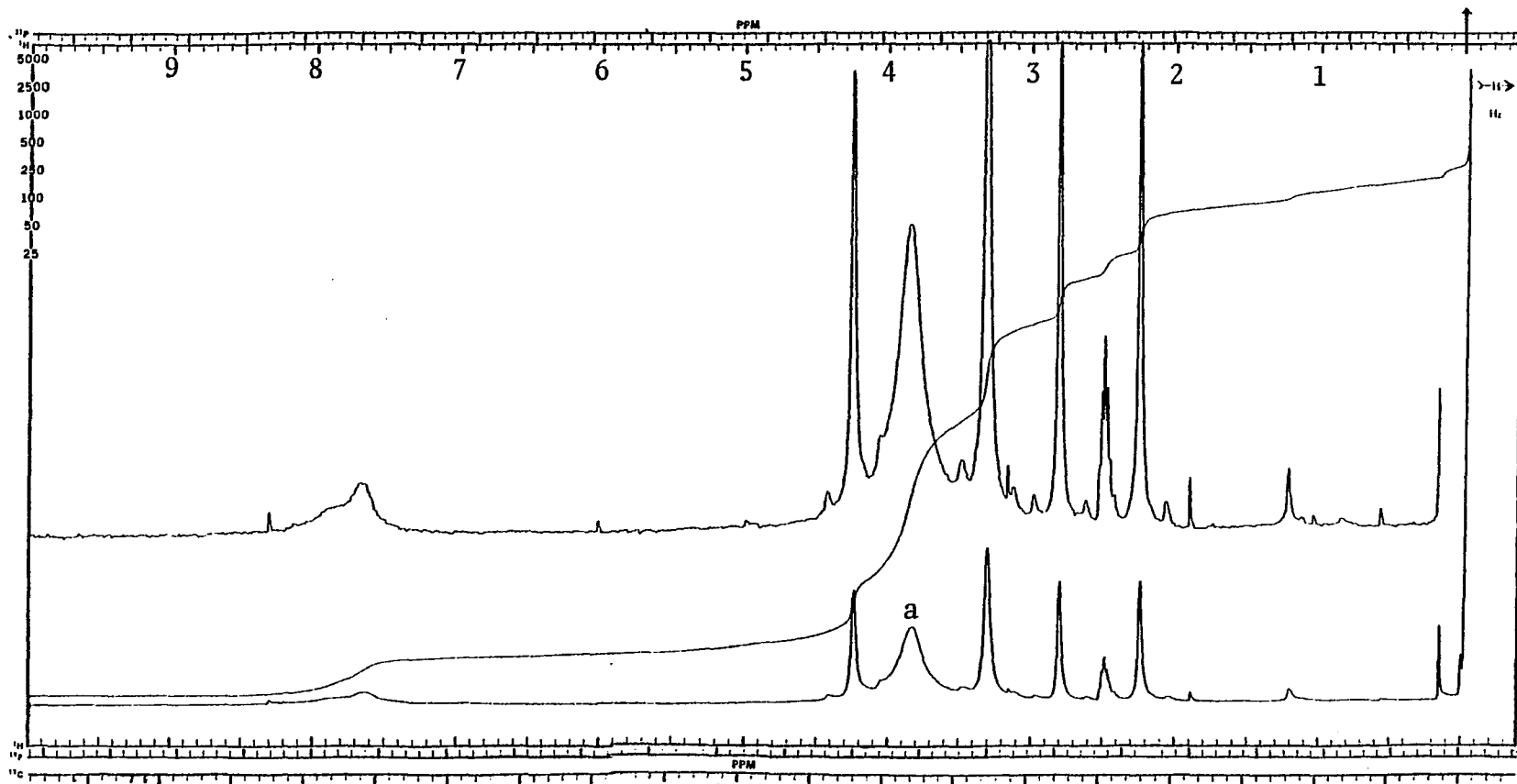


Figure 7. Mass spectrum of
2-acetamido-3-methyl-5-dimethylamino-3H-pseudozanthoxanthin (4).



$^a\text{H}_2\text{O}$

Figure 8. ^1H NMR spectrum of
2-acetamido-3-methyl-5-dimethylamino-3H-pseudozoanthoxanthin (4) in $\text{Me}_2\text{SO}-d_6$.



Figure 9. UV spectrum of
2-acetamino-3-methyl-5-dimethylamino-3H-pseudoanthoxanthin (4) in MeOH.

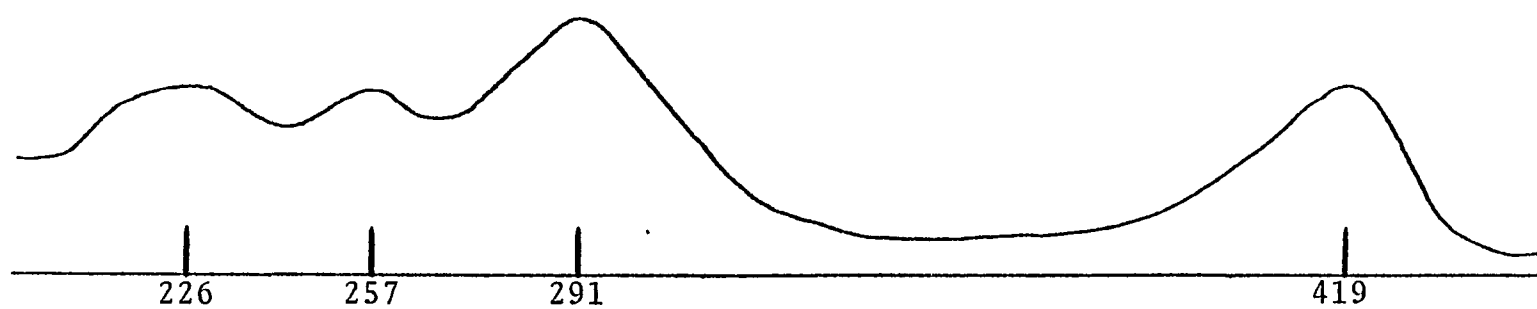


Figure 10. UV spectrum of
2-acetamino-3-methyl-5-dimethylamino-3H-pseudozoanthoxanthin (4) in MeOH₂⁺.

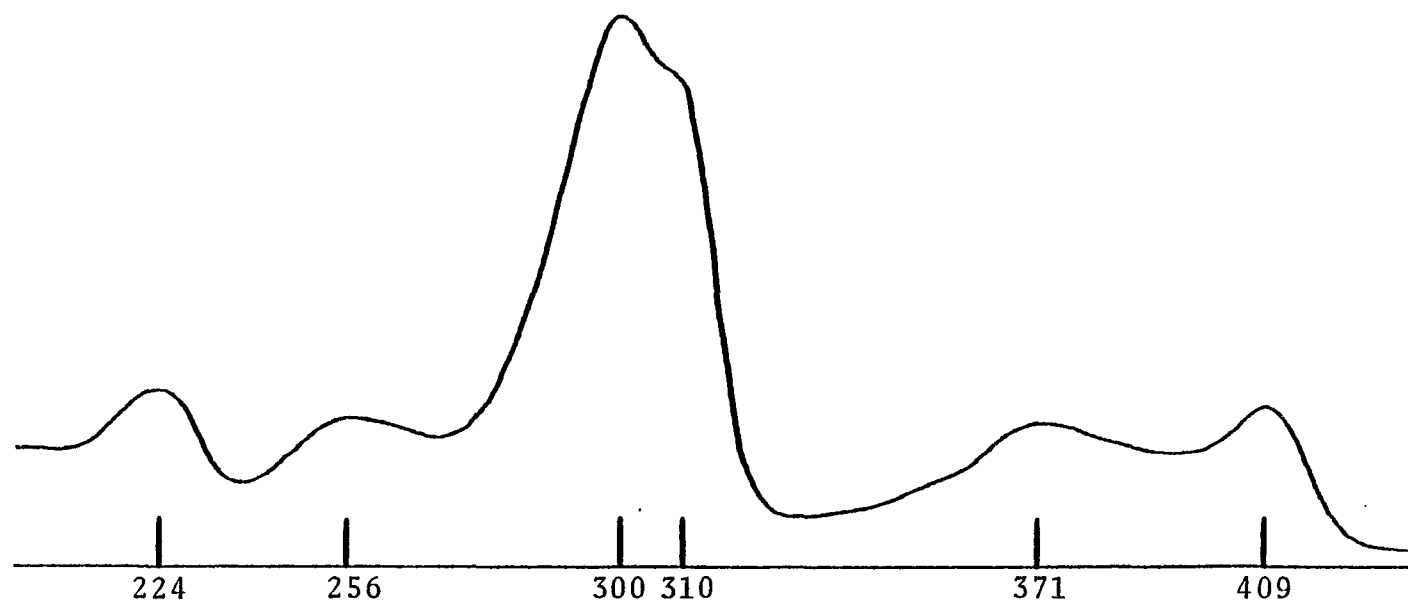


Figure 11. UV spectrum of
2-amino-3-methyl-5-methylamino-3H-pseudoanthoxanthin (6) in MeOH.

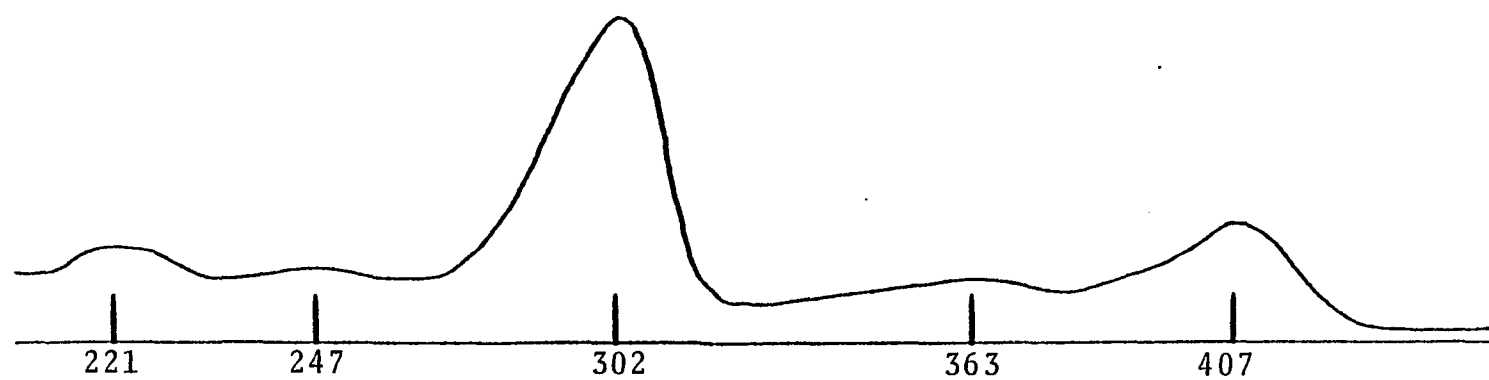


Figure 12. UV spectrum of
2-amino-3-methyl-5-methylamino-3H-pseudozoanthoxanthin (6) in MeOH₂⁺

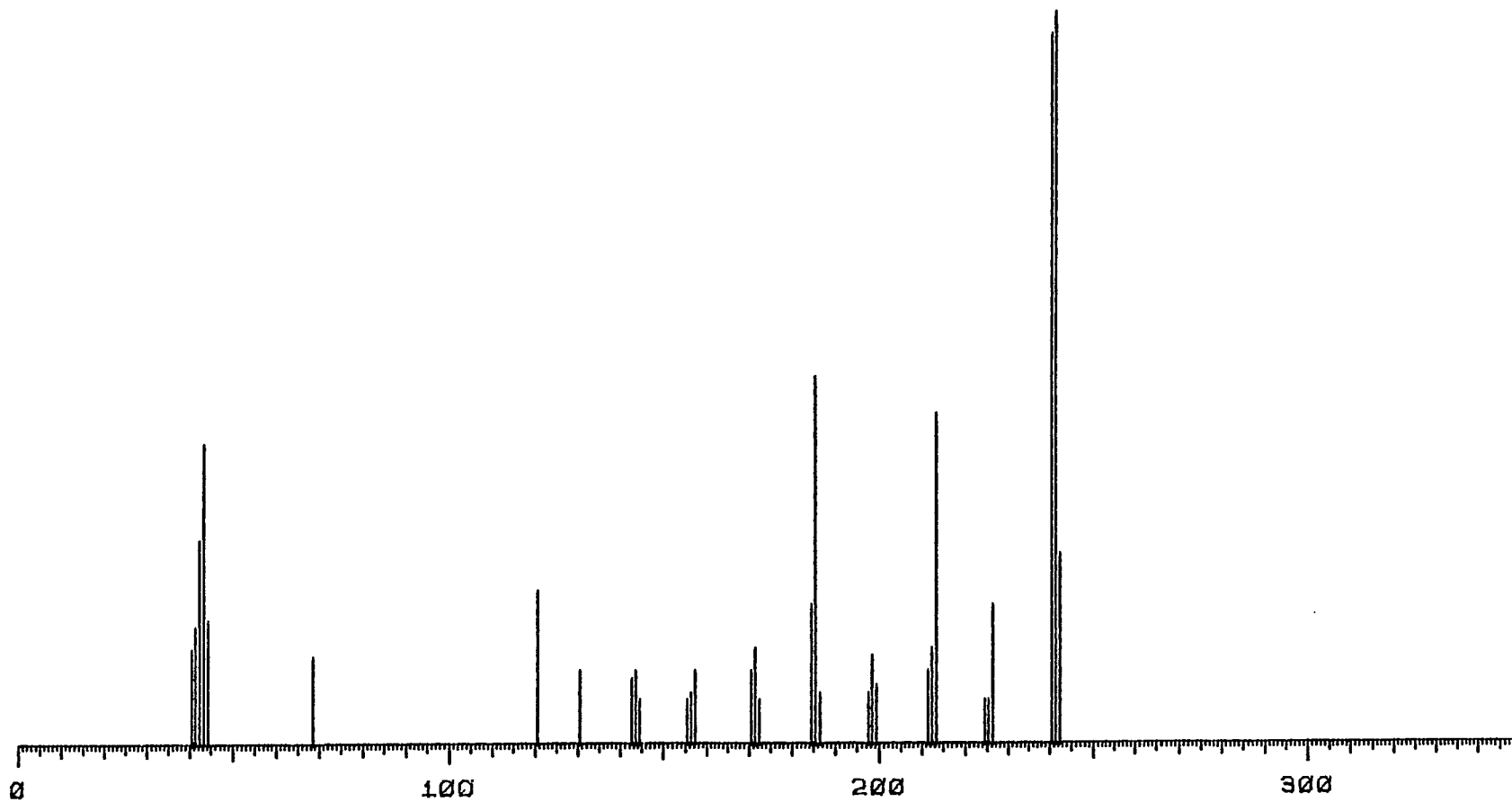
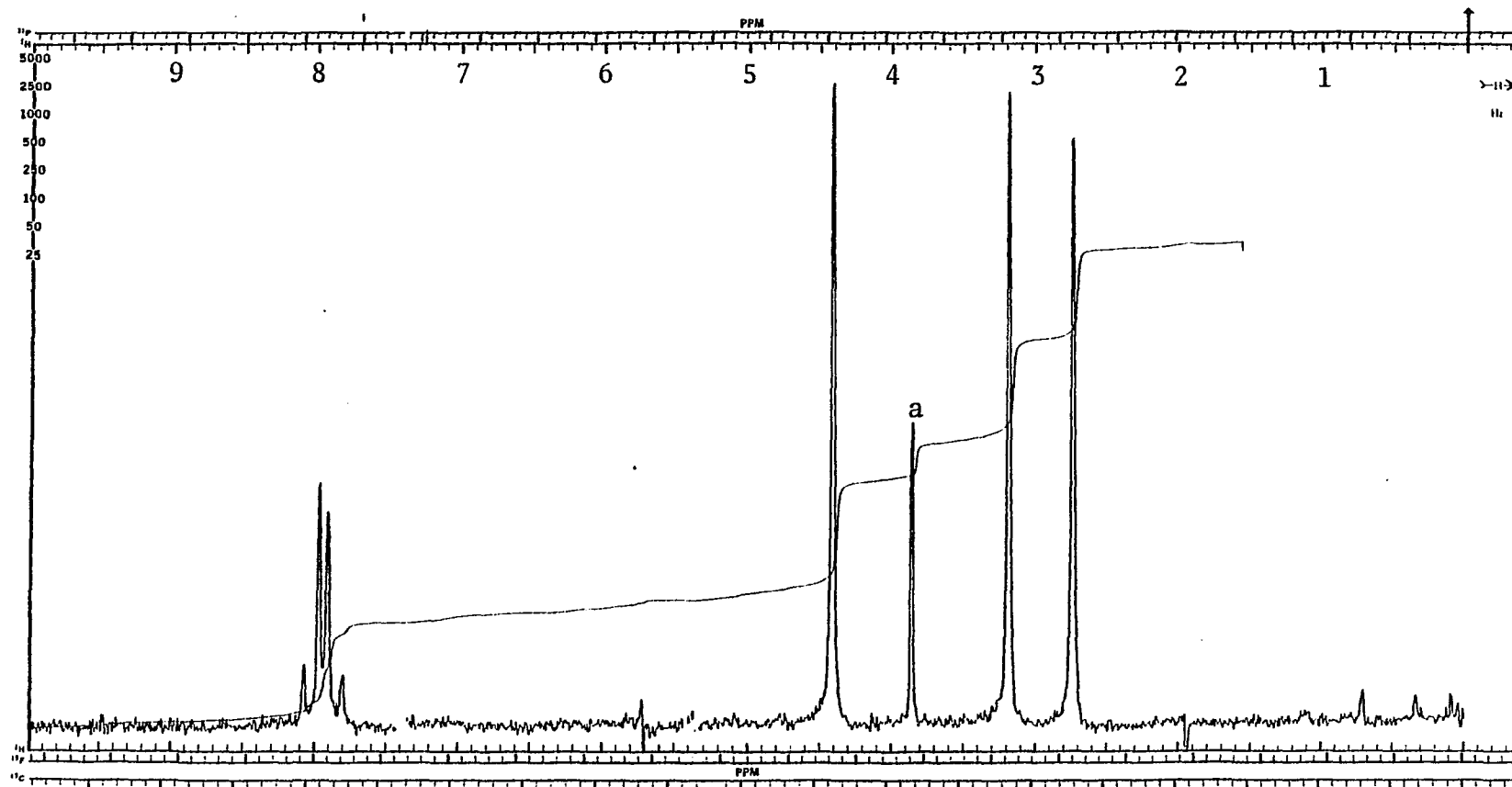
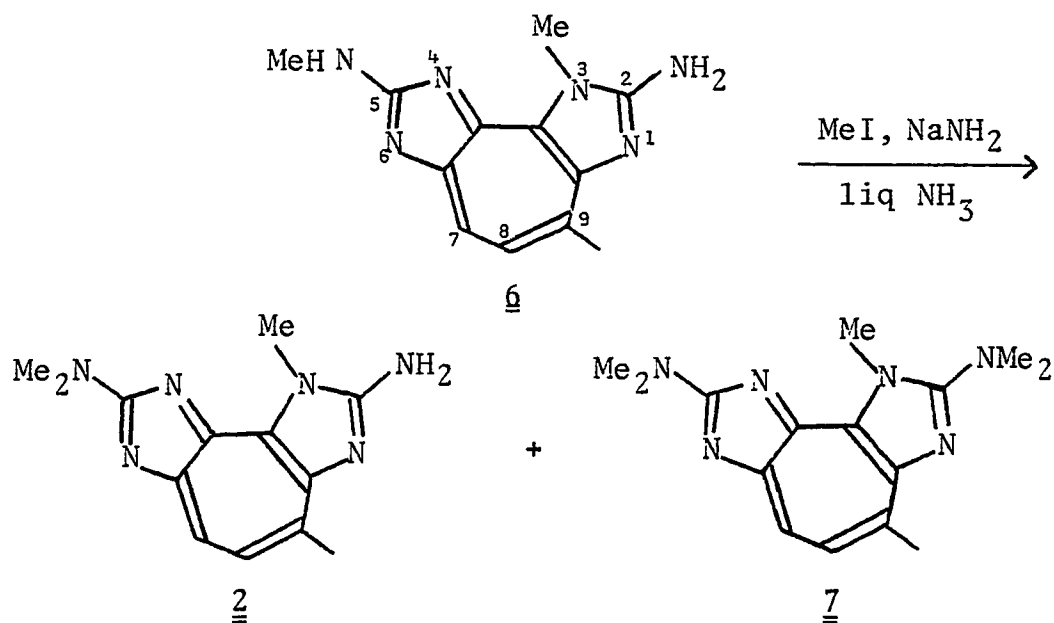


Figure 13. Mass spectrum of
2-amino-3-methyl-5-methylamino-3H-pseudozoanthoxanthin (6).



^a impurity

Figure 14. ^1H NMR spectrum of
2-amino-3-methyl-5-methylamino- 3H -pseudoanthoxanthin (6) in $\text{CF}_3\text{CO}_2\text{D}$.



Scheme 1

The fully N-methylated compound, 2,5-bisdimethylamino-3-methyl-3H-pseudoanthoxanthin (7), was also isolated (22% yield), as well as a third compound which was not characterized. The mass spectrum of compound 7 (Fig. 15) has a molecular ion at m/z 284, indicating a formula of $C_{15}H_{20}N_6$ via high-resolution mass measurement. The 1H NMR spectrum of 7 (CF_3CO_2D , Fig. 16, Table 2) illustrates the small but finite difference in the chemical shifts of the two sets of N,N-dimethyls. Because the molecule is not completely symmetric one group resonates at δ 3.62, the other at δ 3.54--a difference of only 0.08 ppm.

Transformation of 6 to 2 via methylation proves that the structure of 6 is 2-amino-3,9-dimethyl-5-methylamino-3H-1,3,4,6-tetraazacyclopent[e]azulene (Scheme 1).

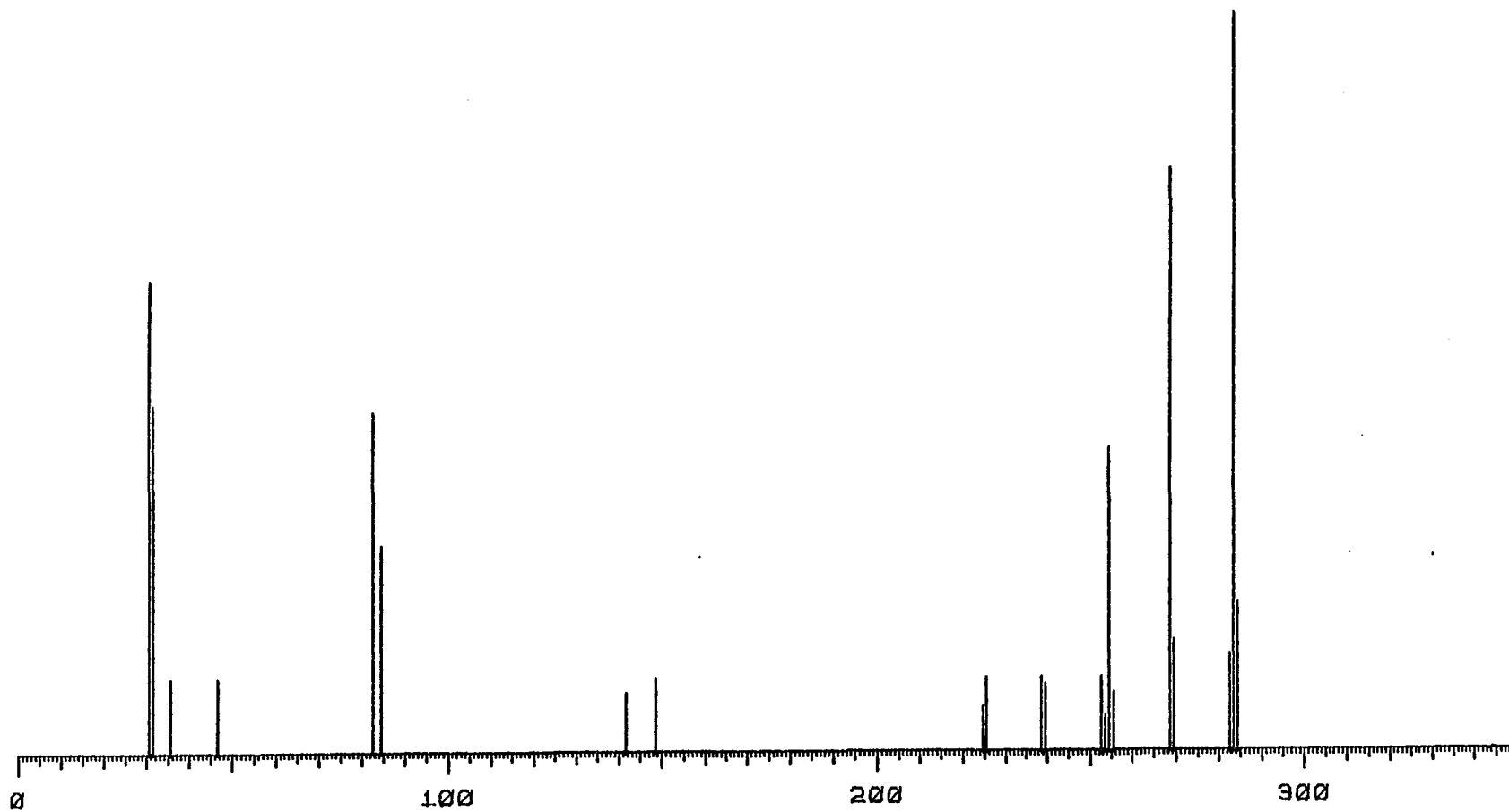


Figure 15. Mass spectrum of
2,5-bisdimethylamino-3-methyl-3H-pseudoanthoxanthin (7).

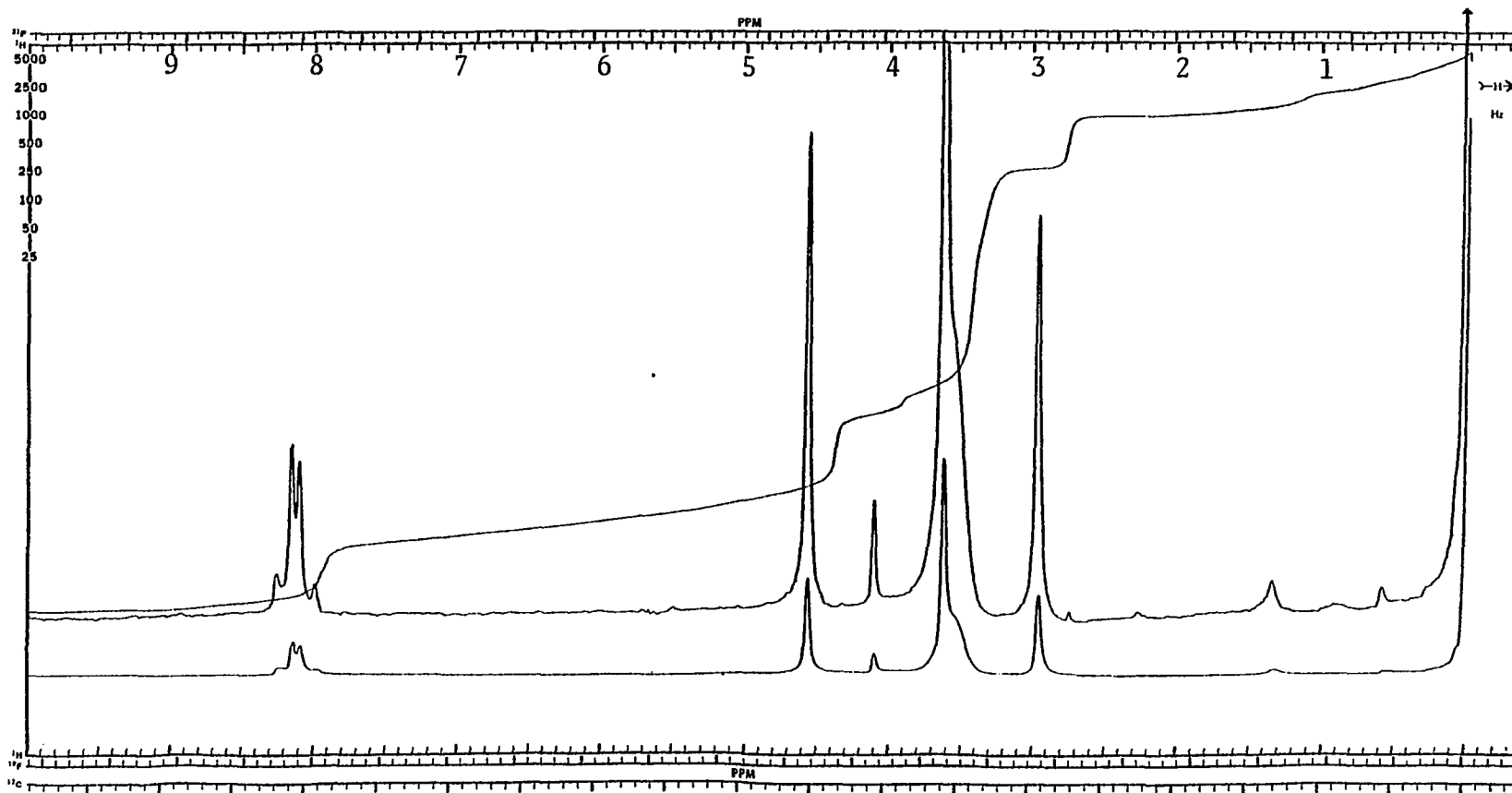


Figure 16. ^1H NMR spectrum of
 2,5-bisdimethylamino-3-methyl-3H-pseudoanthoxanthin (7) in $\text{CF}_3\text{CO}_2\text{D}$.

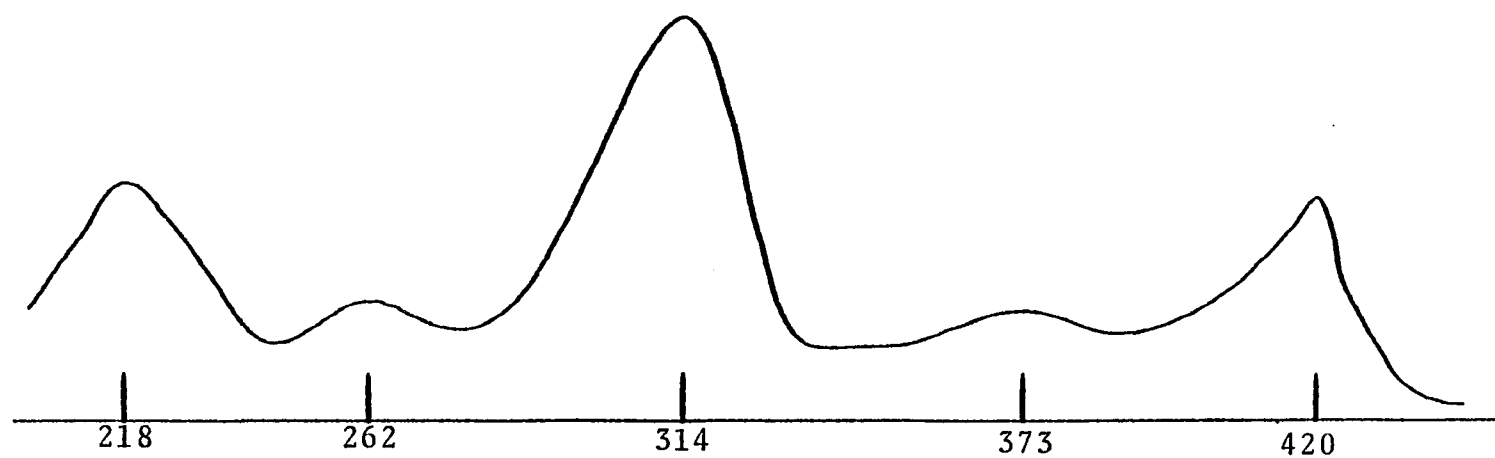


Figure 17. UV spectrum of
2,5-bisdimethylamino-3-methyl-3H-pseudoanthoxanthin (7) in MeOH.

C. Feeding Experiments with 2-Amino-3-methyl-5-dimethyl-
amino-3H-pseudozoanthoxanthin (2)

Samples of bread crumbs coated with different quantities of compound 2 were prepared, fed to fish, and their feeding behavior observed. Sample A was a control and contained no zoanthoxanthin. Sample B contained 0.5 mg of 2 per gram of bread; sample C contained 1 mg of 2 per gram of bread; sample D contained 1.5 mg of 2 per gram of bread; and sample E contained 2.5 mg of 2 per gram of bread.

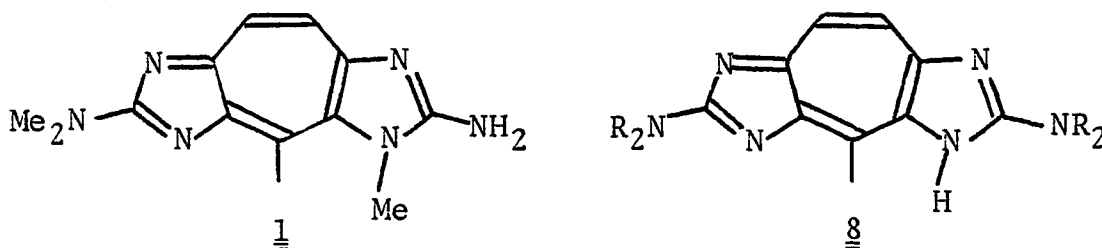
The results of the experiment are simple and clear. All samples (A-E) presented to the fish were eaten as rapidly as they left my hand; no inhibition of feeding was observed with any of the samples. This indicates that zoanthoxanthins, in quantities up to 2.5 mg, do not act as trophic toxins.

IV. RELATED RESEARCH BY OTHERS

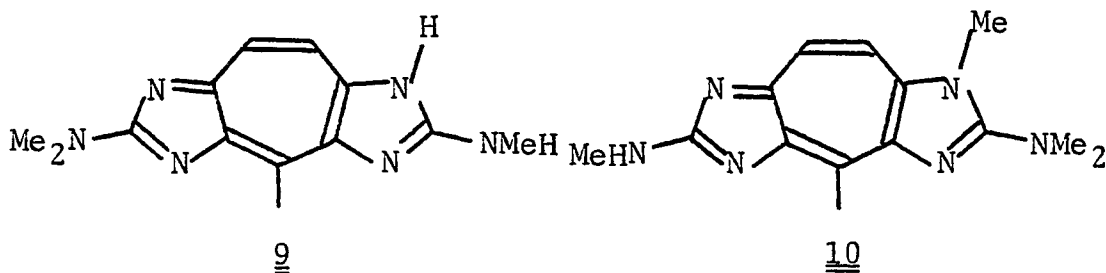
A. Previously Isolated Zoanthoxanthins and Their Nomenclature

Prota and coworkers are responsible for most of the available information on zoanthoxanthin chemistry. As stated previously, they first isolated zoanthoxanthin (1) in 1973 and determined its structure by single-crystal X-ray analysis of a monochloro derivative.^{11,12}

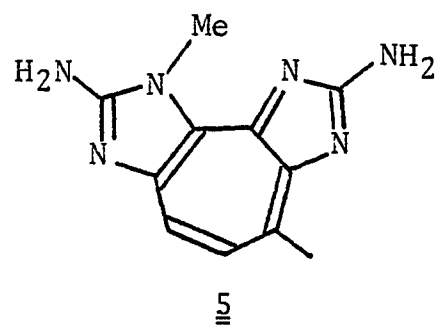
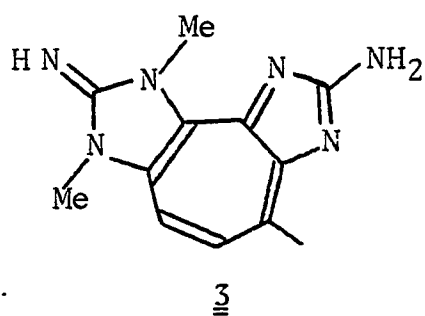
Parazoanthoxanthins (8, R = Me, H), also isolated by Prota



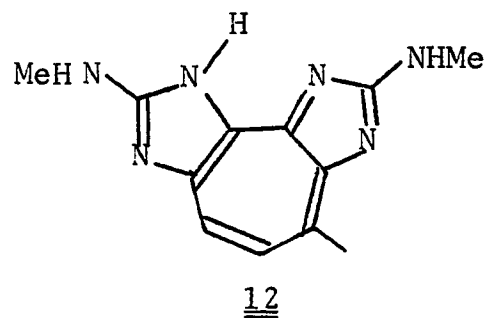
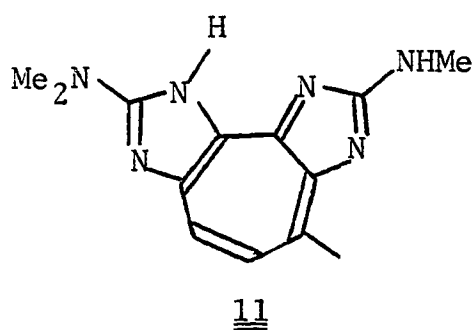
and coworkers, differ from zoanthoxanthin by the absence of the nuclear N-methyl.¹⁶ At about the same time, epizoanthoxanthin-A (9) and B (10) were isolated from what was thought



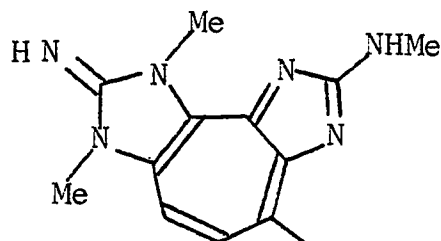
to be Epizoanthus arenaceus,¹³ but was later shown to be Parazoanthus axinellae.¹⁰ From this same organism pseudozoanthoxanthin (3) and norpseudozoanthoxanthin (5), the first examples of the angular zoanthoxanthin ring systems, were isolated.¹³



Komoda and coworkers later isolated two more angular zoanthoxanthins and, evidently unaware of the nomenclature introduced by the Italian researchers, named their compounds paragraccine (11) and norparagraccine (12).^{17,18}

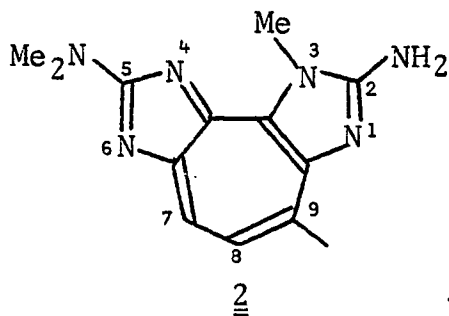
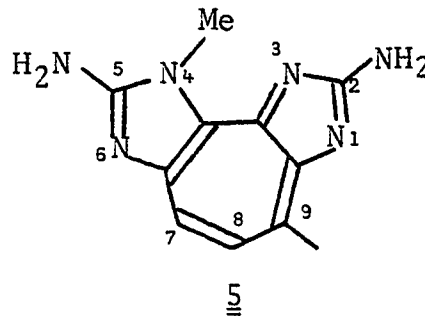


Finally, in 1979 Prota and coworkers reported the isolation of homopseudozoanthoxanthin (13), a minor constituent of Zoanthus sociatus and Palythoa sp.¹⁰

13

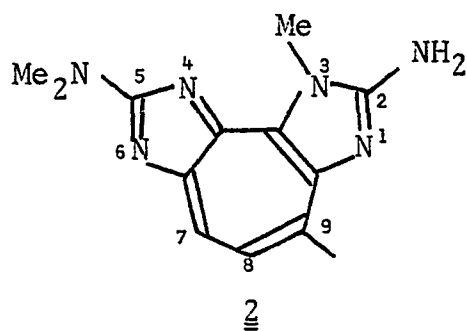
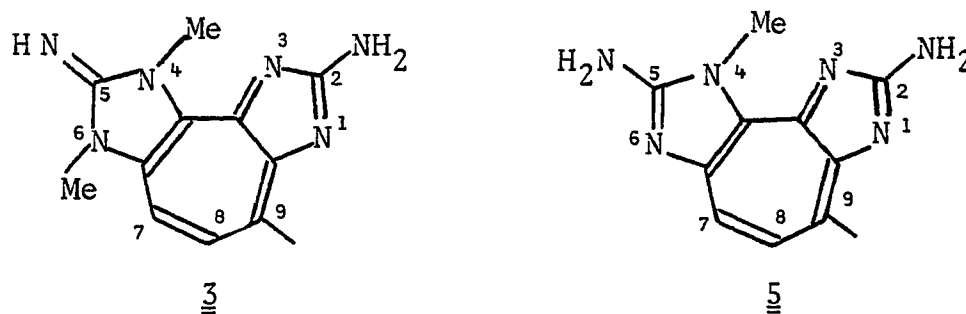
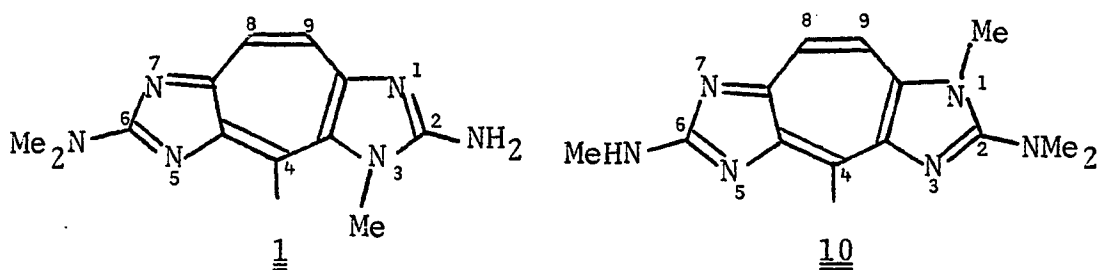
The IUPAC names for zanthoxanthins are long and complex. For example, compound 2 is 2-amino-3,9-dimethyl-5-dimethylamino-3H-1,3,4,6-tetrazacyclopent[e]azulene. These names render writing and discussion difficult. The trivial nomenclature, which has evolved from the work of the Italian and Japanese researchers, is inconsistent and confusing, as it is based on methylation patterns and/or the generic source. Prota and coworkers even stated in their latest zanthoxanthin publication that they are "awaiting a more rational nomenclature for all the members of the zanthoxanthin class."¹⁰

If one compares 2 with norpseudozanthoxanthin (5), one sees that the major structural difference is the relationship between the C-methyl on C-9 and the nuclear N-methyl on N-3 or

25

N-4. I have suggested that this critical relationship be made the basis of a more logical trivial nomenclature.¹⁵

I propose to call the linear system zoanthoxanthin (1, 10) and the angular system pseudozoanthoxanthin (2, 3, 5) and to number the rings so that the C-methyl in zoanthoxanthin is always at C-4 and in pseudozoanthoxanthin at C-9.

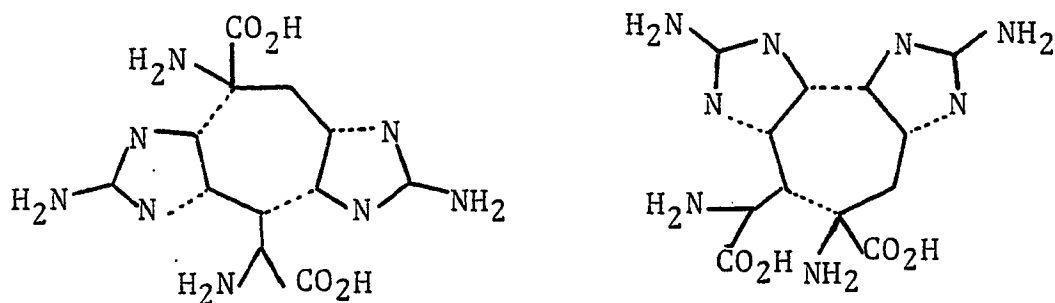


The position number of the saturated nuclear nitrogen followed by an H will then distinguish between the major

groups of zoanthoxanthins. For example, 1 becomes a 3H-zoanthoxanthin, 10 a 1H-zoanthoxanthin, 5 a 4H-pseudozoanthoxanthin, 3 a 4H,6H-pseudozoanthoxanthin, and 2 a 3H-pseudozoanthoxanthin.

B. Biogenesis of Zoanthoxanthins

Prota and coworkers postulated that zoanthoxanthins arise biogenetically from two arginine-derived C_5N_3 units,



as depicted in these two formulas. Subsequent methylation generates various zoanthoxanthins.¹⁶ Although no labelling studies have been carried out, the structures of all zoanthoxanthins isolated so far are consistent with this hypothesis. Since 3H-pseudozoanthoxanthins are identical to 4H-pseudozoanthoxanthins prior to methylation, it seems reasonable that compounds 2 and 6, from Gerardia sp., are also biosynthesized via arginine coupling.

There are no symbiotic zooxanthellae associated with Gerardia sp., as one would expect for a coral that grows in the darkness found 350 m below the surface. The only possible sources of these zoanthoxanthins, therefore, are the diet or through in vivo coupling of amino acids. It

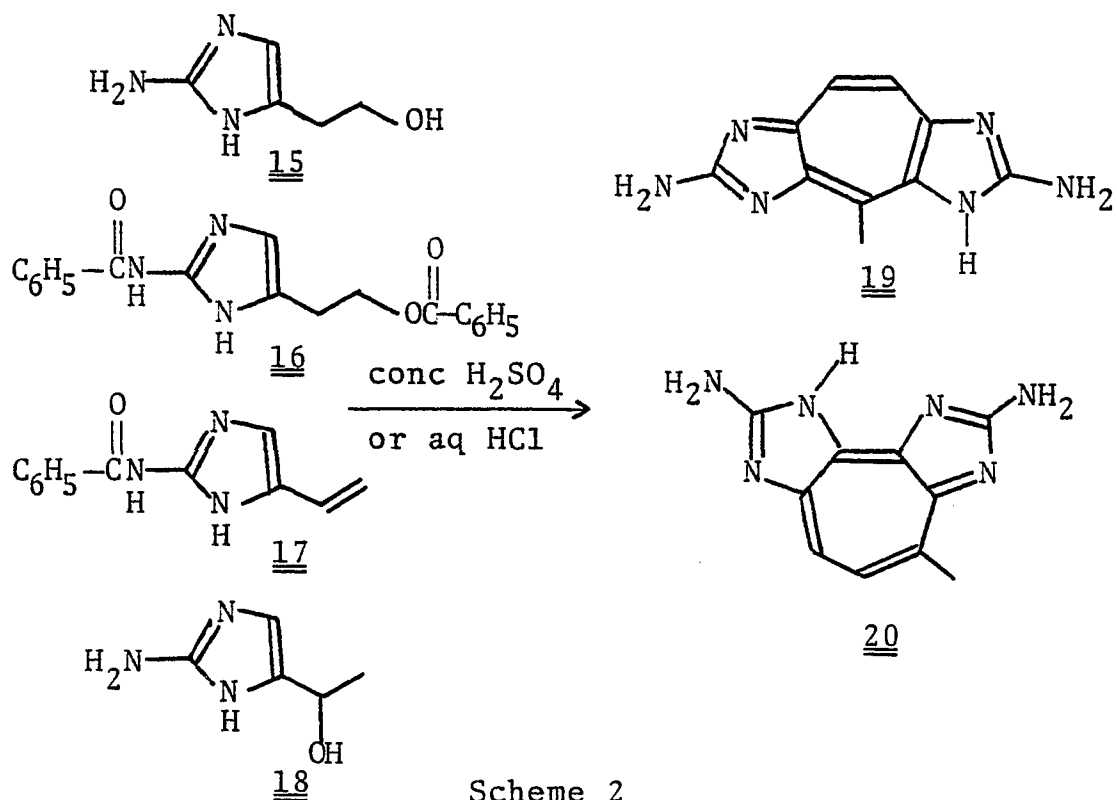
seems improbable that this organism would be capable of concentrating such large amounts (≈ 3 g/kg endoskeleton and polyps) of zoanthoxanthins from its diet. Moreover, possible dietary sources with significant amounts of these pigments have never been discovered, though a number of other organisms have been investigated. Organisms that have been examined include species from the phyla Cnidaria (22 species), Ctenophora (3 species), Tentacula (2 species), Mollusca (16 species), Annelida (7 species), Arthropoda (1 species), and Echinodermata (13 species).¹⁰ It is likely, therefore, that ^3H -pseudozoanthoxanthins are biogenetically derived from the coupling of amino acids by the coral Gerardia sp.

On the other hand, zoanthoxanthins were found in minute quantities in the genera Epizoanthus (1 species), Zoanthus (2 species), and Palythoa (3 species)--all belonging to the order Zoanthidea. A survey by Prota and coworkers indicates that Parazoanthus is the only genus which produces significant amounts of these compounds. The type and amounts of zoanthoxanthins found in these three genera may be useful chemotaxonomic markers.¹⁰ Such an approach to taxonomy should be used with caution, however, since I have observed trace amounts of $\underline{2}$ in almost every deep-sea organism which I have examined, including an unidentified sponge, bamboo coral (Lepidisis olapa), Narella sp., and smoky gold coral (Callogorgia sp.) (see Preface). I believe that, during or after collection, these organisms came into contact with

Gerardia sp. Even extremely small amounts of contamination are detectable because of the strong UV absorbance of these pigments. In fact, they are difficult to miss. Since I had no control over collecting procedures at Maui Divers, Inc., I have never been able to confirm that the presence of zoanthoxanthins in organisms other than Gerardia sp. is due to contamination.

C. Synthesis of Zoanthoxanthins

Büchi and coworkers have developed biomimetic syntheses of the zoanthoxanthin and pseudozoanthoxanthin ring systems based on the dimerization of a variety of suitably functionalized C_5N_3 units (15-18). By starting with the correct

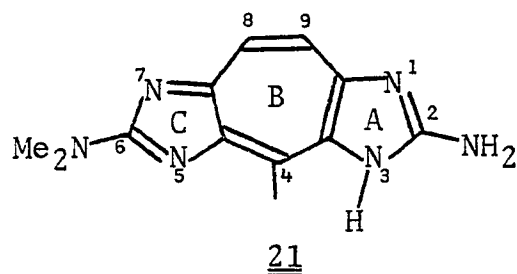


Scheme 2

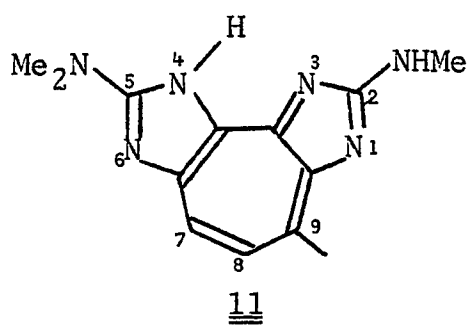
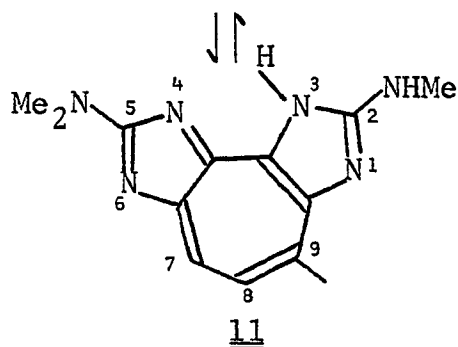
C_5N_3 unit and choosing the appropriate acid for the oxidative dimerization, either concentrated sulfuric acid or aqueous hydrochloric acid, they selectively synthesized the zoanthoxanthin (19) or pseudozoanthoxanthin (20) skeleton as illustrated in Scheme 2.^{19,20}

The synthetic work of Büchi and coworkers is complemented by the research of Prota and coworkers on the methylation of zoanthoxanthins. This is a crucial piece of work, in which Prota's group described the selective methylation of different zoanthoxanthins. They developed methods which they used to prove the structures of many trace zoanthoxanthins through transformations to or from known compounds. These methods can also be used to methylate 19 and 20 to produce specific zoanthoxanthins. Their research indicates that under neutral (dimethyl sulphoxide and methyl iodide) or acidic (boron trifluoride etherate and diazomethane) conditions methylation occurs at one of the nuclear N-methyls; however, under basic conditions (sodium azide and methyl iodide in liquid ammonia), methylation takes place exclusively at the amino nitrogen.²¹

Some insight into the aromaticity of the zoanthoxanthin ring system was also gained as a result of this research. Regardless of the alkylating conditions utilized on 21, methylation only occurs on the nitrogens of ring A. This suggested to Prota and coworkers that rings B and C form a fully aromatic diazazulene, with tautomerism of the imino proton limited to N-1 and N-3.²¹



The single-crystal X-ray structure of paragraccine (11), on the other hand, indicates that N-3 and N-4 share one hydrogen atom in the ratio 1:2.¹⁸ This implies that


 $\frac{2}{3}$

 $\frac{1}{3}$

paragraccine tautomerizes as shown above. The differences in aromaticity observed between 21 and 11 are most likely due to the fact that 21 is a linear zoanthoxanthin, while 11 is an angular pseudozoanthoxanthin.

D. Biological Activity of Zoanthoxanthins

Paragraine (11) may be a desirable synthetic target since Komoda and coworkers reported that it possesses a variety of physiological activities. These activities include anti-BaCl₂, anti-histamine, anti-bradykinin, anti-acetylcholine, and anti-adrenalin activities on the contraction of a number of isolated smooth muscles. It is also reported to decrease the pulse rate of isolated rabbit atria.¹⁸

Similar activity has never been reported for other zoanthoxanthins, though perhaps they have not been tested. I attempted to test for the presence of biological activity in compound 2, but it was not sufficiently soluble, even as its dihydrochloride salt, for such tests. Perhaps the Japanese researchers have discovered a better method of solubilizing these compounds, although it has never been mentioned in the literature.

V. CONCLUSION

The chemistry of zoanthoxanthins is fairly well understood at the present time. A variety of zoanthoxanthins have been isolated and their structures elucidated.¹⁰⁻¹⁸ A reasonable biogenetic scheme has been proposed,¹⁶ although it remains to be confirmed by experimentation. And a scheme for the total synthesis of these pigments has been devised.¹⁹⁻²¹

The function of the zoanthoxanthins, however, remains a mystery. They apparently are not antifeedants. Perhaps these compounds are necessary for the zoanthid to defend itself against its host. Alternately, they may be involved in bioluminescence, with their unusual light absorbing and emitting properties. Perhaps they are simply nontoxic byproducts of some biochemical reaction, which accumulate in this organism. These questions, of course, can only be answered by further experimentation.

PART TWO

CONSTITUENTS OF
CORALLIUM SP.

I. INTRODUCTION

Gorgonians are anthozoans belonging to the subclass Alcyonacea (see Preface). Of the 94 species of gorgonians found in Hawaiian waters, only one shallow-water (0 to ~ 75 m) species (Acabaria bicolor) is known. This is in sharp contrast to both the West Indies and the East Indies where more than 40 percent of the gorgonian species are found at depths of less than 50 m.³

One explanation for this unusual distribution involves the geographic isolation of the Hawaiian Islands. During the early Tertiary period there were many shallow-water stepping stones across the Pacific, which could be used by both shallow and deep-water gorgonians for migration. However, it is believed that the Hawaiian Islands did not appear until the middle Tertiary, so that perhaps there was no habitat available for the shallow-water organisms when they arrived.³ This, of course, does not explain how other shallow-water corals migrated to the Hawaiian Islands.

Pink coral is a gorgonian belonging to the family Coralliidae, and the genus Corallium.^{*} Corallium sp. has a pink endoskeleton, yellow and orange polyps, and is fan-shaped with a thick base and many branches. This species is found

*This species of pink coral was previously identified as Corallium secundum; however, Katherine Muzik at the United States National Museum feels that it is a new species. I will, therefore, refer to it as Corallium sp.

approximately 350 m below the surface in the Molokai Channel off Makapuu Point, Oahu.

Most gorgonians differ from soft corals (alcyonaceans) by a rigid endoskeleton made of a horn-like, proteinaceous substance called gorgonin.⁷ In the genus Corallium, however, gorgonin is absent and is replaced by a solid axis of calcareous spicules and organic polymer, usually red or pink in color. This hard, colored endoskeleton is the coral of jewelry.⁷ Hawaii is known for its extremely light-colored pink coral, which is referred to in the jewelry industry as "angel skin."

Man's penchant for precious corals dates back to the Paleolithic period about 25,000 years ago. Pieces of pink coral were found, along with other Paleolithic artifacts, in an archeological excavation in Germany. Pink coral was later collected by skin divers in the shallow grottoes of the Mediterranean. Eventually the Arabs invented a device called an ingegno. An ingegno is a cross that is covered with rope mops which, when dragged over the ocean floor, breaks off and entangles coral trees and everything else in its path.²²

In Hawaii, pink coral (Corallium sp.) is collected commercially for the production of jewelry by Maui Divers, Inc. Using the minisubmersible Star II the pilot, Boh Bartko, can be selective about the colonies of pink coral which he collects.

In coral industries elsewhere a general pattern developed--exploration followed by discovery, exploitation, and depletion. The Hawaiian pink coral industry, however, practices two forms of conservation as outlined by coral ecologist Richard Grigg. The first is a minimum size of 30 cm, which allows for a long period (>10 years) of sexual maturity. The second form of conservation is an annual harvest limit of 1000 kg (approximately 4% of the standing crop), which takes into consideration the replacement rate of pink coral.²³

One of the benefits of the development of this industry is the opportunity for scientists, such as Richard Grigg and Katherine Muzik, to investigate deep-sea organisms in their natural habitats. Although I have never observed these organisms in their deep-sea environment, I was provided with specimens of pink coral. I will discuss the constituents of pink coral in Part Two of this Dissertation.

II. EXPERIMENTAL

A. Apparatus, Methods and Materials

Natural abundance ^{13}C NMR spectra were recorded on a Varian XL-100 Fourier transform spectrometer at 25.2 MHz. The deuterium signal of CDCl_3 provided field/frequency locking. Proton NMR spectra were recorded on a Varian XL-100 NMR spectrometer at 100 MHz; field/frequency locking was provided by the deuterium signals of CDCl_3 and C_6D_6 . Two hundred twenty MHz ^1H NMR spectra were obtained on a Varian HR 220 NMR spectrometer; TMS was used as an internal reference. Three hundred sixty MHz ^1H NMR spectra were recorded on a Nicolet NTC 360 NMR spectrometer; field/frequency locking was provided by the deuterium signals of CDCl_3 and C_6D_6 . The ^1H NMR spectra of many compounds contain signals which appear to be triplets but are due to coupling with two nonequivalent protons and, therefore, are referred to as doublets of doublets (dd).

Mass spectra were determined on a Varian MAT 311 high resolution mass spectrometer at an ionizing voltage of 70 eV. To eliminate impurity peaks from H_2O ($\underline{m/z}$ 18) and N_2 ($\underline{m/z}$ 28), fragments with masses less than $\underline{m/z}$ 35 were not included in the mass spectral reproductions. Field desorption mass spectra were obtained using a Varian MAT 731 high resolution mass spectrometer equipped with a field desorption ion source.

Infrared spectra were recorded on a Perkin-Elmer 467 grating infrared spectrophotometer. A Beckman ACTA III

spectrophotometer was used for the UV spectra. Optical rotations were obtained on an ETL-NPL type 143A automatic polarimeter.

Melting points were taken on a Fisher-Johns apparatus. New England Nuclear silica gel OF 250 μ plates were used for all TLC's.

Many separations were performed on a Waters Associates HPLC system consisting of an M-6000 solvent delivery system, a U6K injector, an R401 differential refractometer, a 440 absorbance detector, and a Varian 9176 recorder. A Whatman Partisil PXS 10 μ , 25 cm column or a Whatman Partisil M9 10 μ , 25 cm column was used for all separations requiring HPLC. Waters Associates silica gel Sep-Paks were often used for preliminary clean-up of mixtures to be separated by HPLC.

B. Isolation

Seven hundred sixty gram of freshly collected pink coral (Corallium sp.) was stepped in MeOH 3X. This extract was filtered, concentrated, and partitioned between CH_2Cl_2 and water; the aqueous extract was discarded.

The CH_2Cl_2 layer (\approx 2.2 g) was chromatographed on Bio-Sil A using CH_2Cl_2 as the eluent. Final purification of most compounds was accomplished by HPLC with 10 μ Partisil as the adsorbent and the eluents as indicated for each particular compound.

C Coraxeniolide-A (22)

Coraxeniolide-A (22) was purified by HPLC with CH_2Cl_2 as the eluent; approximately 500 mg of 22 was present in the CH_2Cl_2 extract. Compound 22 forms white, plate-like crystals upon concentration, mp 88-91°C, R_f 0.38, CH_2Cl_2 , and chars red with H_2SO_4 /vanillin; $\text{C}_{20}\text{H}_{30}\text{O}_2$ (calcd 302.224 586; found 302.224 28), $\text{C}_{14}\text{H}_{20}\text{O}_2$ (calcd 220.146 334; found 220.142 98) m/z 302 (57%, M^+), 259 (13, $\text{M}^+ - \text{C}_3\text{H}_7$), 220 (72, $\text{M}^+ - \text{C}_6\text{H}_{10}$), 219 (57, $\text{M}^+ - \text{C}_6\text{H}_{11}$) (Fig. 20). ^{13}C NMR: (CDCl_3) 175.16 (s), 153.06 (s), 140.73 (d), 139.97 (s), 124.00 (d), 123.47 (d), 112.20 (t), 70.80 (t), 49.93 (d), 44.39 (d), 42.98 (d), 39.89 (t), 35.84 (t), 31.35 (d), 30.03 (t), 25.28 (t), 22.90 (q), 22.90 (q), 16.73 (q) ppm. ^1H NMR: (220 MHz, CDCl_3 , Fig. 19) 5.50 1H dd ($J = 15$ Hz, $J = 6$ Hz), 5.36 2H m, 4.98 2H s, 4.19 1H dd ($J = 12$ Hz, $J = 7$ Hz), 3.93 1H dd ($J = 12$ Hz, $J = 12$ Hz), 2.80 1H m, 1.70 3H bs, 1.00 6H d ($J = 7$ Hz) ppm; (100 MHz, C_6D_6) 5.58-5.12 3H m, 4.66 1H s, 3.82 1H dd ($J = 12$ Hz, $J = 7$ Hz), 3.48 1H dd ($J = 12$ Hz, $J = 12$ Hz), 1.41 3H d ($J = 1.5$ Hz), 0.97 6H d ($J = 7$ Hz) ppm. Decoupling: (220 MHz, CDCl_3) irr 4.19 1H dd, 3.93 1H dd-d; irr 3.93 1H dd, 4.19 1H dd-d. UV: (MeOH) end absorption. IR: (CH_2Cl_2 , Fig. 18) 1748 (lactone C=O), 1640 (C=C), 1391 (CMe_2), 898 ($\text{C}=\text{CH}_2$) cm^{-1} . $[\alpha]_D^{25} + 82^\circ$ (c 0.95, CHCl_3).

D. Hexacoraxeniolide-A (23) and Hexacoraxeniolide-A' (24)
(from 22)

Twenty-three milligram of 22 were dissolved in MeOH and stirred overnight with 10% Pd/C in an H₂ atmosphere. The reaction mixture was filtered, concentrated, and chromatographed by HPLC (CH₂Cl₂) to give 19 mg of an inseparable mixture of 23 and 24. This mixture is a colorless oil, R_f 0.42 (single spot), CH₂Cl₂, and chars red with H₂SO₄/vanillin; C₂₀H₃₆O₂ (calcd 308.271 537; found 308.270 16) m/z 308 (9%, M⁺), 224 (100, M⁺-C₆H₁₂) (Fig. 22). ¹³C NMR: (CDCl₃, Fig. 21) 176.22, 175.78, 69.57, 68.87 ppm and a large number of overlapping aliphatic carbons. ¹H NMR: (360 MHz, CDCl₃, Fig. 23) 4.20-4.05 m, 2.50-2.37 m, 2.13-2.04 m, 0.95-0.82 8 3H d (J = 8 Hz) ppm (for an expansion of the methyl region see Fig. 24). UV: (MeOH) end absorption. IR: (CH₂Cl₂, Fig. 25) 1741 cm⁻¹ (lactone C=O), no C=C stretch in the region 1550-1650 cm⁻¹.

E. Coraxendiol-A (25 from 22)

Eighteen milligram of 22 was reduced with LiAlH₄ in anhydrous Et₂O in an argon atmosphere. The reaction mixture was filtered, concentrated, and chromatographed by HPLC with EtOAc/CH₂Cl₂ (7:3) as the eluent to give 4.5 mg of 25. Coraxendiol-A (25) is a colorless oil, R_f 0.39, EtOAc, and chars red with H₂SO₄/vanillin; C₂₀H₃₄O₂, C₂₀H₃₂O (calcd 288.245 321; found 288.248 66) m/z 306 (1%, M⁺),

288 (7, $M^+ - H_2O$), 257 (33, $M^+ - H_2O, CH_2OH$) (Fig. 26). 1H NMR: (360 MHz, C_6D_6 , Fig. 27) 5.40 1H dd ($J = 15$ Hz, $J = 6$ Hz), 5.32-5.27 2H m, 4.73 1H ms, 4.72 1H ms, 3.65 1H dd ($J = 11$ Hz, $J = 6$ Hz), 3.50 1H dd ($J = 11$ Hz, $J = 6$ Hz), 3.29 1H dd ($J = 11$ Hz, $J = 7$ Hz), 3.24 ($J = 11$ Hz, $J = 7$ Hz), 1.51 3H s, 0.96 3H d ($J = 7$ Hz) ppm. UV: (MeOH) end absorption.

F. Coraxeniolide-B (26)

Approximately 250 mg of 26 was isolated from the crude extract by HPLC with CH_2Cl_2 as the eluent. Although coraxeniolide-B (26) is chromatographically similar to coraxeniolide-C' (38), 26 was obtained with purity greater than 99%. Coraxeniolide-B (26) is a colorless oil, R_f 0.28, CH_2Cl_2 , and chars blue with H_2SO_4 /vanillin; $C_{20}H_{28}O_2$ (calcd 300.208 936; found 300.210 33) m/z 300 (20%, M^+), 257 (40, $M^+ - C_3H_7$) (Fig. 34). ^{13}C NMR: ($CDCl_3$) 171.38 (s), 151.74 (s), 151.38 (d), 138.26 (d), 137.03 (s), 131.31 (s), 124.70 (d), 121.09 (d), 113.52 (t), 71.07 (dd) (Fig. 29), 49.76 (d), 43.59 (d), 40.69 (t), 38.31 (t), 34.70 (t), 32.14 (d), 25.28 (q), 22.28 (q), 16.73 (q) ppm. 1H NMR: (100 MHz, $CDCl_3$, Fig. 33, Table 3) 6.86 1H d ($J = 10$ Hz), 6.40-6.04 2H m, 5.38 1H m, 4.94 1H s, 4.82 1H s, 4.05 1H dd ($J = 12$ Hz, $J = 6$ Hz), 3.54 1H dd ($J = 12$ Hz, $J = 12$ Hz), 3.00 1H m, 1.69 3H d ($J = 1$ Hz), 1.04 6H d ($J = 7$ Hz) ppm; (100 MHz, C_6D_6 , Fig. 32, Table 3) 7.16 1H d ($J = 12$ Hz), 6.38 1H bdd ($J = 15$ Hz, $J = 12$ Hz), 5.84 1H dd ($J = 15$ Hz, $J = 8$ Hz),

5.37 1H m, 4.71 2H s, 3.88 1H dd (J = 12 Hz, J = 6 Hz),
 3.46 1H dd (J = 12 Hz, J = 12 Hz), 3.05 1H m, 1.46 3H d
 (J = 1.5 Hz), 0.91 6H d (J = 6 Hz) ppm. Decoupling:
 (100 MHz, C₆D₆) irr 7.16 1H d, 6.38 1H dd-d; irr 6.38 1H
 bdd, 7.16 1H d-s, 5.84 1H dd-m; irr 5.84 1H dd, 6.38 1H dd-m;
 irr 3.88 1H dd, 3.46 1H dd-m; irr 3.46 1H dd, 3.88 1H dd-m;
 irr 0.91 6H d, 6.38 1H bdd-ddd (J = 15 Hz, J = 12 Hz, J = 1 Hz).
 UV λ_{\max} (log ϵ): (MeOH, Fig. 31) 270 nm (4.08). IR:
 (CH₂Cl₂, Fig. 30) 1729 (lactone C=O), 1640 (C=C), 890
 (C-CH₂)^{cm⁻¹}. $[\alpha]_D^{27} + 35^\circ$ (c 1.38, CH₂Cl₂).

G. Coraxeniolide-C (34)

Approximately 50 mg of 34 was isolated and purified
 from the CH₂Cl₂ extract by HPLC with CH₂Cl₂ as the eluent.
 Coraxeniolide-C (34) is a white, crystalline solid,
 mp 68-69°C, R_f 0.44, CH₂Cl₂, and chars blue with H₂SO₄/
 vanillin; C₂₀H₂₈O₂ (calcd 300.208 936; found 300.207 40)
 m/z 300 (100%, M⁺), 257 (14, M⁺-C₃H₇) (Fig. 35). ¹³C NMR:
 (CDCl₃) 169.44 (s), 152.44 (s), 137.12 (d), 135.62 (s),
 133.77 (s), 133.07 (s), 124.26 (d), 121.00 (d), 112.81 (t),
 71.16 (dd) (Fig. 37), 51.77 (d), 50.02 (d), 40.16 (t),
 38.04 (t), 35.23 (t), 28.27 (t), 25.89 (q), 25.01 (t),
 18.05 (q), 16.56 (q) ppm. ¹H NMR: (100 MHz, CDCl₃,
 Fig. 39) 5.79 1H t (J = 7 Hz), 5.33 1H m, 5.22 1H bt
 (J = 7 Hz), 4.91 1H s, 4.85 1H s, 4.05 1H dd (J = 12 Hz,
 J = 6 Hz), 3.56 1H dd (J = 12 Hz, J = 12 Hz), 3.02 2H bdd

($J = 7$ Hz, $J = 7$ Hz), 1.68 6H s, 1.62 3H s ppm; (100 MHz, C_6D_6 , Fig. 40, Table 4) 5.61 1H t ($J = 8$ Hz), 5.28 2H m, 4.73 1H s, 4.69 1H s, 3.81 1H dd ($J = 12$ Hz, $J = 7$ Hz), 3.48 1H dd ($J = 12$ Hz, $J = 12$ Hz), 3.25 2H bdd ($J = 8$ Hz, $J = 8$ Hz), 1.66 3H bs, 1.62 3H bs, 1.40 3H d ($J = 1$ Hz) ppm. Decoupling: irr 5.79 1H t, 3.02 1H bdd-d; irr 5.22 1H bt, 3.02 1H bdd-d; irr 4.05 1H dd, 3.56 1H dd-d; irr 3.56 1H dd, 4.05 1H dd-d; irr 3.02 2H bdd, 5.79 1H t-s, 5.22 1H bt-d ($J = 1.5$ Hz); irr 1.68 6H bs, 5.22 1H bt-t, 3.02 2H bdd-dd. UV λ_{max} ($\log \epsilon$): (MeOH, Fig. 38) 215 nm (3.89). IR: (CH_2Cl_2 , Fig. 36) 1737 (lactone C=O), 1643 (C=C), 1388 (CH₃), 900 (C=CH₂) cm^{-1} . $[\alpha]_D^{25} +113^\circ$ (c 1.24, $CHCl_3$).

Twenty-eight milligram of coraxeniolide-C (34) was dissolved in toluene and stirred overnight with 23 μ l of DBU. The reaction mixture was passed through a silica gel Sep-Pak, concentrated, and chromatographed by HPLC (CH_2Cl_2) to give 7.2 mg of coraxeniolide-D (36) and 5.6 mg of coraxeniolide-D' (37).

H. Coraxeniolide-D (36 from 34)

Coraxeniolide-D (36) forms white, plate-like crystals upon purification and concentration, mp 127-129°C, R_f 0.41, CH_2Cl_2 , and chars red with H_2SO_4 /vanillin; $C_{20}H_{28}O_2$ (calcd 300.208 936; found 300.207 40) m/z 300 (28%, M^+), 219 (13, $M^+ - C_6H_9$) (Fig. 43). 1H NMR: (100 MHz, $CDCl_3$, Fig. 44, Table 4) 6.39 1H dd ($J = 15$ Hz, $J = 10$ Hz), 5.90 1H dd

($J = 15$ Hz, $J = 7$ Hz), 5.89 1H bd ($J = 10$ Hz), 5.34 1H bt ($J = 7$ Hz), 5.04 1H s, 5.01 1H s, 4.21 1H dd ($J = 12$ Hz, $J = 8$ Hz), 3.96 1H dd ($J = 12$ Hz, $J = 12$ Hz), 3.58 1H bdd ($J = 7$ Hz, $J = 7$ Hz), 1.78 6H bs, 1.68 3H d ($J = 2$ Hz) ppm.
 Decoupling: (100 MHz, CDCl_3) irr 6.39 1H dd, 5.90 1H dd-d, 5.89 1H d-s; irr 3.58 1H dd, 5.90 1H dd-d; irr 1.78 6H bs, 5.89 1H bd-d. UV λ_{max} (log ϵ): (MeOH, Fig. 42) 239 nm (4.11). IR: (CH_2Cl_2 , Fig. 41) 1745 (lactone C=O), 1637 (C=C), 890 ($\text{C}=\text{CH}_2$) cm^{-1} . $[\alpha]_{\text{D}}^{28} + 31^\circ$ (c 0.65, CH_2Cl_2).

I. Hexacoraxeniolide-A (23) and Hexacoraxeniolide-A' (24)
 (from 36)

Four milligram of coraxeniolide-D (36) was hydrogenated by stirring overnight with 10% Pd/C in MeOH in an H_2 atmosphere. The reaction mixture was filtered and concentrated to give 2.9 mg of a mixture of two products identical to hexacoraxeniolides 23 and 24 (from 22). The mixture of 23 and 24 (from 36) is a colorless oil, R_f 0.44, CH_2Cl_2 , and chars red with H_2SO_4 /vanillin; $\text{C}_{20}\text{H}_{36}\text{O}_2$ (calcd 308.271 537; found 308.270 16) m/z 308 (12%, M^+), 224 (100, $\text{M}^+ - \text{C}_6\text{H}_{12}$). ^1H NMR: (100 MHz, CDCl_3) 4.20-4.05 m (Fig. 45), 2.60-2.25 m, 0.85-0.92 (envelope of CH_3 doublets). UV: (MeOH) end absorption. IR: (CH_2Cl_2) 1739 cm^{-1} (lactone C=O), no C=C stretch in the region 1550-1650 cm^{-1} .

J. Coraxeniolide-D' (37 from 34)

Compound 37 forms a white, amorphous solid upon isolation and concentration, mp 115-118°C, R_f 0.35, CH_2Cl_2 , and chars red with H_2SO_4 /vanillin; $\text{C}_{20}\text{H}_{28}\text{O}_2$ (calcd 300.208 936; found 300.207 06) m/z 300 (100%, M^+), 219 (12, $\text{M}^+ - \text{C}_6\text{H}_9$) (Fig. 46). ^1H NMR: (360 MHz, CDCl_3 , Fig. 49) 6.35 1H dd ($J = 15$ Hz, $J = 10$ Hz), 5.86 1H bd ($J = 10$ Hz), 5.51 1H dd ($J = 15$ Hz, $J = 8$ Hz), 5.32 1H bt ($J = 8$ Hz), 4.89 1H s, 4.78 1H s, 4.15 1H dd ($J = 12$ Hz, $J = 4.5$ Hz), 4.05 1H dd ($J = 12$ Hz, $J = 3.5$ Hz), 2.89 1H dd ($J = 8$ Hz, $J = 8$ Hz), 1.76 3H bs, 1.73 3H s, 1.67 3H bs ppm; (100 MHz, CDCl_3 , Fig. 48, Table 4) 6.26 1H dd ($J = 15$ Hz, $J = 10$ Hz), 5.85 1H bd ($J = 10$ Hz), 5.52 1H dd ($J = 15$ Hz, $J = 8$ Hz), 5.31 1H m, 4.89 1H s, 4.79 1H s, 4.16 1H dd ($J = 12$ Hz, $J = 4$ Hz), 4.00 1H dd ($J = 12$ Hz, $J = 4$ Hz), 2.89 1H dd ($J = 8$ Hz, $J = 8$ Hz), 1.76 3H bs, 1.73 3H bs, 1.67 3H d ($J = 1$ Hz) ppm. Decoupling: (100 MHz, CDCl_3) irr 6.26 1H dd, 5.85 1H bd-bs, 5.52 1H dd-m; irr 5.85 1H bd, 6.26 1H dd-m; irr 5.52 1H dd, 6.30 1H dd-m, 2.89 1H dd-d; irr 5.31 1H m, 1.67 3H d-s; irr 2.89 1H dd, 5.52 1H dd-bd.

UV λ_{max} (log ϵ): (MeOH, Fig. 47) 237 nm (4.00). IR: (CH_2Cl_2 , Fig. 50) 1735 (lactone C=O), 890 ($\text{C}=\text{CH}_2$).

$[\alpha]_{\text{D}}^{27} -96^\circ$ (c 0.56, CH_2Cl_2).

K. Coraxeniolide-C' (38)

Final purification of coraxeniolide-C' (38) was accomplished by HPLC (CH_2Cl_2); the crude extract from pink coral contains approximately 150 mg of 38. Due to its chromatographic similarity to coraxeniolide-B (26), coraxeniolide-C' (38) was obtained in small quantities and its purity was somewhat greater than 90%. It is a colorless oil, R_f 0.36, CH_2Cl_2 , and chars red with H_2SO_4 /vanillin; $\text{C}_{20}\text{H}_{28}\text{O}_2$ (calcd 300.208 936; found 300.210 33) m/z 300 (11%, M^+), 257 (10, $\text{M}^+ - \text{C}_3\text{H}_7$) (Fig. 52). ^{13}C NMR: (CDCl_3) 171.29, 152.44, 137.82, 135.53, 134.30, 133.77, 124.52, 119.86, 113.08, 71.07, 49.67, 43.68, 40.51, 38.04, 34.87, 27.04, 25.89, 25.10, 18.14, 16.64 ppm. ^1H NMR: (100 MHz, CDCl_3) 6.41 1H t ($J = 8$ Hz), 5.41 1H m, 5.11 1H bd ($J = 8$ Hz), 4.94 1H s, 4.80 1H s, 4.06 1H dd ($J = 11$ Hz, $J = 6$ Hz), 3.54 1H dd ($J = 11$ Hz, $J = 11$ Hz), 2.87 2H bdd ($J = 8$ Hz, $J = 8$ Hz), 1.71 6H bs, 1.66 3H bs ppm; (100 MHz, C_6D_6 , Fig. 55, Table 4) 6.57 1H t ($J = 8$ Hz), 5.34 1H m, 5.08 1H mt ($J = 8$ Hz), 4.72 1H s, 4.67 1H s, 3.84 1H dd ($J = 12$ Hz, $J = 6$ Hz), 3.38 1H dd ($J = 12$ Hz, $J = 12$ Hz), 2.72 2H bdd ($J = 8$ Hz, $J = 8$ Hz), 1.62 3H bs, 1.50 3H bs, 1.42 3H d ($J = 1$ Hz) ppm. Decoupling: (100 MHz, C_6D_6) irr 6.57 1H t, 2.72 2H bdd-d; irr 5.34 1H m, 1.42 3H d-s; irr 5.08 1H mt, 2.72 2H bdd-d; irr 2.72 2H bdd, 6.57 1H t-s, 5.08 1H mt-bs; irr 1.62 bs, 5.08 1H mt-bt; irr 1.50 bs, 5.08 1H mt-bt.

UV λ_{max} (log ϵ): (MeOH, Fig. 54) 213 nm (3.81).

IR: (CH_2Cl_2 , Fig. 53) 1730 (lactone C=O), 1640 (C=C), 892 ($\text{C}=\text{CH}_2$) cm^{-1} . $[\alpha]_D^{26} +85^\circ$ (c 1.08, CHCl_3).

Thirteen milligram of coraxeniolide-C' (38) was dissolved in toluene and stirred overnight with 30 μl of DBU. The reaction mixture was then passed through a silica gel Sep-Pak, concentrated, and chromatographed by HPLC (CH_2Cl_2) to give 3.7 mg of coraxeniolide-D (36) and 5.0 mg of coraxeniolide-D' (37).

L. Coraxeniolide-D (36 from 38)

Coraxeniolide-D (36), from the reaction of coraxeniolide-C' (38) with base, forms white, plate-like crystals upon concentration, mp 128-131°C, R_f 0.41, CH_2Cl_2 , and chars red with H_2SO_4 /vanillin; $\text{C}_{20}\text{H}_{28}\text{O}_2$ (calcd 300.208 936; found 300.208 40) m/z 300 (45%, M^+), 219 (21, $\text{M}^+ - \text{C}_6\text{H}_9$). ^1H NMR: (100 MHz, CDCl_3 , Table 4) 6.39 1H dd ($J = 15$ Hz, $J = 10$ Hz), 5.90 1H dd ($J = 15$ Hz, $J = 7$ Hz), 5.89 1H bd ($J = 10$ Hz), 5.32 1H bt ($J = 7$ Hz), 5.04 1H s, 5.00 1H s, 4.20 1H dd ($J = 12$ Hz, $J = 8$ Hz), 3.95 1H dd ($J = 12$ Hz, $J = 12$ Hz), 3.59 1H dd ($J = 7$ Hz, $J = 7$ Hz), 1.77 6H bs, 1.67 3H d ($J = 2$ Hz) ppm. Decoupling: (100 MHz, CDCl_3) irr 6.39 1H dd, 5.90 1H dd-d, 5.89 1H bd-s; irr 3.59, 5.90 1H dd-d; irr 1.77 6H bs, 5.89 1H bd-d. UV λ_{max} (log ϵ): (MeOH) 240 nm (4.13). IR: (CH_2Cl_2) 1742 (lactone C=O), 1633 (C=C), 890 ($\text{C}=\text{CH}_2$) cm^{-1} .

M. Coraxeniolide-D' (37 from 38)

Coraxeniolide-D' (37) is a white, amorphous solid, mp 116-118°C, R_f 0.35, CH_2Cl_2 . and chars red with H_2SO_4 /vanillin; $\text{C}_{20}\text{H}_{28}\text{O}_2$ (calcd 300.208 936; found 300.210 33) m/z 300 (100%, M^+), 219 (17, $\text{M}^+ - \text{C}_6\text{H}_9$). ^1H NMR: (100 MHz, CDCl_3 , Table 4) 6.29 1H dd ($J = 15$ Hz, $J = 10$ Hz), 5.87 1H bd ($J = 10$ Hz), 5.52 1H dd ($J = 15$ Hz, $J = 8$ Hz), 5.32 1H m, 4.90 1H s, 4.81 1H s, 4.17 1H dd ($J = 12$ Hz, $J = 4$ Hz), 4.02 1H dd ($J = 12$ Hz, $J = 4$ Hz), 2.90 1H dd ($J = 8$ Hz, $J = 8$ Hz), 1.78 3H bs, 1.75 3H bs, 1.69 3H d ($J = 1$ Hz) ppm. Decoupling: (100 MHz, CDCl_3) irr 6.30 1H dd, 5.89 1H bd-bs, 5.56 1H dd-m; irr 5.89 1H bd, 6.30 1H dd-d; irr 5.56 1H dd, 6.30 1H dd-d, 2.92 1H dd-d; irr 5.30 1H m, 1.71 3H d-s; irr 2.92 1H dd, 5.56 1H dd-d. UV λ_{max} (log ϵ): (MeOH) 237 nm (4.04). IR: 1740 (lactone C=O), 895 ($\text{C}=\text{CH}_2$) cm^{-1} .

N. Corbohcin (47)

Approximately 25 mg of corbohcin (47) was isolated by HPLC with CH_2Cl_2 /hexane (1:1) as the eluent. Corbohcin (47) is a colorless oil, R_f 0.55, CH_2Cl_2 , and chars red with H_2SO_4 /vanillin; $\text{C}_{22}\text{H}_{34}\text{O}_2$ (field desorption, calcd 330.255 67; found 330.255 68), $\text{C}_{20}\text{H}_{30}$ (field desorption, calcd 270.234 59; found 270.234 64), $\text{C}_{17}\text{H}_{23}$ (70 eV, calcd 227.179 980; found 227.182 27) m/z (70 eV) 330 (4%, M^+), 270 (43, $\text{M}^+ - \text{CH}_3\text{CO}_2\text{H}$), 227 (77, $\text{M}^+ - \text{CH}_3\text{CO}_2\text{H}, \text{C}_3\text{H}_7$), 201 (59, $\text{M}^+ - \text{CH}_3\text{CO}_2\text{H}, \text{C}_5\text{H}_9$) (Fig. 56). ^{13}C NMR: (CDCl_3) 170.85 (s),

152.71 (s), 147.33 (s), 136.15 (s), 131.83 (s), 124.60 (d),
124.50 (d), 117.58 (t), 109.03 (t), 65.52 (t), 52.31 (d),
47.73 (d), 40.25 (t), 33.91 (t), 32.23 (t), 31.26 (t),
28.71 (t), 26.68 (t), 26.33 (q), 21.22 (q), 18.14 (q),
17.97 (q) ppm. ^1H NMR: (220 MHz, CDCl_3 , Fig. 58) 5.28 1H bd
($J = 8$ Hz), 5.15 1H m, 4.91 2H s, 4.82 1H s, 4.71 1H s,
4.01 1H dd ($J = 12$ Hz, $J = 6$ Hz), 3.81 1H dd ($J = 12$ Hz, $J = 12$
Hz), 1.94 3H s, 1.69 3H s, 1.63 3H s, 1.57 3H s ppm.
Decoupling: (220 MHz, CDCl_3) irr 5.28 1H bd, 1.57 3H s
enhanced; irr 5.15 1H m, 1.63 3H s enhanced, 1.69 3H s
enhanced. UV: (MeOH) end absorption. IR: (CH_2Cl_2 , Fig. 59)
1732 (lactone C=O), 1640 (C=C), 1386 (CH_3), 890 ($\text{C}=\text{CH}_2$) cm^{-1} .
 $[\alpha]_{\text{D}}^{27} - 169^\circ$ (c 0.71, CHCl_3).

III. RESULTS AND DISCUSSION

A. Structural Determination of Coraxeniolide-A (22)

Pink coral (Corallium sp.), endoskeleton and polyps, contains approximately 650 mg/kg of coraxeniolide-A (22). It is the major secondary metabolite in this organism. Coraxeniolide-A (22) is a crystalline, white solid, mp 88-91°C, with composition $C_{20}H_{30}O_2$, indicating six unsaturations.

The IR spectrum (Fig. 18) exhibits a lactone or ester absorbance at 1748 cm^{-1} and an exocyclic double bond absorbance at 898 cm^{-1} . The ^{13}C NMR spectrum confirms the presence of a lactone or ester with signals at 175.16 (s) ppm for the carbonyl and 70.78 (t) ppm for the carbon bearing oxygen. Additionally, it reveals three double bonds with six absorbances at 153.06 (s), 140.73 (d), 139.97 (s), 124.00 (d), 123.47 (d), and 112.20 (t) ppm; the 112.20 (t) ppm absorbance confirms the presence of an exocyclic methylene. One unsaturation for the carbonyl and three for double bonds leaves two unsaturations for rings in the structure of coraxeniolide-A (22).

The ^1H NMR spectrum of 22 (220 MHz, CDCl_3 , Fig. 19) contains a doublet of doublets at δ 5.50, indicating a trans double bond proton adjacent to a methine. The exocyclic methylene is seen as a two-hydrogen singlet at δ 4.98, and two other olefinic protons appear as a multiplet at δ 5.36.

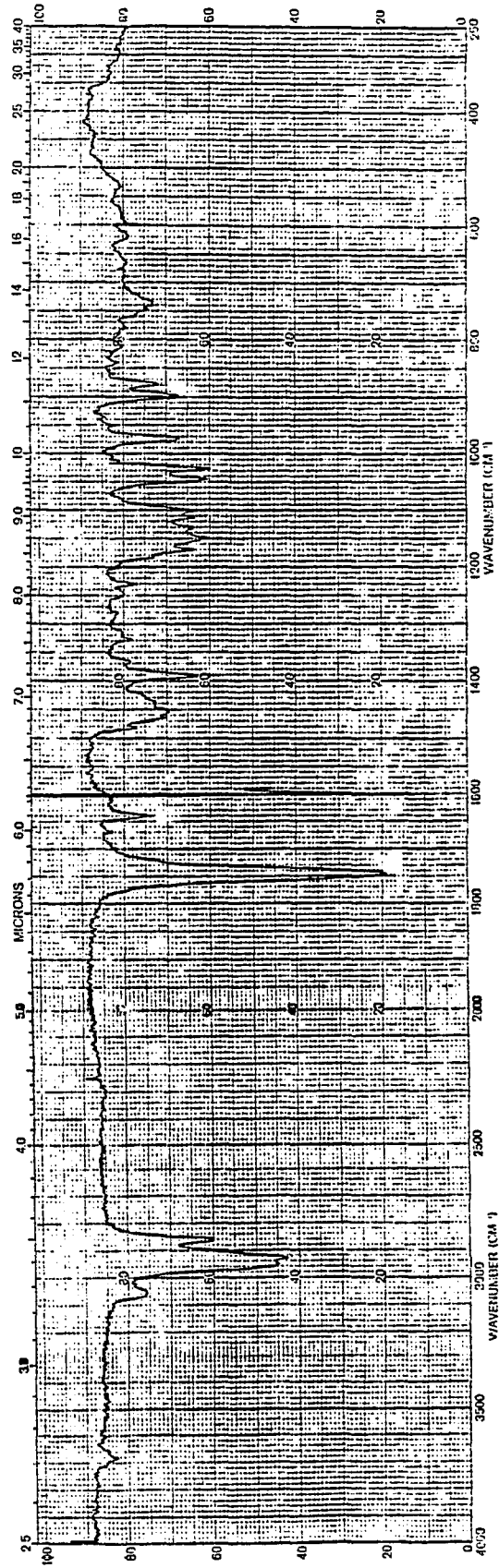


Figure 18. IR spectrum of coraxeniolide-A (22).

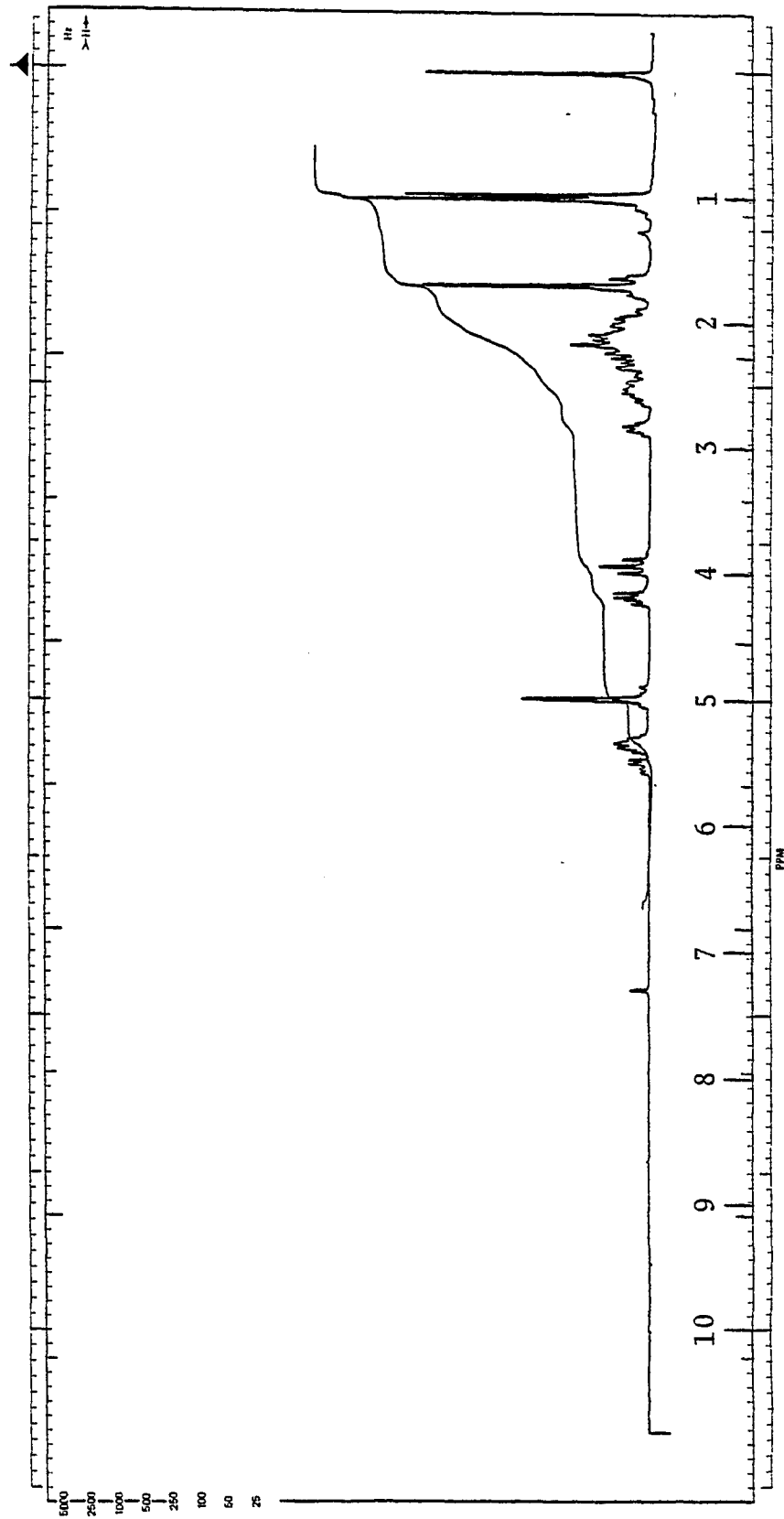


Figure 19. 220 MHz ^1H NMR spectrum of
coraxeniolide-A (22) in CDCl_3 .

The methylene bonded to oxygen is apparently in a rigid system as illustrated by the nonequivalence (δ 4.19 and δ 3.93) and geminal coupling ($J = 12$ Hz) of its protons. These protons are vicinally coupled to a methine with different coupling constants, $J = 6$ Hz and $J = 12$ Hz, respectively, which also suggests an inflexible ring system. There is a methine adjacent to the carbonyl as indicated by the one-hydrogen multiplet at δ 2.80, a vinyl methyl at δ 1.70, and an isopropyl group which appears as a doublet ($J = 7$ Hz) at δ 1.00.

The presence of an isopropyl group is confirmed by the loss of 43 mass units (m/z 259) from the molecular ion in the mass spectrum of 22 (Fig. 20). A loss of C_6H_{11} (m/z 219) from the molecular ion, as well as a rearranged fragment at m/z 220, are also observed in the mass spectrum.

Coraxeniolide-A (22) was hydrogenated with 10% Pd/C in a hydrogen atmosphere to give an inseparable mixture of two hexacoraxeniolides, 23 and 24. The product appeared to be one compound by thin layer chromatography, high performance liquid chromatography, and gas chromatography. A mixture, however, was apparent in the ^{13}C NMR spectrum (Fig. 21), which revealed two carbonyls at 176.22 and 175.78 ppm and two oxygen-bearing carbons at 69.57 and 68.87 ppm. The absence of any carbons in the region 110-160 ppm, along with the molecular ion in the mass spectrum of 23 and 24 (Fig. 22) at m/z 308 ($C_{20}H_{36}O_2$), confirms the presence of three double bonds in coraxeniolide-A (22).

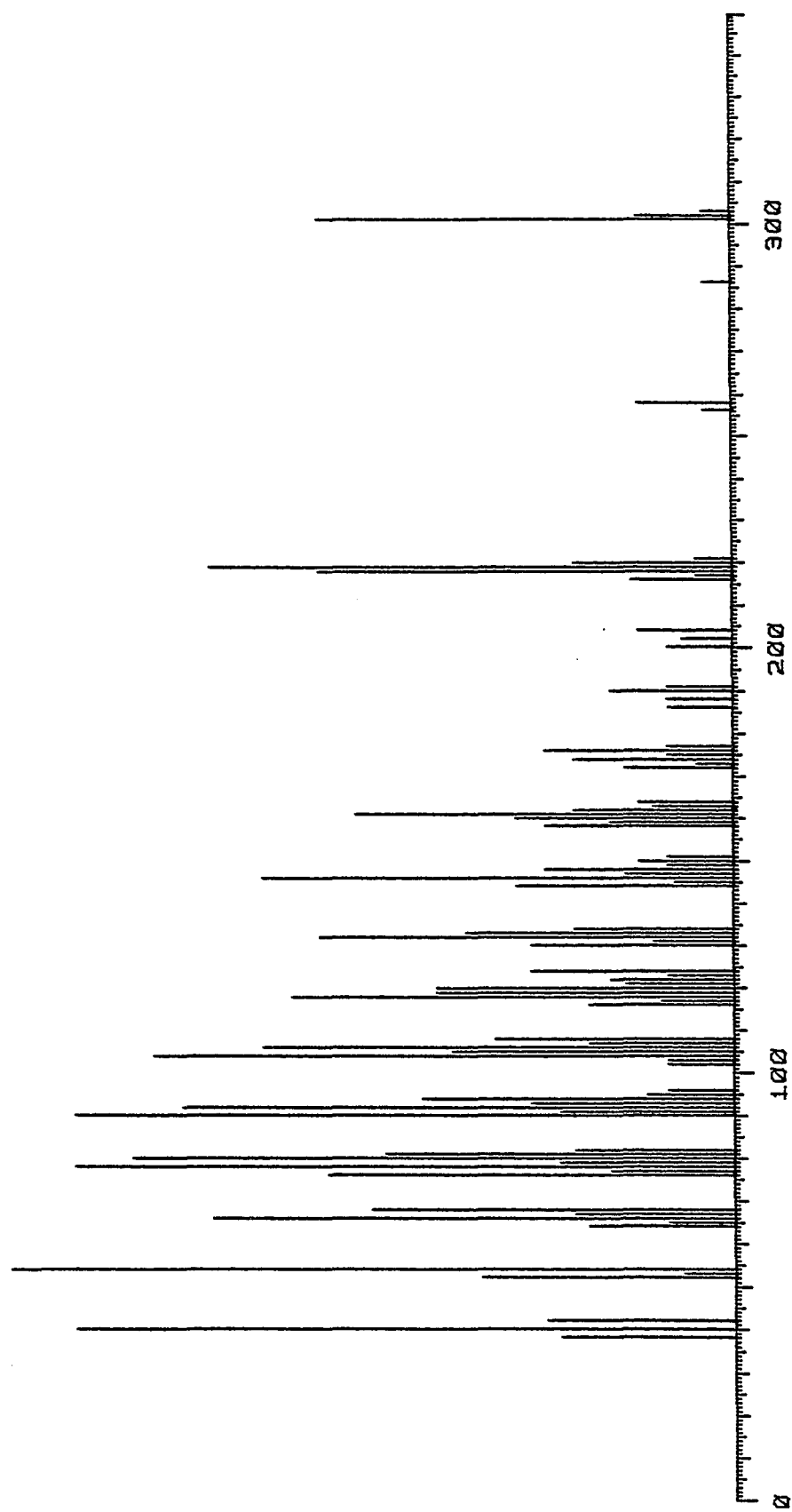


Figure 20. Mass spectrum of coraxeniolide-A (22).

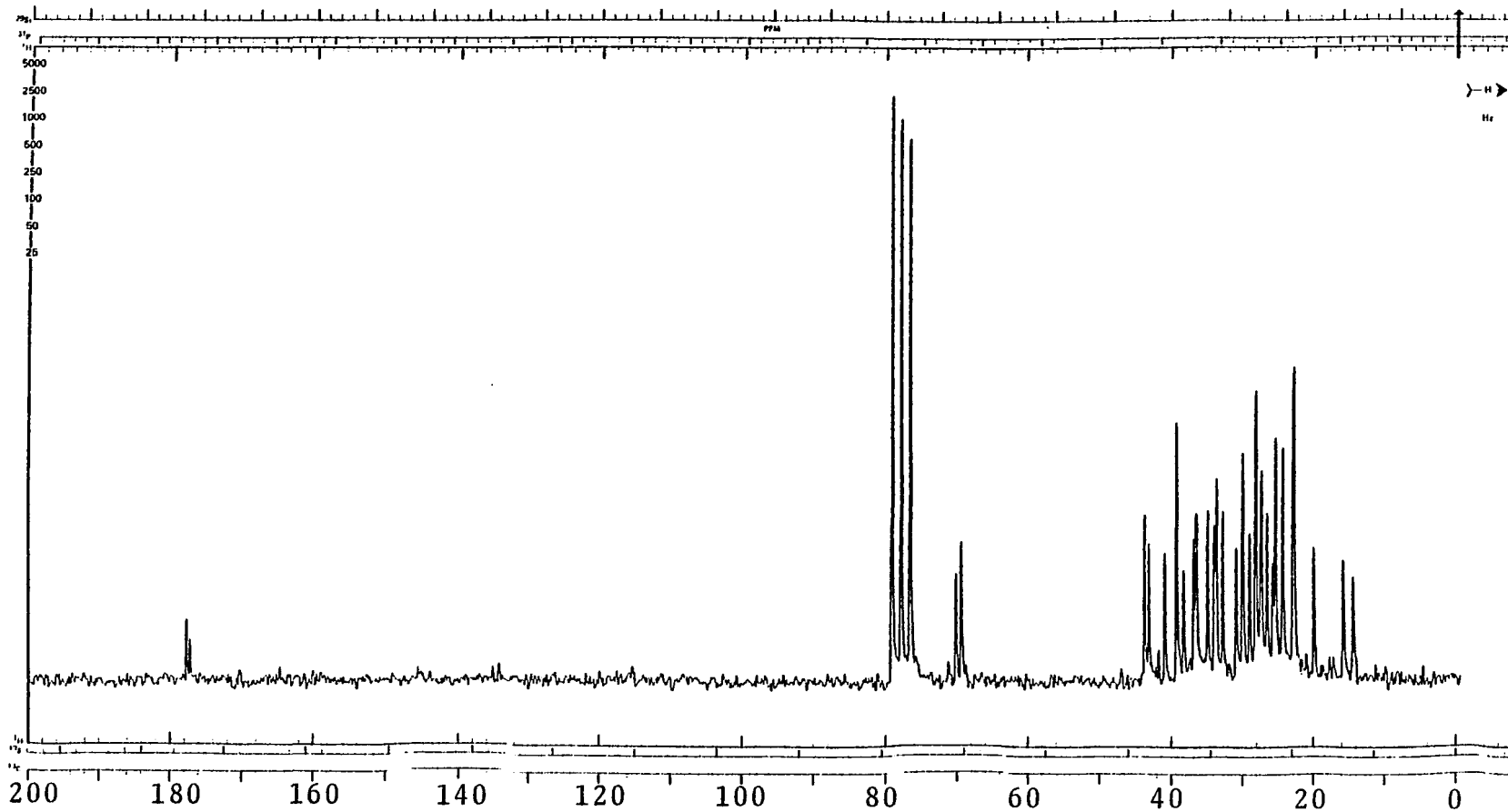


Figure 21. ^{13}C NMR spectrum of hexacoraxeniolide-A (23) and hexacoraxeniolide-A' (24) in CDCl_3 .

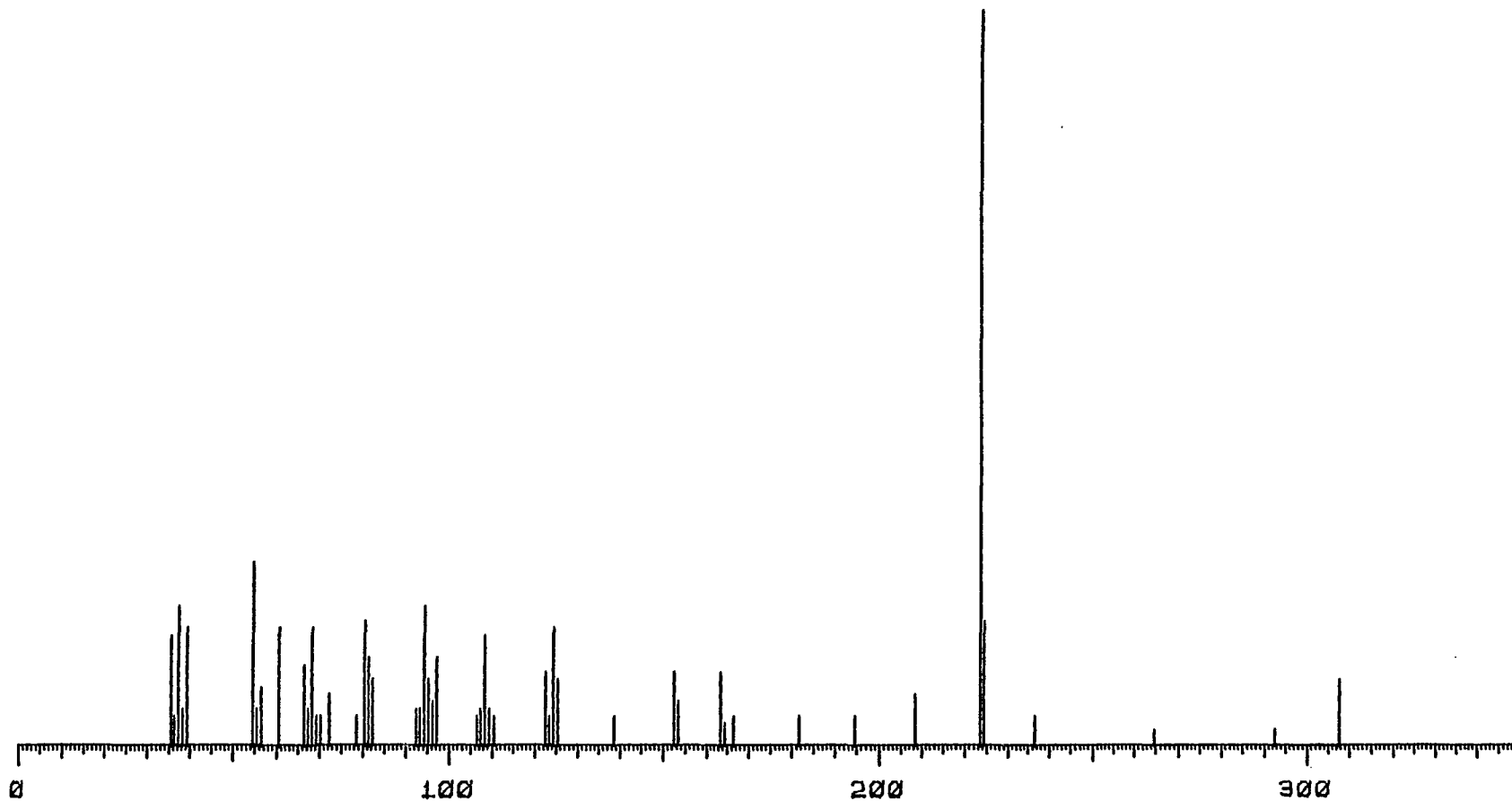


Figure 22. Mass spectrum of
hexacoraxeniolide-A (23) and hexacoraxeniolide-A' (24).

A detailed interpretation of the 360 MHz ^1H NMR spectrum of this mixture (CDCl_3 , Fig. 23) was impossible. Expansion of the methyl region (Fig. 24), however, revealed the presence of eight methyl doublets, as would be expected for a mixture of two compounds containing four methyl doublets each.

Coraxeniolide-A (22) was also reduced to the diol 25, with composition $\text{C}_{20}\text{H}_{34}\text{O}_2$. The molecular ion at m/z 306 in the mass spectrum of 25 (Fig. 26) represents only one percent of the base peak and, therefore, the molecular formula of coraxendiol-A (25) could not be obtained directly. However, high resolution mass measurement of a more intense peak at m/z 288 indicates a formula of $\text{C}_{20}\text{H}_{32}\text{O}$. This corresponds to loss of a molecule of water from the molecular ion, $\text{C}_{20}\text{H}_{34}\text{O}_2$, a common phenomenon in compounds containing hydroxyls.

In the 360 MHz ^1H NMR spectrum of coraxendiol-A (25) (C_6D_6 , Fig. 27) the protons bonded to hydroxyl-bearing carbons appear as four distinct doublets of doublets at δ 3.65 ($J = 11$ Hz, $J = 6$ Hz), δ 3.50 ($J = 11$ Hz, $J = 6$ Hz), δ 3.29 ($J = 11$ Hz, $J = 7$ Hz), and δ 3.24 ($J = 11$ Hz, $J = 7$ Hz). Neither methylene, therefore, is free to rotate as implied by the nonequivalence and geminal coupling of their protons. This is probably due to the bulkiness of these substituents as well as to intramolecular hydrogen bonding. Both methylenes are adjacent to methines in 25 which confirms

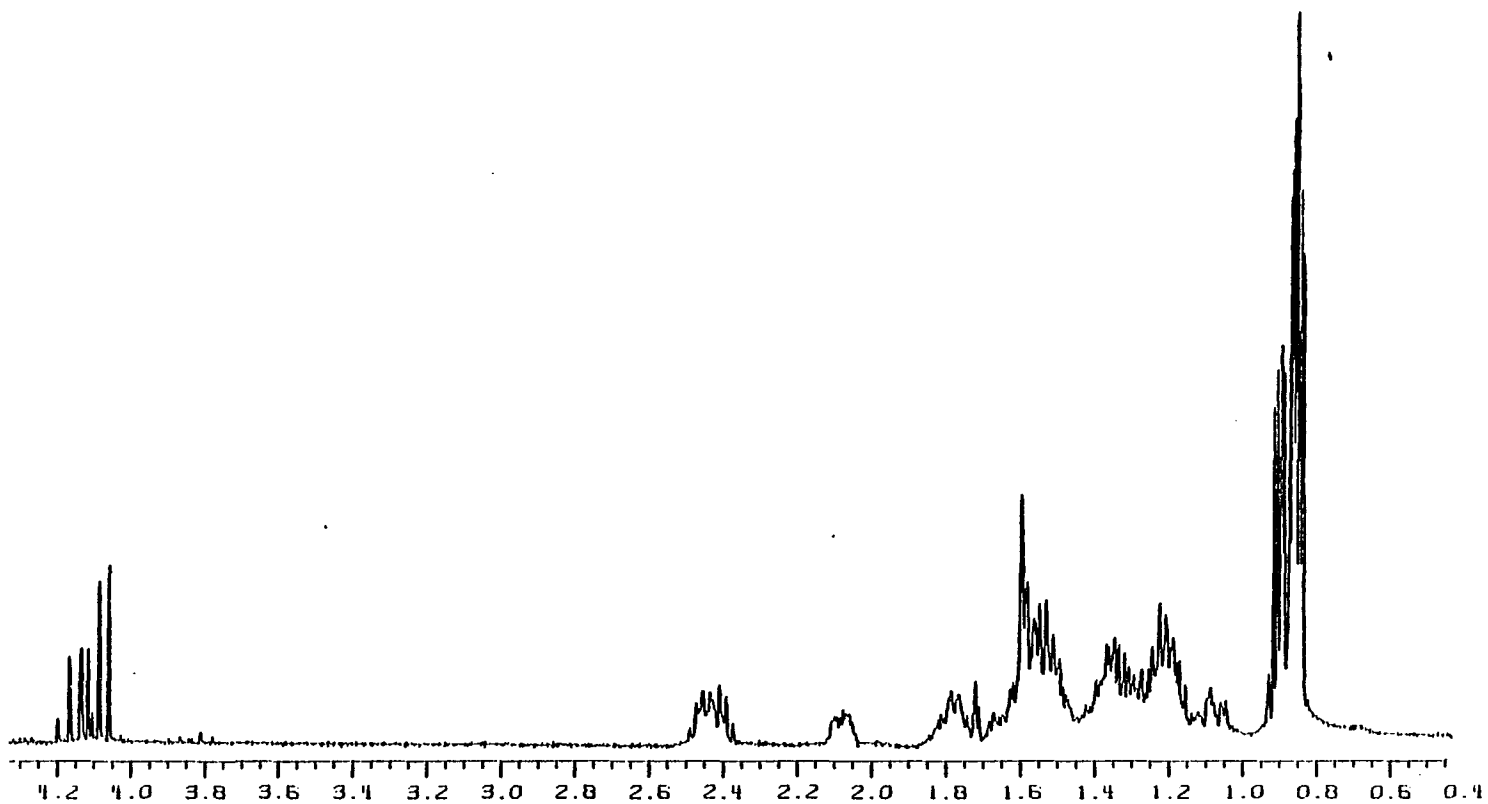


Figure 23. 360 MHz ^1H NMR spectrum of hexacoraxeniolide-A (23) and hexacoraxeniolide-A' (24) in CDCl_3 .

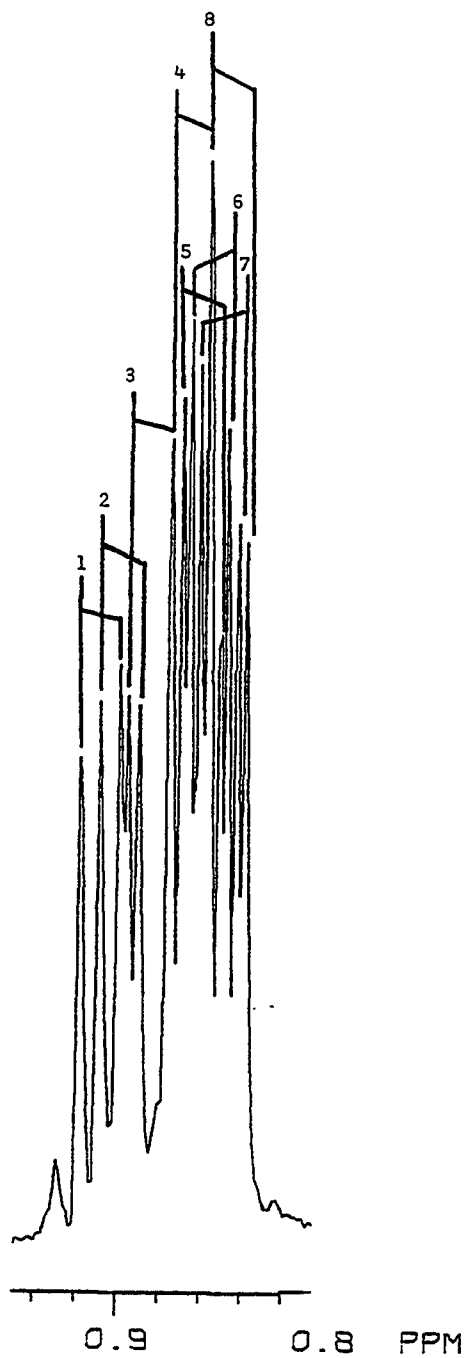


Figure 24. Expansion of the methyl region of the 360 MHz ^1H NMR spectrum of hexacoraxeniolide-A (23) and hexacoraxeniolide-A' (24) in CDCl_3 .

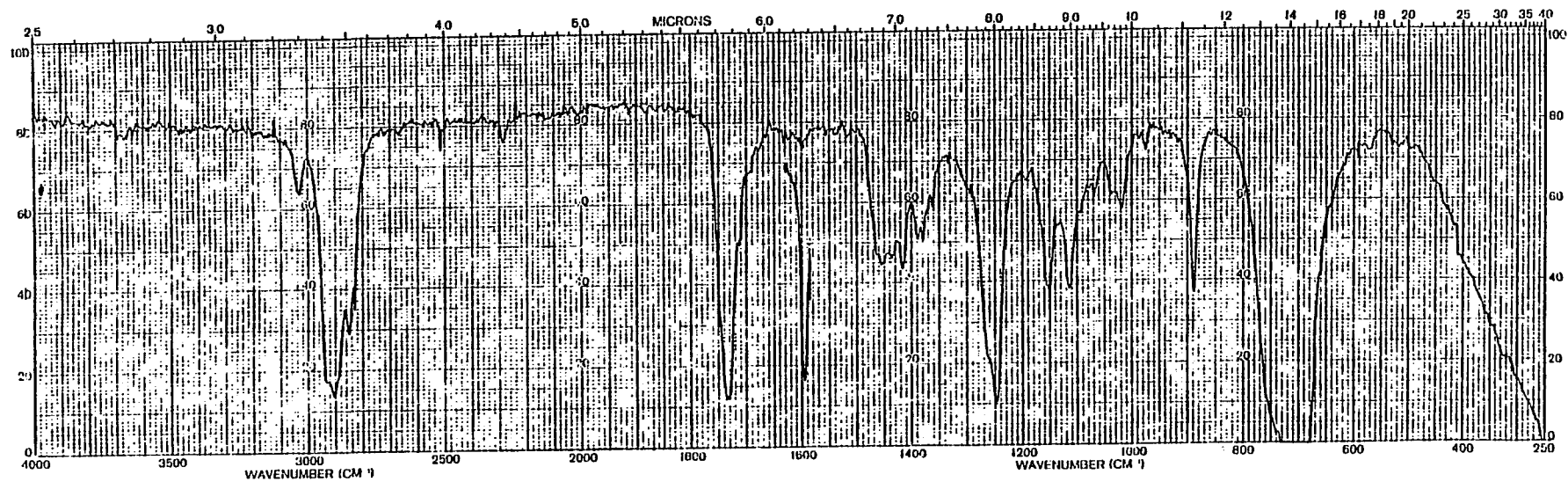


Figure 25. IR spectrum of
hexacoraxeniolide-A (23) and hexacoraxeniolide-A' (24).

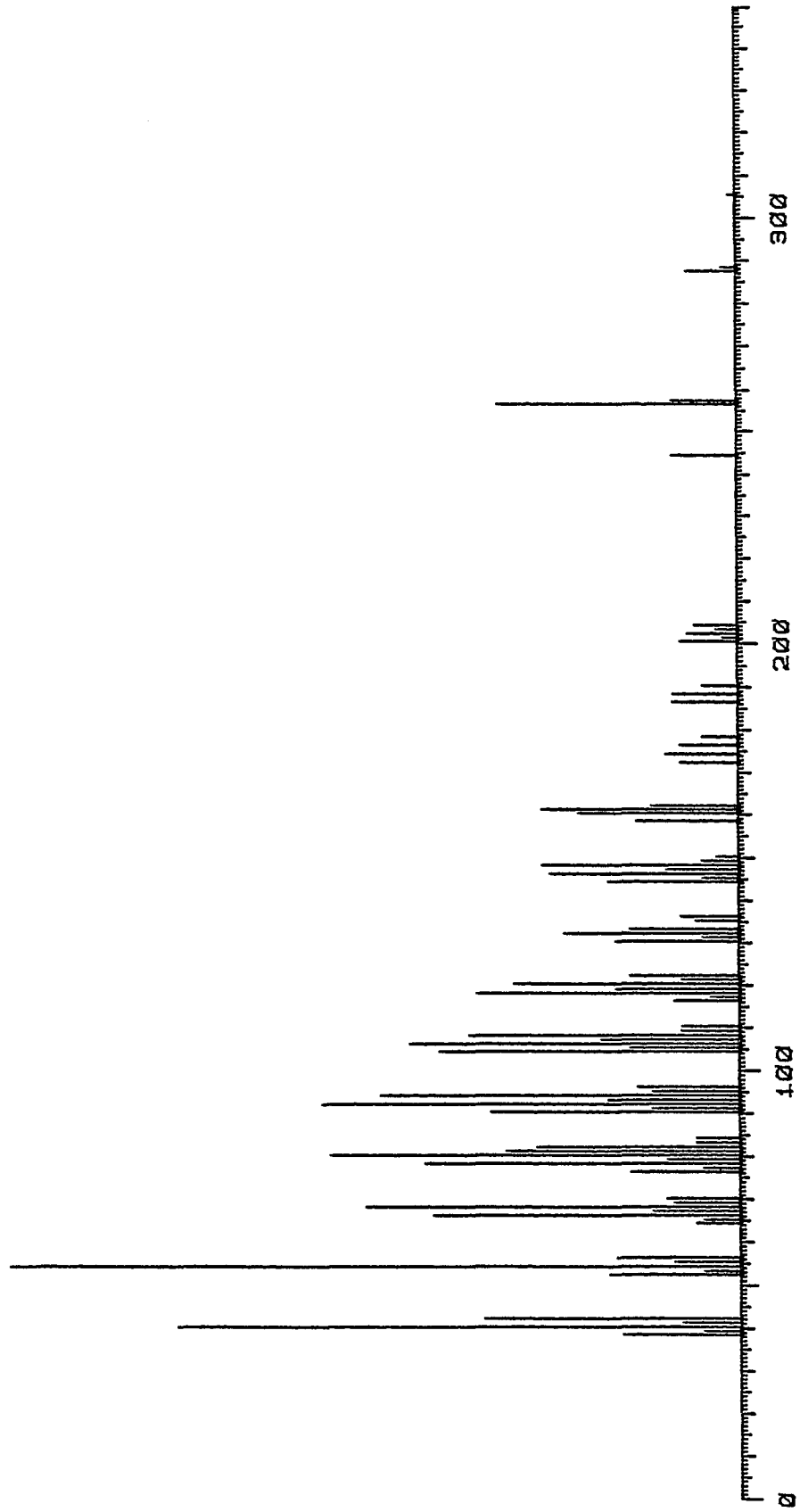


Figure 26. Mass spectrum of coraxendiol-A (25).

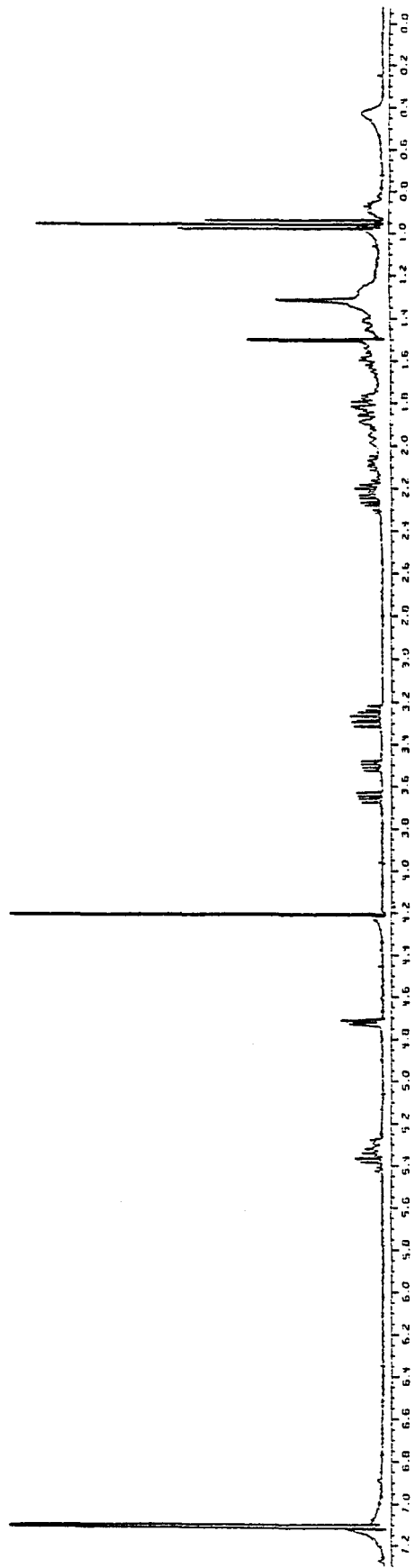


Figure 27. 360 MHz ^1H NMR spectrum of coraxendiol-A (25) in C_6D_6 .

that the carbons adjacent to the carbonyl and oxygen-bearing carbons in coraxeniolide-A (22) are also methines.

A number of attempts were made to cleave the double bonds of coraxeniolide-A (22) by ozonolysis and by osmium tetroxide/sodium periodate with a variety of oxidative and reductive workups. These reactions, however, always resulted in a large number of products, none of which could be isolated in sufficient quantities for structure elucidation.

A concentrated solution of coraxeniolide-A (22) in dichloromethane was placed in the freezer for several weeks, after which time a cubic crystal approximately 5 mm on a face was discovered. A small fragment was cut from this large crystal and submitted for single-crystal X-ray analysis. The structure of coraxeniolide-A (22) is shown in Fig. 28. The numbering system used for coraxeniolide-A (22, p. 80) was suggested by Schmitz and coworkers²⁴ who isolated xenicin, which is closely related to coraxeniolide-A.

Coraxeniolide-A (22) is an unrearranged diterpene with a δ -lactone ring trans-fused to a nine-membered carbocyclic ring. The δ -lactone is in the boat form (C-1 and C-4 down) with the cyclononene ring approximately perpendicular to it--forming an extremely rigid system. Below is a Newman projection looking down the C-11a(1) bond of 22. The dihedral angle between the methine on C-11a and H-1 α (δ 3.93) is 180°, which explains the 12 Hz vicinal coupling seen in

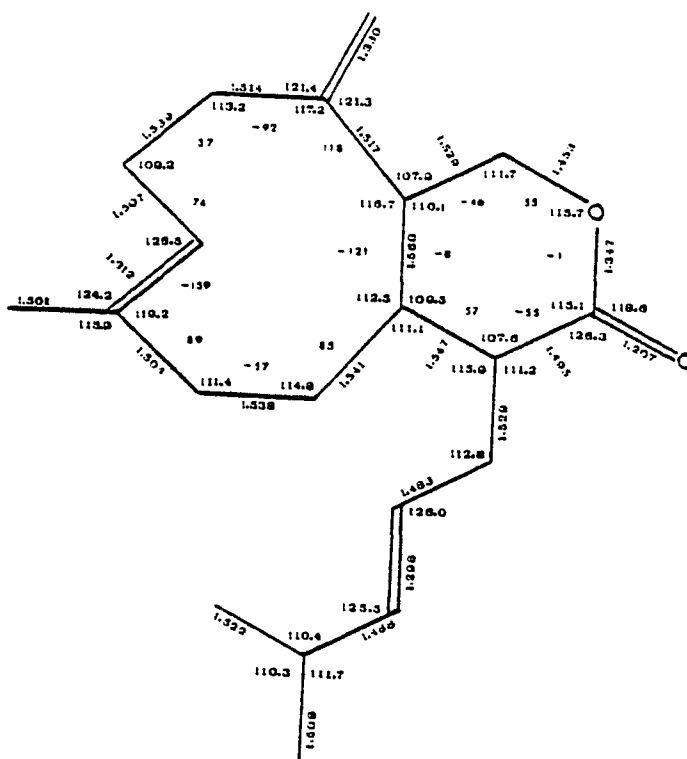
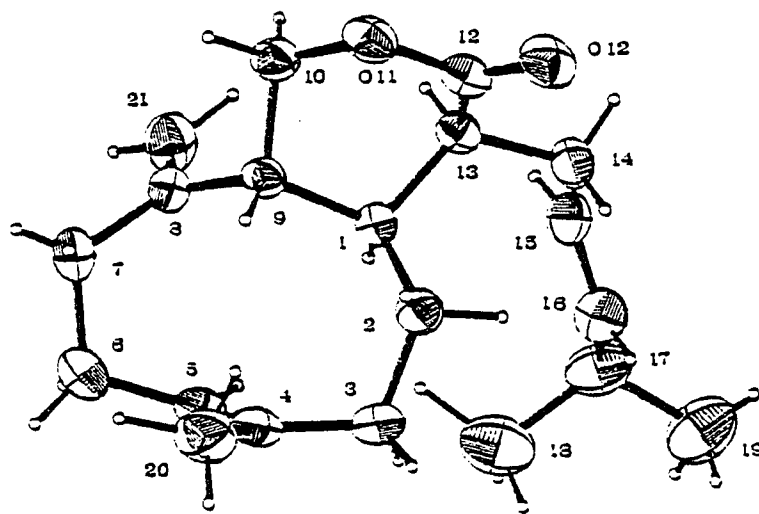
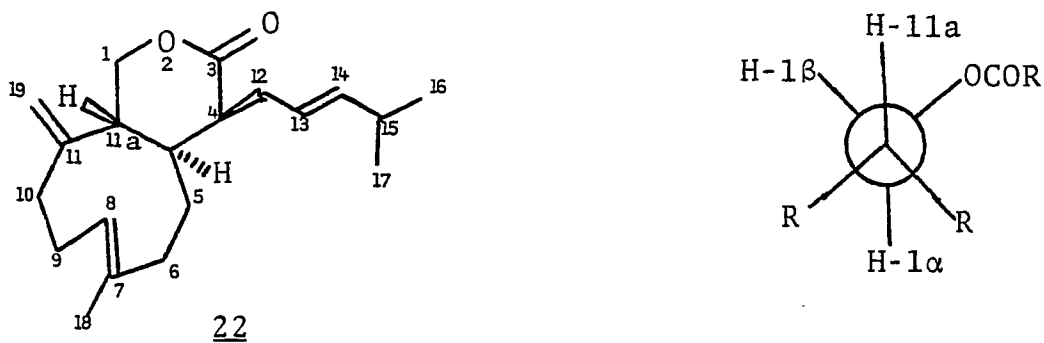
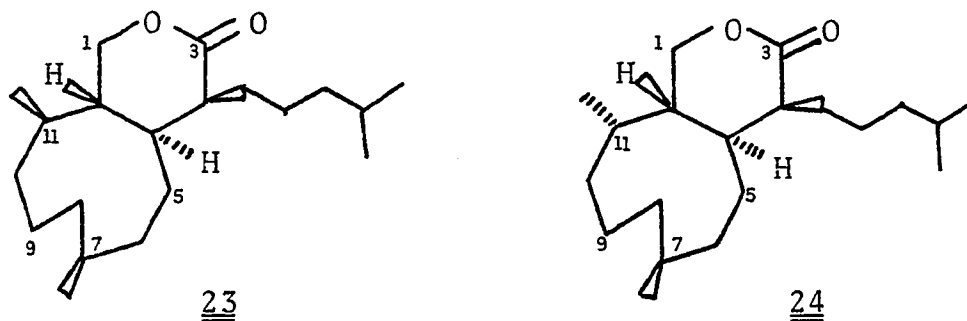


Figure 28. Single-crystal X-ray structure of coraxeniolide-A (22).

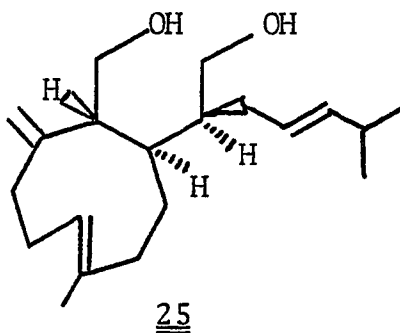


this signal. The β -proton on C-1 (δ 4.19), on the other hand, forms a 30° dihedral angle with H-11a, which accounts for the observed 6 Hz vicinal coupling. The isopropyl unit, trans double bond adjacent to a methine, exocyclic methylene, vinyl methyl, and three double bonds predicted from spectral and chemical data are all present in the single-crystal X-ray structure of coraxeniolide-A (22).

Heterogeneous hydrogenation of coraxeniolide-A (22) could theoretically lead to a mixture of four compounds since the double bonds at C-7(8) and C-11(19) can be attacked from either side and produce a mixture of two epimers each. As a result of the conformation of 22, however, the double bond at C-7(8) can only be attacked from one side, i.e., the outside of the ring, since the rest of the ring is blocking attack from the inside. Therefore, only the hexacoraxeniolides 23 and 24, which are epimeric at C-11, are produced from the hydrogenation of 22.



The structure of compound 25, resulting from the reduction of 22 with LiAlH_4 is shown below.



I would like to suggest the name coraxeniolide for the series of non-hydroxylated, diterpene lactones isolated from Corallium sp. Xen refers to the structural relationship of these compounds to the xeniolides (xenicin), which will be detailed in Section B. In particular, I would like to name compound 22 coraxeniolide-A, making compound 23 hexacoraxeniolide-A, compound 24 hexacoraxeniolide-A', and compound 25 coraxendiol-A.

B. Structural Determination of Coraxeniolide-B (26)

A second major constituent (≈ 325 mg/kg) of Corallium sp. is coraxeniolide-B (26). Coraxeniolide-B (26) is a colorless oil with composition $C_{20}H_{28}O_2$, having one more unsaturation than coraxeniolide-A (22). This additional unsaturation is another double bond as revealed by the eight olefinic carbon signals at 151.74 (s), 151.38 (d), 138.26 (d), 137.03 (s), 131.31 (s), 124.70 (d), 121.09 (d), 113.52 (t) ppm in the ^{13}C NMR spectrum of 26. The chemical shift (113.52 ppm) and multiplicity (t) of the high field carbon indicate that it is part of an exocyclic methylene, while signals at 171.38 (s) and 71.07 (dd) (Fig. 29) are interpreted as the carbonyl and oxygen-bearing carbon of a lactone. The reason that the methylene carbon bonded to oxygen appears as a doublet of doublets, rather than as a triplet, will be discussed shortly. Four double bonds and a lactone leave one unsaturation for an additional ring in the structure of coraxeniolide-B (26).

The IR spectrum of 26 (Fig. 30) confirms the presence of the lactone (1729 cm^{-1}) and the exocyclic methylene (890 cm^{-1}). The maximum at 270 nm in the UV spectrum of 26 (Fig. 31) reveals a highly conjugated system.

The 1H NMR spectrum (100 MHz, C_6D_6 , Fig. 32, Table 3) and decoupling data, in combination with the information already presented, suggest structure 26 for coraxeniolide-B.

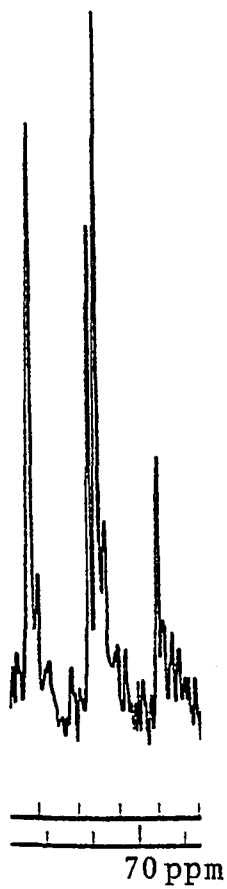


Figure 29. Expansion of the 71.07 ppm signal
in the off-resonance ^{13}C NMR spectrum of
coraxeniolide-B (26).

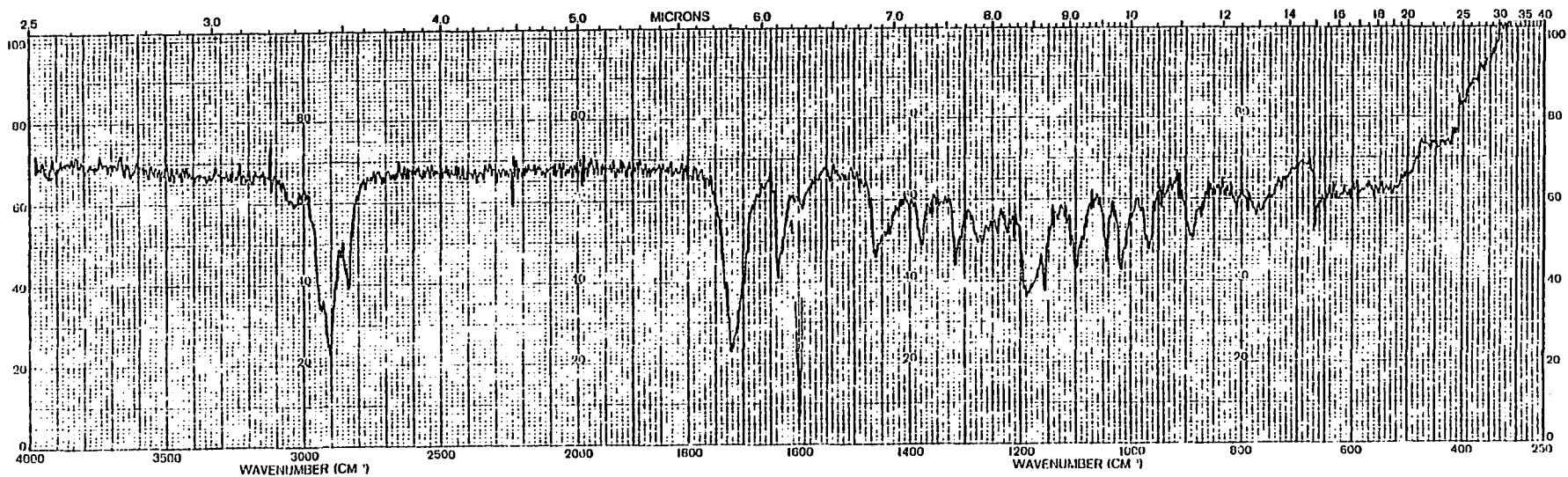


Figure 30. IR spectrum of coraxeniolide-B (26).

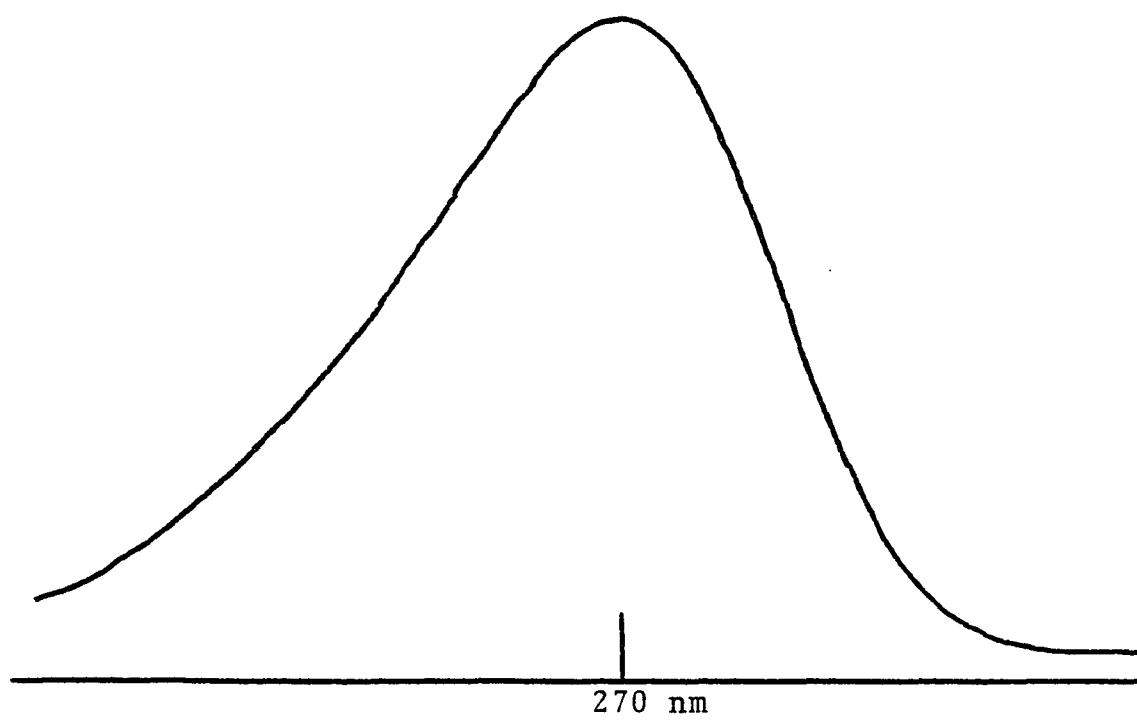


Figure 31. UV spectrum of coraxeniolide-B (26).

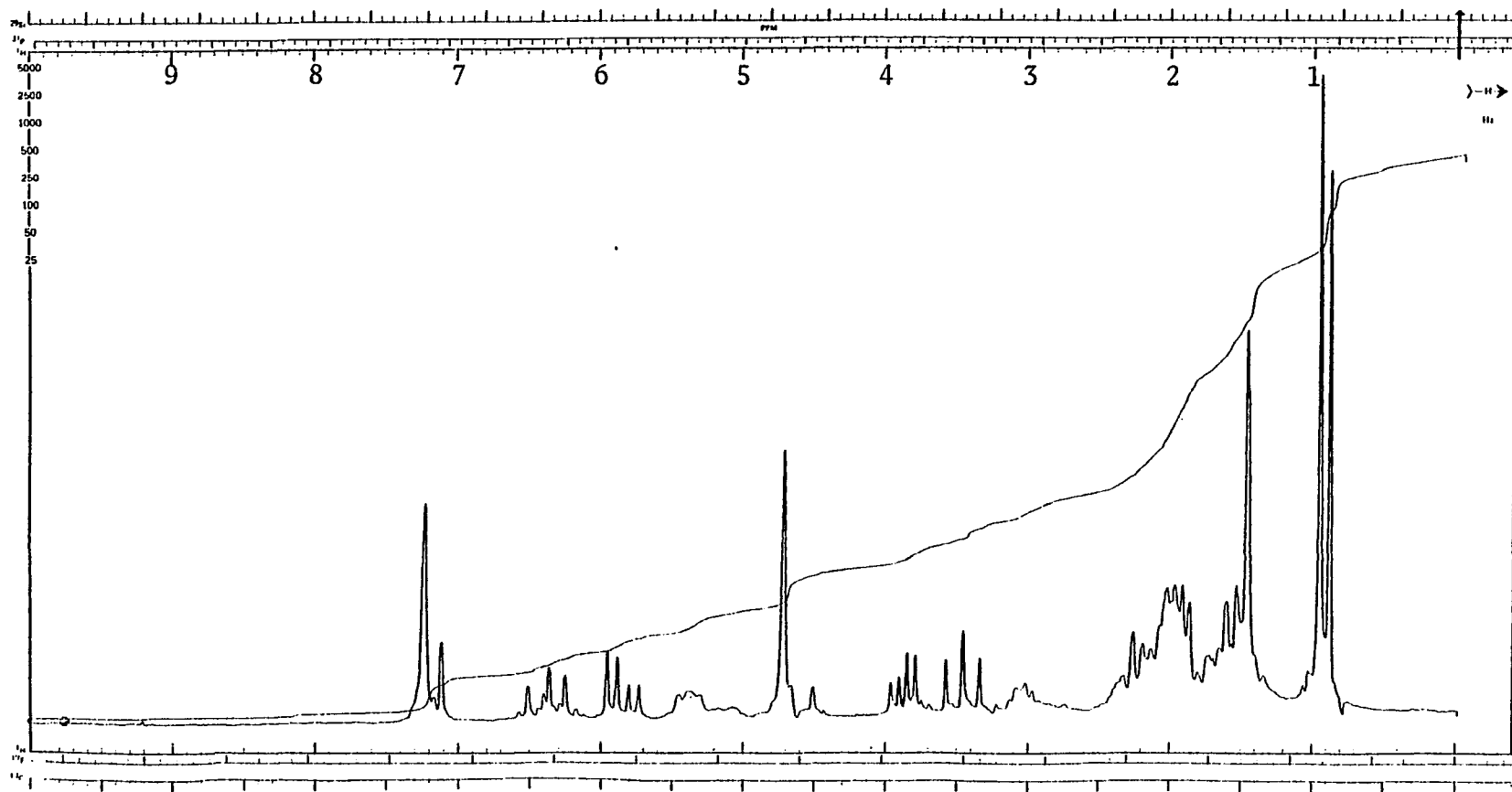
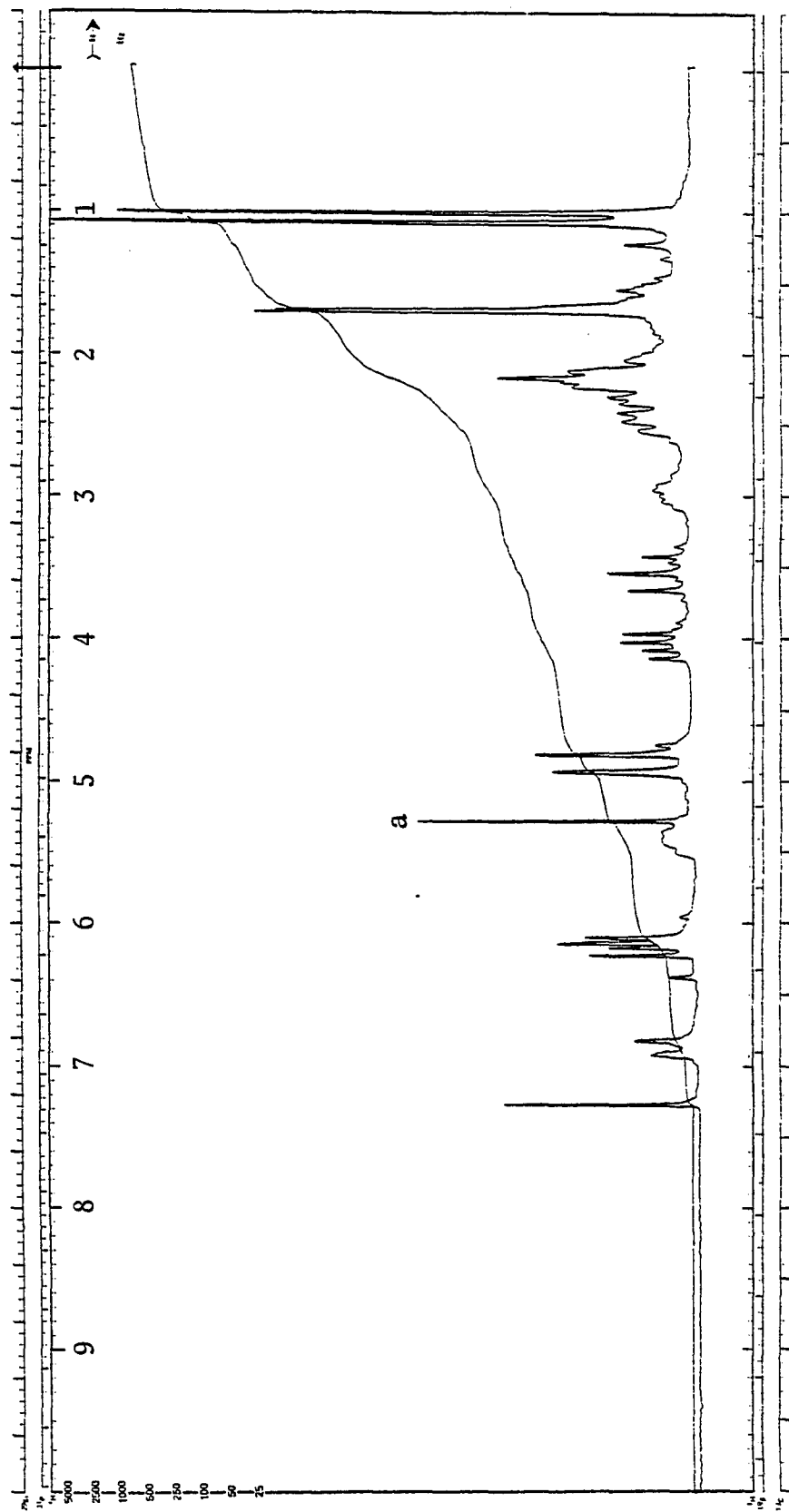
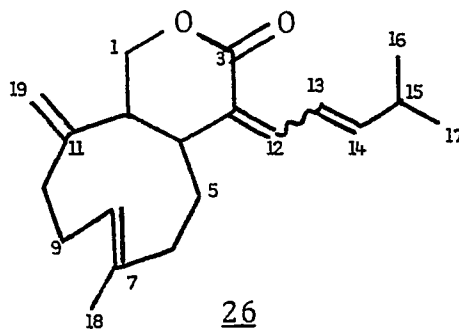


Figure 32. 100 MHz ^1H NMR spectrum of coraxeniolide-B (26) in C_6D_6 .



CH_2Cl_2

Figure 33. 100 MHz ^1H NMR spectrum of coraxeniolide-B (26) in CDCl_3 .



The proton on C-12 is a doublet ($J = 12$ Hz) at δ 7.16, coupled to H-13 which appears as a broad doublet of doublets ($J = 15$ Hz, $J = 12$ Hz) at δ 6.38. This H-13 proton at δ 6.38 is also trans-coupled to a doublet of doublets ($J = 15$ Hz, $J = 8$ Hz) at δ 5.84, which is assigned to H-14. The proton at δ 5.84 is undoubtedly coupled to H-15, although this signal could not be located.

An isopropyl group appears as a six-hydrogen doublet ($J = 7$ Hz) at δ 1.04 in the ^1H NMR spectrum of coraxeniolide-B (26). Its presence is also supported by the loss of 43 mass units (m/z 257) from the molecular ion in the mass spectrum of 26 (Fig. 34). The exocyclic methylene protons are seen as two one-hydrogen singlets at δ 4.94 and δ 4.82, and the vinyl methyl on C-7 is a doublet ($J = 1$ Hz) at δ 1.69, allylically coupled to H-8.

The geminal coupling ($J = 12$ Hz) and vicinal coupling ($J = 12$ Hz, $J = 6$ Hz) of the C-1 protons in the CDCl_3 spectrum of 26 (100 MHz, Fig. 33, Table 3) are very similar to the

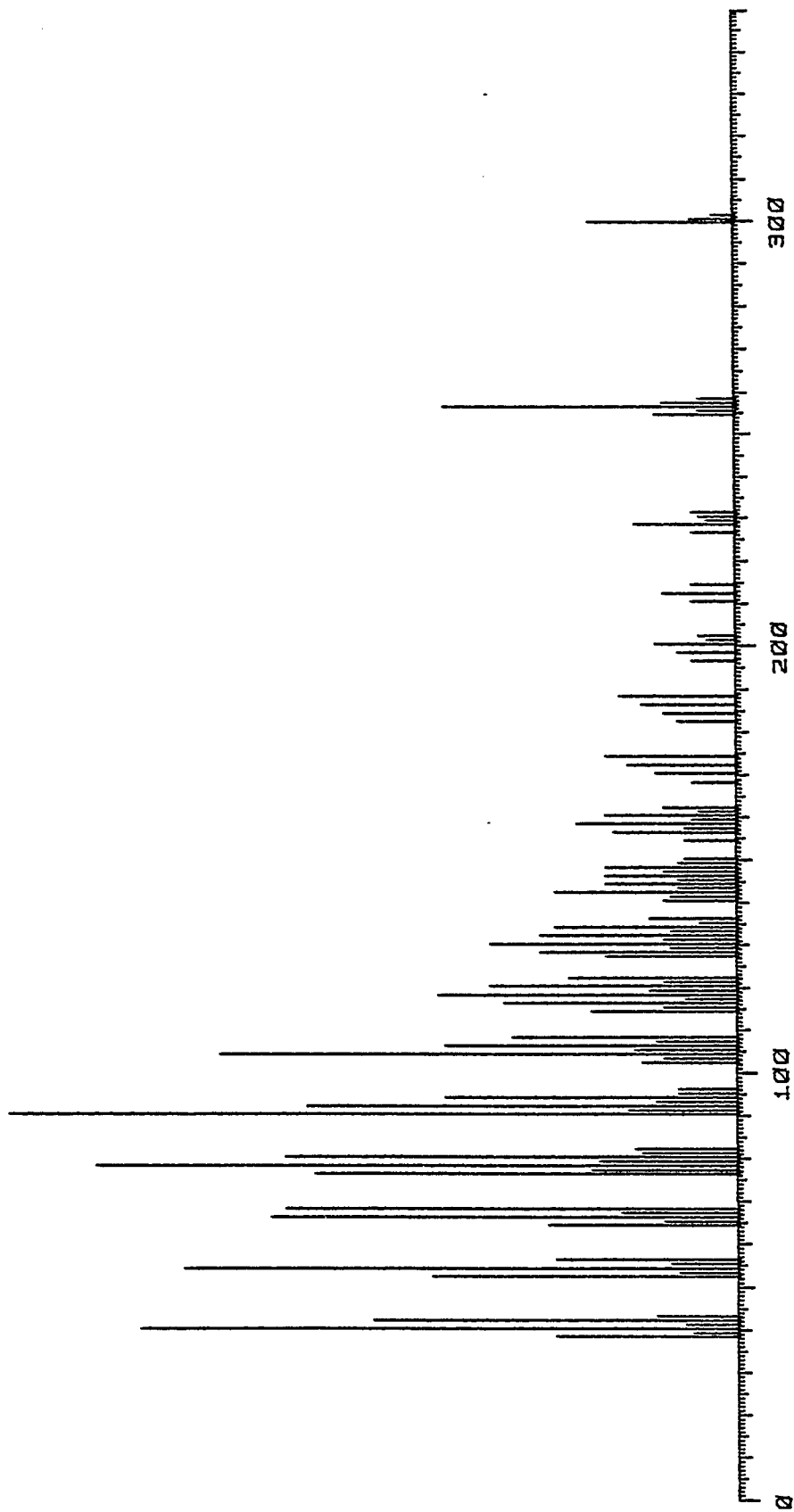
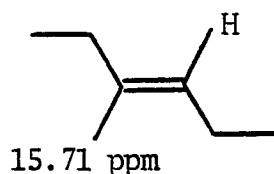
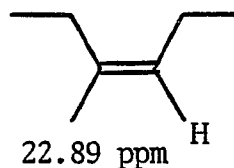


Figure 34. Mass spectrum of coraxeniolide-B (26).

geminal ($J = 12$ Hz) and vicinal ($J = 12$ Hz, $J = 7$ Hz) coupling of these protons in coraxeniolide-A (22). These data suggest that coraxeniolide-B (26) and coraxeniolide-A (22) have the same carbon skeletons with similar conformations, that is, a trans ring fusion and a boat conformation for the lactone. The importance of the vicinal coupling constants of the C-1 protons in elucidating conformations will become apparent later when I discuss similar compounds with different conformations.

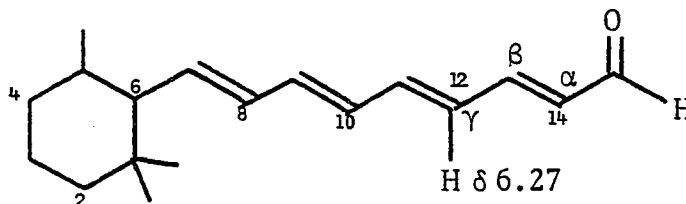
The difference in the chemical shifts of the C-1 protons of coraxeniolide-B (100 MHz, CDCl_3 , $4.05 - 3.54 = 0.51$ ppm) is large compared to the difference in coraxeniolide-A (100 MHz, CDCl_3 , $4.19 - 3.93 = 0.26$ ppm). Hagaman²⁵ has determined that for nonequivalent geminal protons the off-resonance ^{13}C signal will appear as a doublet of doublets, if the difference in the chemical shifts of the protons is greater than three times the geminal coupling. Conversely, if the difference is less than three times the geminal coupling, the signal will appear as a triplet. In coraxeniolide-B the difference in chemical shifts is 51 Hz, which is greater than three times the geminal coupling ($3 \times 12 = 36$ Hz), and C-1 appears as a doublet of doublets (Fig. 29) in the ^{13}C off-resonance spectrum. The 26 Hz difference seen in the ^1H NMR spectrum of coraxeniolide-A (22) is less than three times the geminal coupling ($3 \times 12 = 36$ Hz) and C-1, therefore, appears as a triplet.

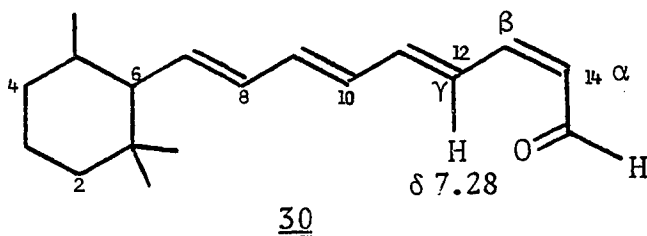
The configuration of the C-7(8) double bond in coraxeniolide-B (26) was resolved by examination of the ^{13}C NMR spectrum. Carbon-18 appears as a quartet at 16.73 ppm, which is typical of E configuration, rather than in the 22-25 ppm region, which is characteristic of Z configuration. The validity of this assignment (20 MHz, CDCl_3) is illustrated by the monoolefins 27 and 28.²⁶ Also,

27 (E)28 (Z)

C-18 in coraxeniolide-A (22), which is known to have E configuration, absorbs at 16.73 ppm, as expected.

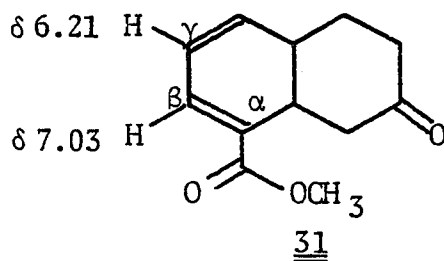
The only remaining point of uncertainty in the structure elucidation of coraxeniolide-B (26) is the stereochemistry of the C-4(12) double bond. The ^1H NMR spectra (220 MHz, CDCl_3) of two model compounds, trans-retinal (29) and 13-cis-retinal (30) helped to resolve this point.²⁷ The proton γ to the carbonyl in 29 (H-12)

29



absorbs at δ 6.27, while the H-12 proton of 30 is found at δ 7.28. The large downfield shift of this proton in 30 must be due to the anisotropic effect of the carbonyl. The chemical shift of the γ -proton of coraxeniolide-B (26) (H-13) is δ 6.38 (100 MHz, C_6D_6) supporting a trans relationship between the lactone carbonyl and C-13.

The 1H NMR spectrum of 31 ($CDCl_3$)²⁸ also supports this assignment. In this compound the β -proton has a cis relationship to the carbonyl, while the γ -carbon is trans to

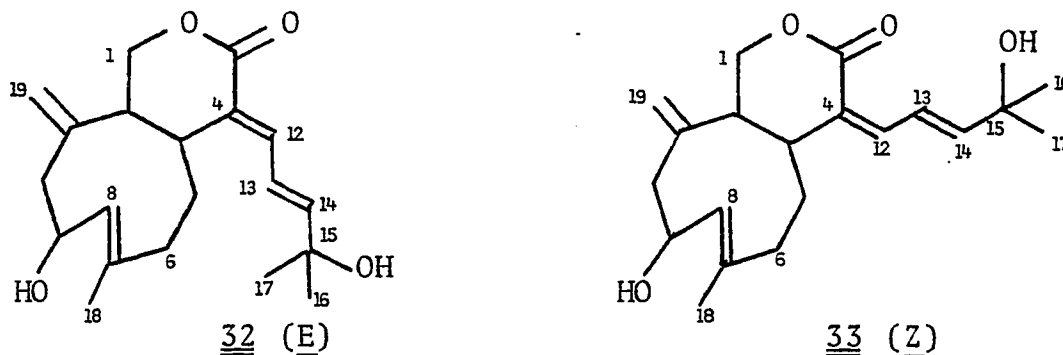


the carbonyl. The β -proton is found at lower field (δ 7.03) than the γ -proton (δ 6.21). This is the same relationship as observed in coraxeniolide-B (26).

Lastly, the 1H NMR spectra of the isomers xeniolide-A (32, 270 MHz)²⁹ and isoxeniolide-A (33, 100 MHz)³⁰ ($CDCl_3$, Table 3) support E stereochemistry for the C-4(12) double

Table 3.
 ^1H NMR Spectral Data of Coraxeniolide-B (26),
 Xeniolide-A (32), and Isoxeniolide-A (33)

	<u>26</u> (100 MHz, C_6D_6)	<u>26</u> (100 MHz, CDCl_3)	<u>32</u> (270 MHz, CDCl_3)	<u>33</u> (100 MHz, CDCl_3)
HC-12	7.16 1H d (J=12 Hz)	6.86 1H d (J=12 Hz)	6.92 1H d (J=11 Hz)	6.39 1H d (J=10 Hz)
HC-13	6.38 1H bdd (J=15,12 Hz)	6.40-6.04 2H m	6.53 1H dd (J=15,11 Hz)	6.85 1H dd (J=15,10 Hz)
HC-14	5.84 1H dd (J=15,8 Hz)		6.26 1H d (J=15 Hz)	6.06 1H d (J=15 Hz)
H_3C -16, 17	0.91 6H d (J=6 Hz)	1.04 6H d (J=7 Hz)	1.38 6H s	1.33 6H s
HC-1 β	3.88 1H dd (J=12,6 Hz)	4.05 1H dd (J=12,6 Hz)	4.08 1H dd (J=11,6 Hz)	4.07 1H dd (J=12,6 Hz)
HC-1 α	3.46 1H dd (J=12,12 Hz)	3.54 1H dd (J=12,12 Hz)	3.61 1H dd (J=11,11 Hz)	3.61 1H dd (J=12,12 Hz)
H_2C -19	4.71 2H s	4.94 1H s 4.82 1H s	5.09 1H s 4.91 1H s	5.09 1H s 4.95 1H s
HC-8	5.37 1H m	5.38 1H m	5.32 1H d (J=8 Hz)	5.24 1H d (J=8 Hz)
H_3C -18	1.46 3H d (J=1.5 Hz)	1.69 3H d (J=1 Hz)	1.70 3H s	1.67 3H s



bond in coraxeniolide-B (26). In xeniolide-A, H-12 is the lowest field proton (δ 6.92 d), as it is in coraxeniolide-B (26) (δ 6.86 d), while H-13 is found at lowest field in isoxeniolide-A (δ 6.85 dd) and H-12 appears at δ 6.39. Also, the UV spectrum of xeniolide-A has a maximum at 268 nm, while the maximum of isoxeniolide-A is found at 263 nm, which again supports E stereochemistry for the C-4(12) double bond of 26 (270 nm).

I would like to suggest the name coraxeniolide-B for compound 26, which implies its source (Corallium sp.), as well as its close structural relationship to the xeniolides.

C. Structural Determination of Coraxeniolide-C (34)

Coraxeniolide-C (34), a minor (65 mg/kg) constituent of Corallium sp., is a white, crystalline solid, mp 68-69°C. The mass spectrum of 34 (Fig. 35) exhibits a molecular ion at m/z 300, with composition $C_{20}H_{28}O_2$, indicating that coraxeniolide-C (34) and coraxeniolide-B (26) are isomeric.

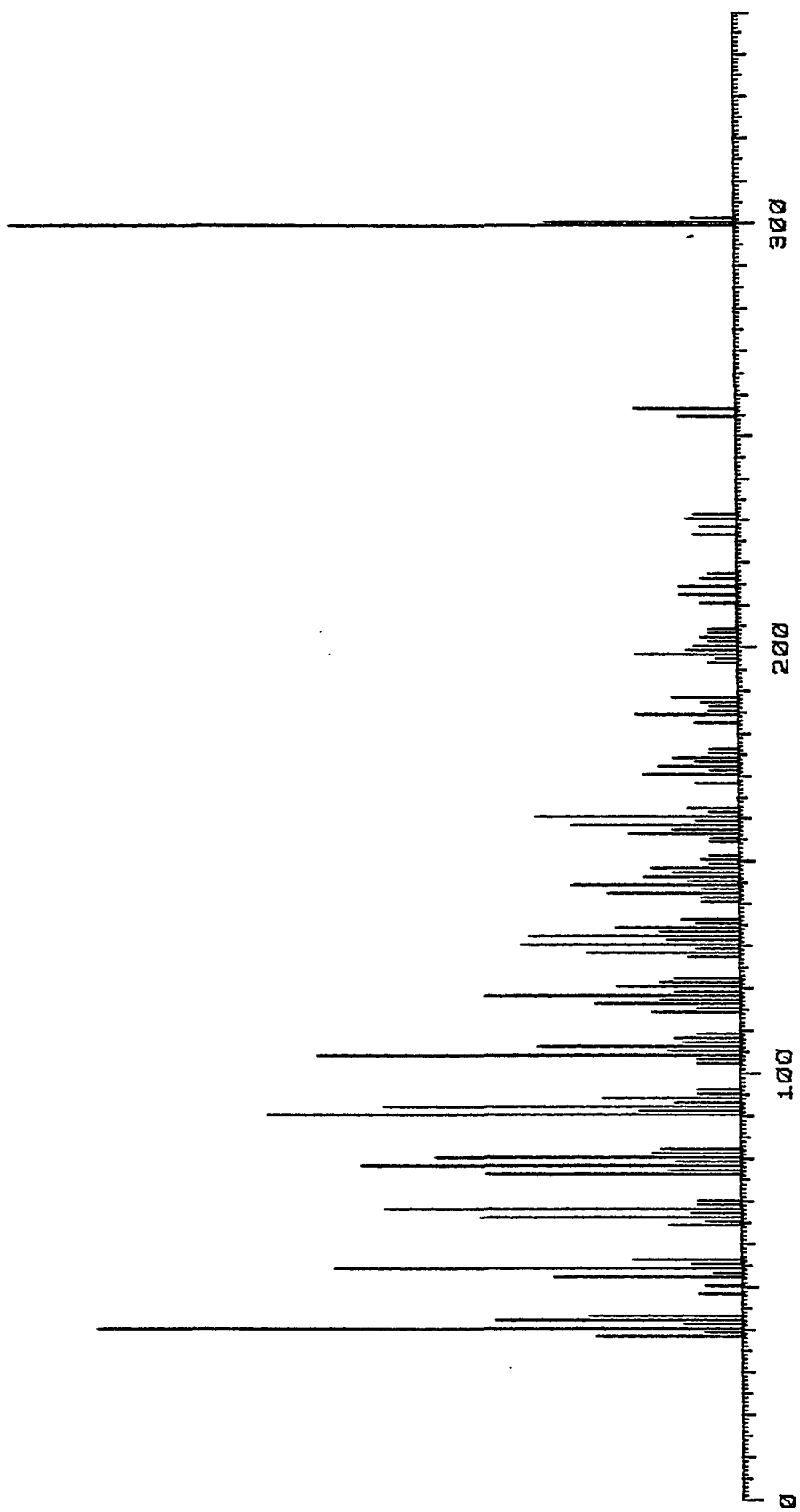
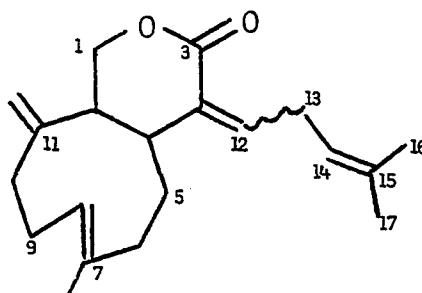


Figure 35. Mass spectrum of coraxeniolide-C (34).

The IR spectrum (Fig. 36) indicates that 34 contains a lactone (1737 cm^{-1}) and an exocyclic methylene (900 cm^{-1}). The ^{13}C NMR spectrum corroborates these assignments with absorbances at 169.44 (s) and 71.66 (dd) ppm (Fig. 37) for the lactone, and a triplet in the off-resonance spectrum at 112.81 ppm for the exocyclic methylene. Seven other olefinic carbons at 152.44 (s), 137.12 (d), 135.62 (s), 133.77 (s), 133.07 (s), 124.26 (d), and 121.00 (d) ppm are evidence for a total of four double bonds. Four unsaturations for double bonds and two for the lactone leave the seventh unsaturation for an additional ring in the structure of coraxeniolide-C (34).

The UV spectrum of 34 (Fig. 38) has a maximum at 215 nm, probably due to the presence of an α,β -unsaturated lactone. This initial characterization, along with the ^1H NMR spectrum (100 MHz, CDCl_3 , Fig. 39), and decoupling data suggest structure 34 for coraxeniolide-C.



34

The proton on C-12 is a triplet ($J = 7\text{ Hz}$) at δ 5.79, coupled to a doublet of doublets ($J = 7\text{ Hz}$, $J = 7\text{ Hz}$) at

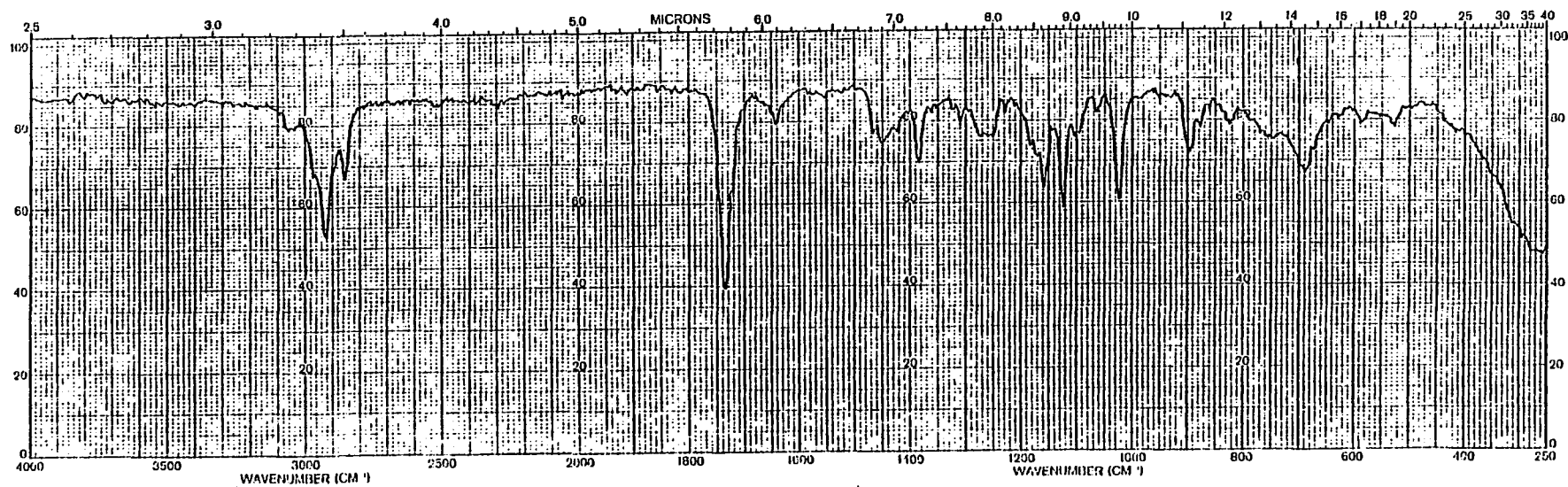


Figure 36. IR spectrum of coraxeniolide-C (34).

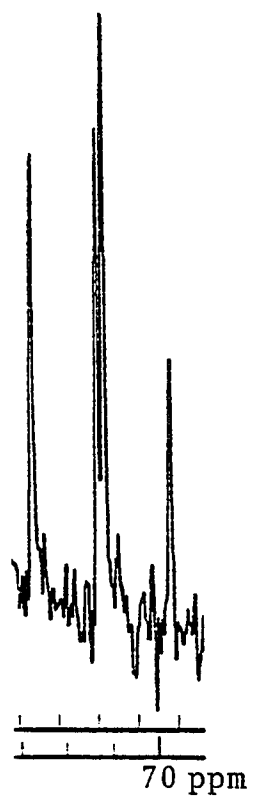


Figure 37. Expansion of the 71.66 ppm signal in the off-resonance ^{13}C NMR spectrum of coraxeniolide-C (34).

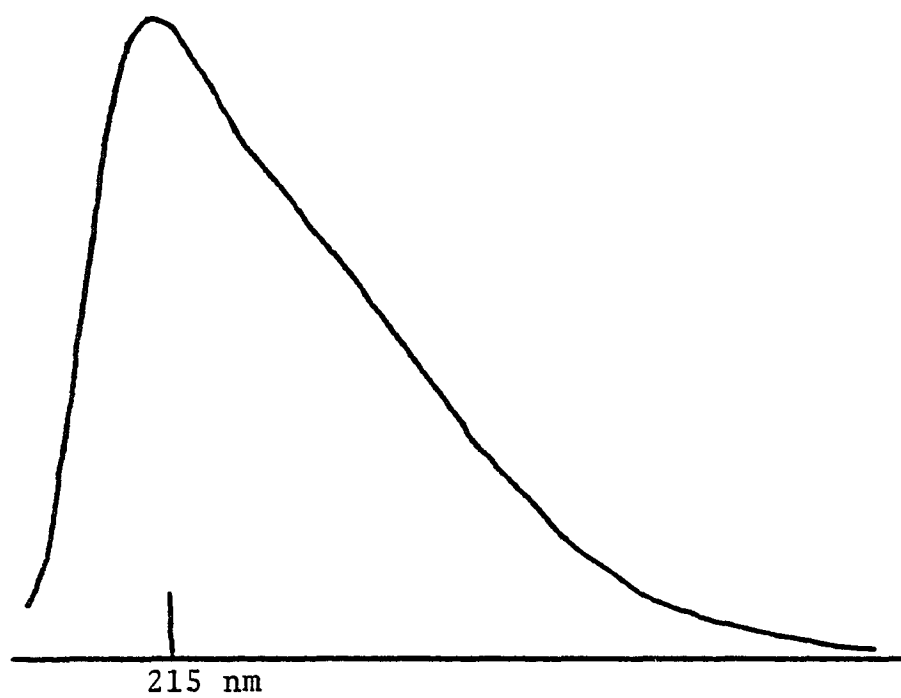


Figure 38. UV spectrum of coraxeniolide-C (34).

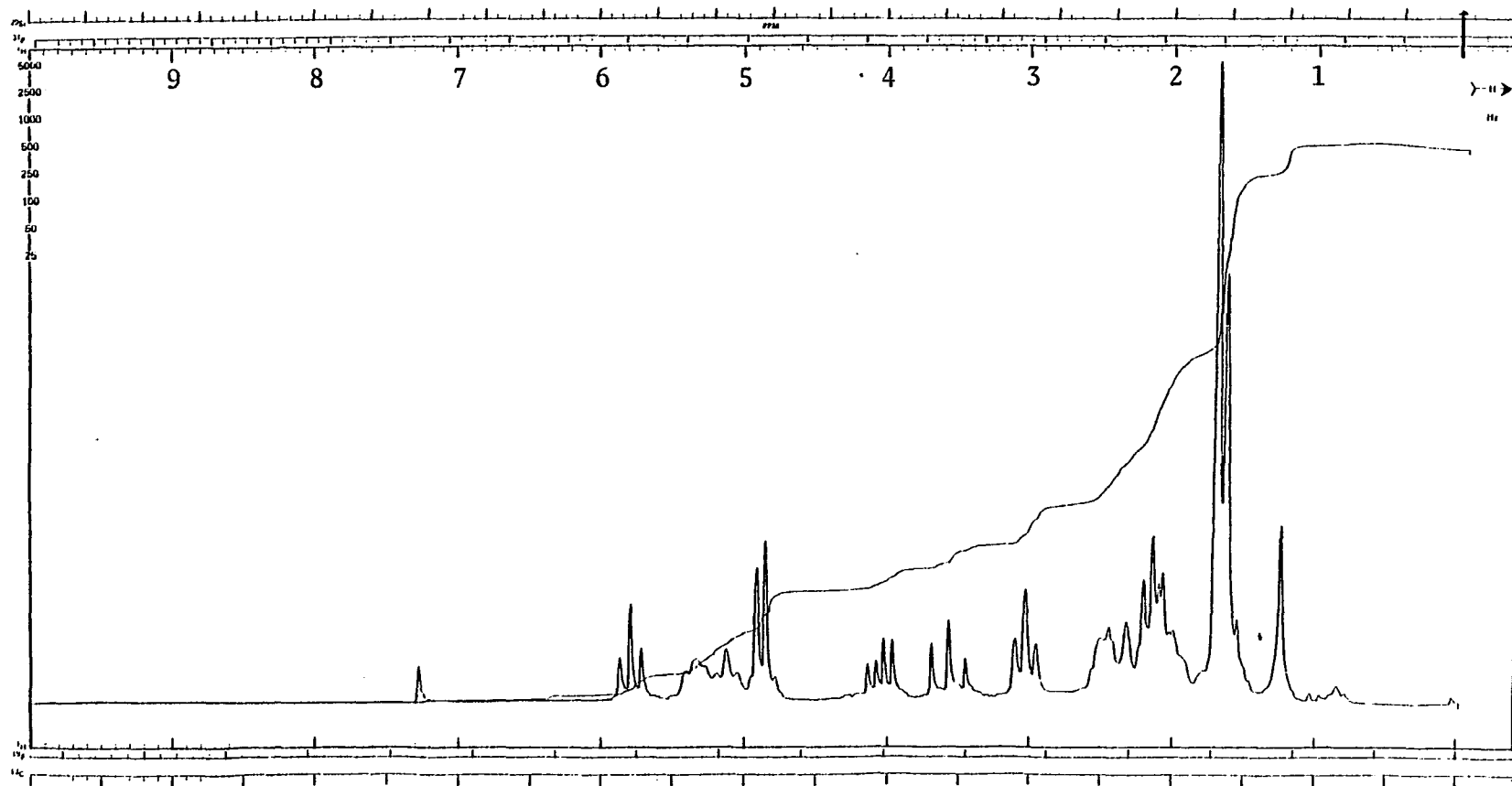


Figure 39. 100 MHz ^1H NMR spectrum of coraxeniolide-C (34) in CDCl_3 .

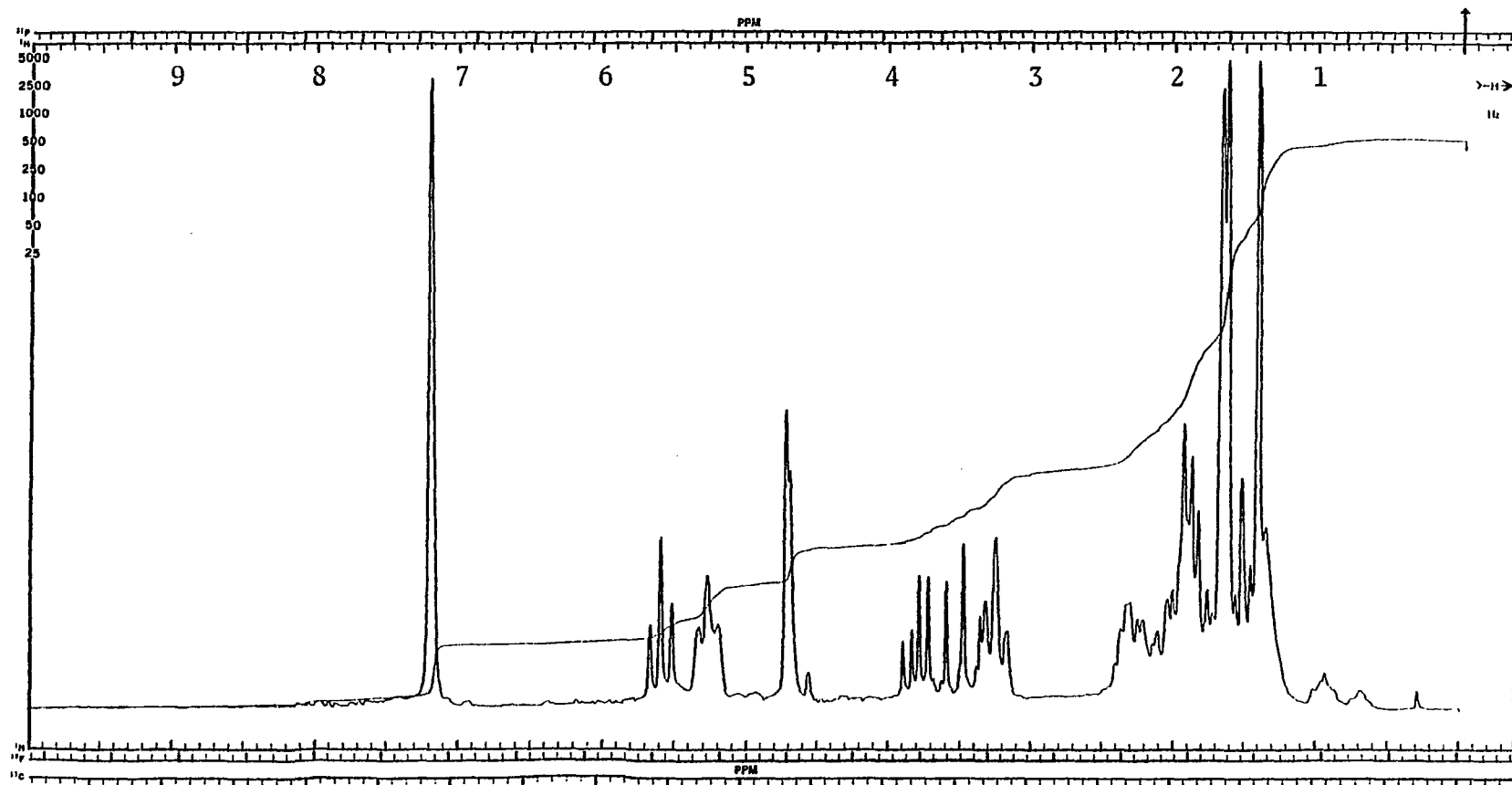
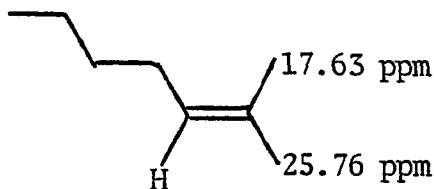


Figure 40. 100 MHz ^1H NMR spectrum of coraxeniolide-C (34) in C_6D_6 .

δ 3.02, which is assigned to the two hydrogens on C-13. These C-13 protons are also coupled to a one-proton broad triplet ($J = 7$ Hz) at δ 5.22 (H-14). The olefinic proton on C-8 is seen as a multiplet at δ 5.33, and the two protons of the exocyclic double bond are singlets at δ 4.91 and δ 4.85. Irradiation of the methyls bonded to C-15 (δ 1.68) cause sharpening of the signals at δ 5.22 and δ 3.02. An additional vinyl methyl absorbs at δ 1.62.

The protons on the methylene bonded to oxygen (C-1) appear as doublet of doublets at δ 4.05 ($J = 12$ Hz, $J = 6$ Hz) and δ 3.56 ($J = 12$ Hz, $J = 12$ Hz). The difference in the chemical shifts of these geminal protons (49 Hz) is again larger than three times the geminal coupling ($3 \times 12 = 36$ Hz). This explains why the ^{13}C off-resonance NMR spectrum contains a doublet of doublets (Fig. 37) for the oxygen-bearing carbon in coraxeniolide-C, instead of a triplet.²⁵

The vinyl methyls seen in the ^{13}C NMR spectrum of coraxeniolide-C (34) can be assigned by comparing them with the model olefin 35.²⁶ By analogy, the vinyl methyl trans



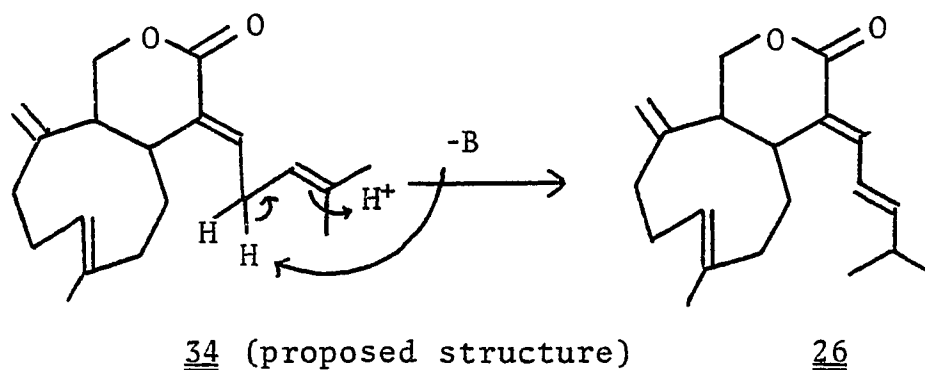
35

to the side chain (C-17) in 34 is assigned to the quartet at 25.89 ppm, while the cis methyl (C-16) is found at 18.05 (q) ppm.

The remaining signal at 16.56 (q) ppm for the vinyl methyl on C-7 indicates E configuration for C-7(8) double bond, as previously discussed for coraxeniolide-B (26).²⁶

The last two points that remain to be resolved in the structure elucidation of coraxeniolide-C (34) are the stereochemistry of the C-4(12) double bond and the stereochemistry of the ring fusion.

Assuming that the side chain bonded to C-12 is trans to the carbonyl of the lactone, I attempted to transform coraxeniolide-C (34) into coraxeniolide-B (26) by base, as illustrated in Scheme 3. The reaction of 34 with diaza-



Scheme 3

bicycloundec-5-ene (DBU) produced a 26% yield of coraxeniolide-D and a 20% yield of coraxeniolide-D', neither of which corresponds to coraxeniolide-B (26).

Coraxeniolide-D (36) is a crystalline, white solid (mp 127-129°C) with composition $C_{20}H_{28}O_2$ and is, therefore, an isomer of coraxeniolide-C (34). The IR spectrum (Fig. 41) has absorbances at 1745 and 890 cm^{-1} , indicating that the

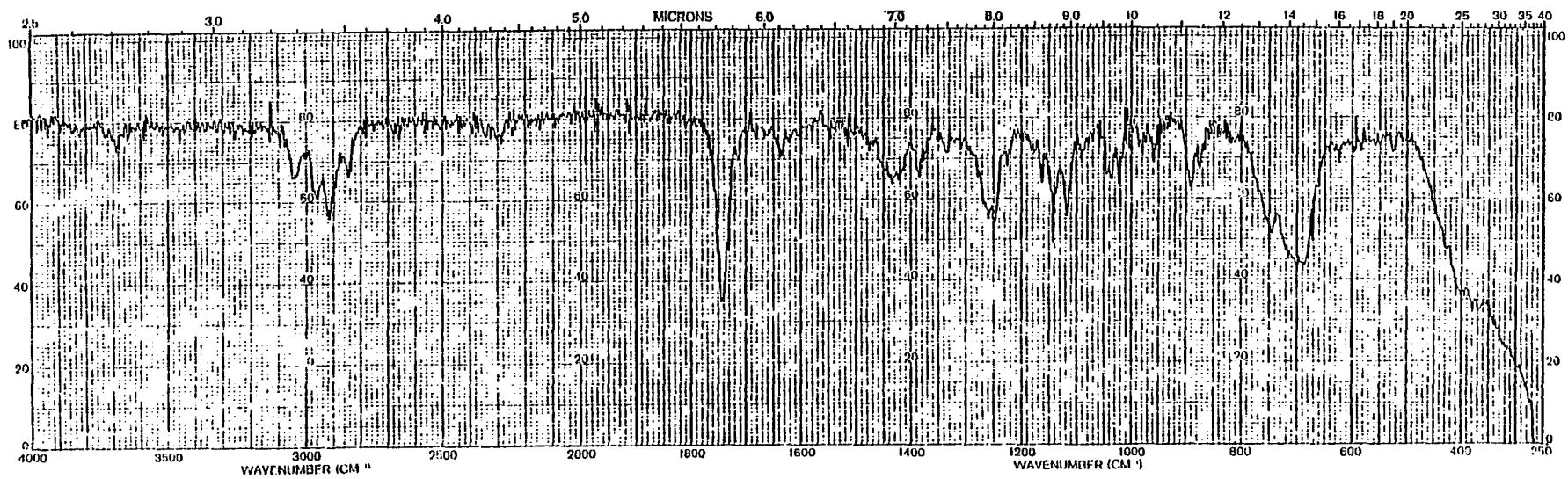
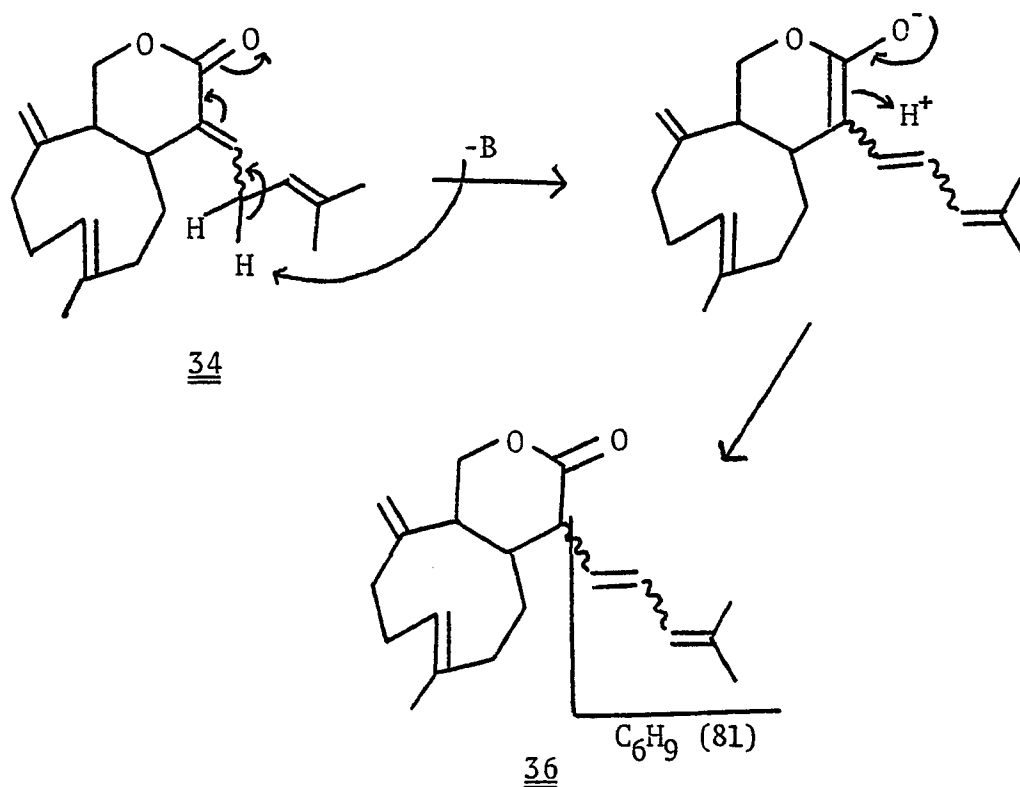


Figure 41. IR spectrum of coraxeniolide-D (36).

lactone and exocyclic methylene from 34 are still intact in 36

The maximum in the UV spectrum has shifted from 215 nm in 34 to 239 nm in 36 (Fig. 42). The maximum should be in the range 260-270 nm for an $\alpha,\beta,\gamma,\delta$ -unsaturated lactone as already seen in coraxeniolide-B (26) (270 nm), xeniolide-A (32) (268 nm),²⁹ and isoxeniolide-A (33) (263 nm).³⁰ An explanation of the UV spectrum is the transformation of 34 into a diene, as seen in Scheme 4. a loss of C_6H_9 (m/z 219, 13%) from the molecular ion in the mass spectrum of 36 (Fig. 43) supports this hypothesis.



Scheme 4

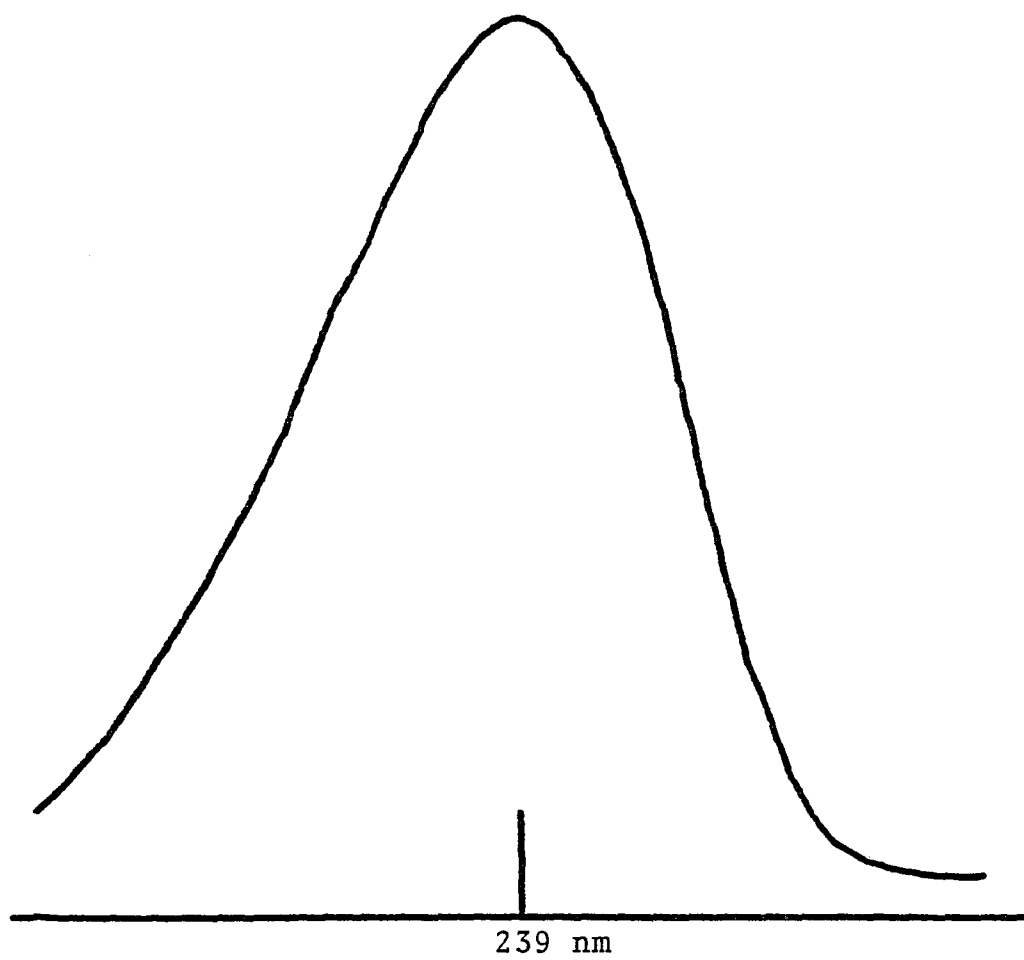


Figure 42. UV spectrum of coraxeniolide-D (36).

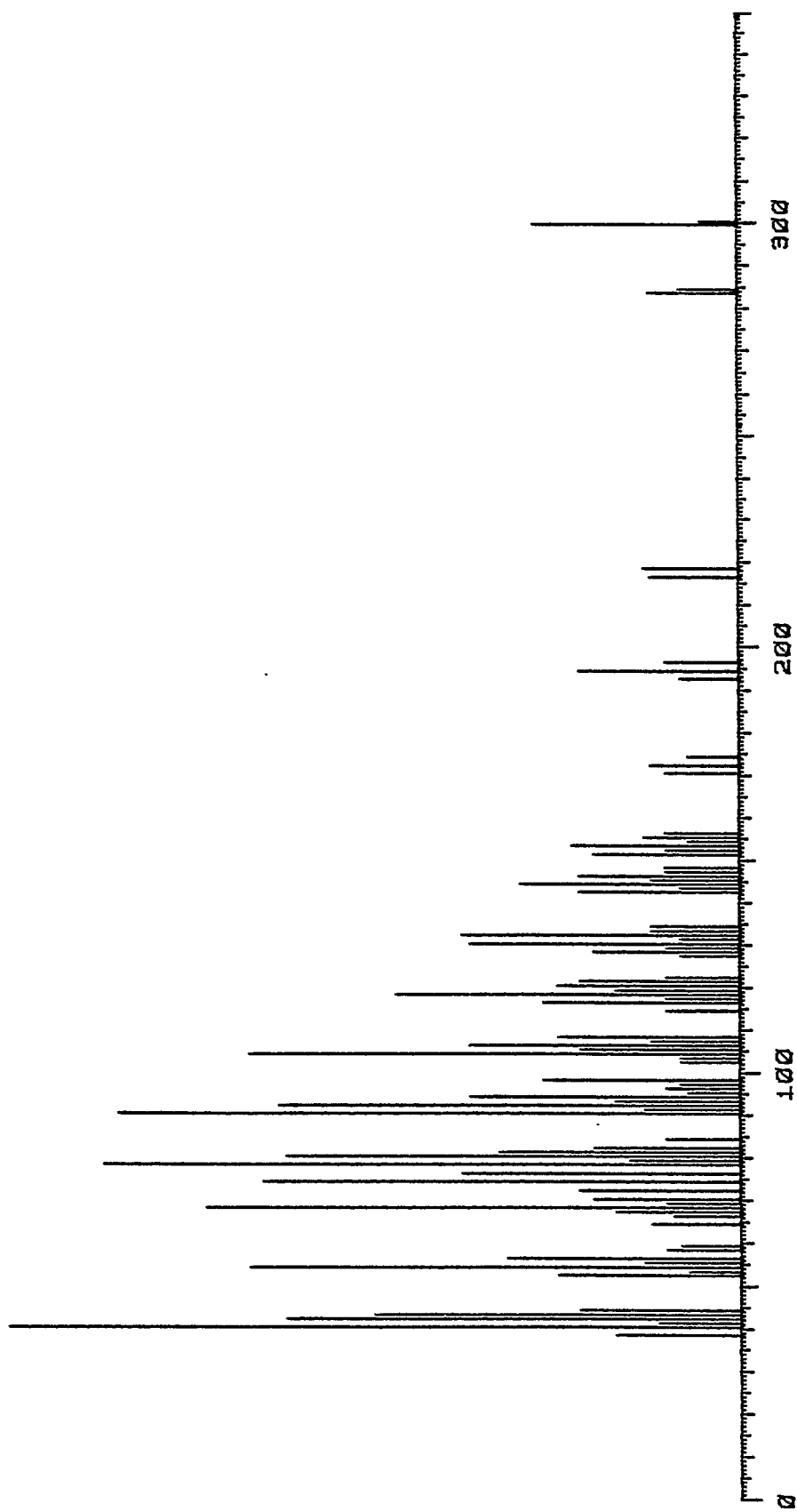
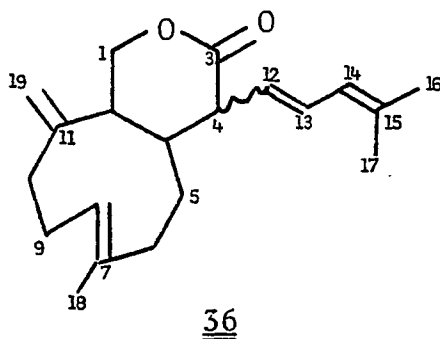


Figure 43. Mass spectrum of coraxeniolide-D (36).

The ^1H NMR spectrum of coraxeniolide-D (100 MHz, CDCl_3 , Fig. 44, Table 4) and decoupling data substantiate this interpretation and, furthermore, establish the stereochemistry of the C-12(13) double bond as seen below.



The proton on C-4 appears as a broad doublet of doublets ($J = 7$ Hz, $J = 7$ Hz) at δ 3.58; it is coupled to H-12, which is a doublet of doublets ($J = 15$ Hz, $J = 7$ Hz) at δ 5.90. This H-12 proton is trans coupled to H-13, which is also a doublet of doublets ($J = 15$ Hz, $J = 10$ Hz) and appears at δ 6.39. The proton on C-13 is in turn coupled to H-14 seen as a broad doublet ($J = 10$ Hz) at δ 5.89. Lastly, irradiation of the six-proton broad singlet at δ 1.78 (C-16, C-17) transforms the broad doublet corresponding to H-14 into a sharp doublet.

The C-1 protons of coraxeniolide-D appear as doublets of doublets at δ 4.21 ($J = 12$ Hz, $J = 8$ Hz) and δ 3.96 ($J = 12$ Hz, $J = 12$ Hz). The proton on C-8 appears as a broad triplet at δ 5.34, while the olefinic protons on C-19 are seen as singlets at δ 5.04 and δ 5.01. The vinyl methyl bonded to C-9 is found at δ 1.68.

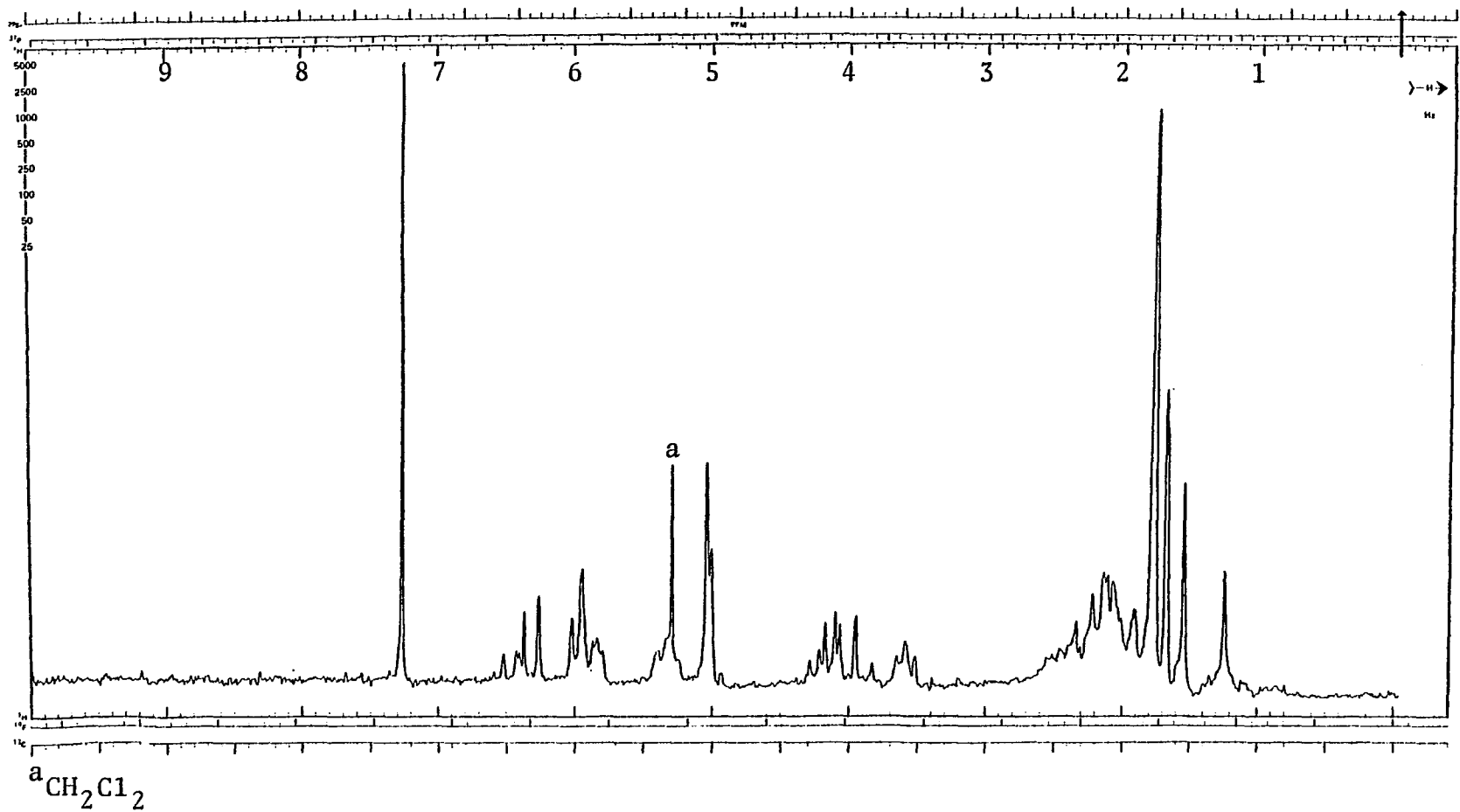
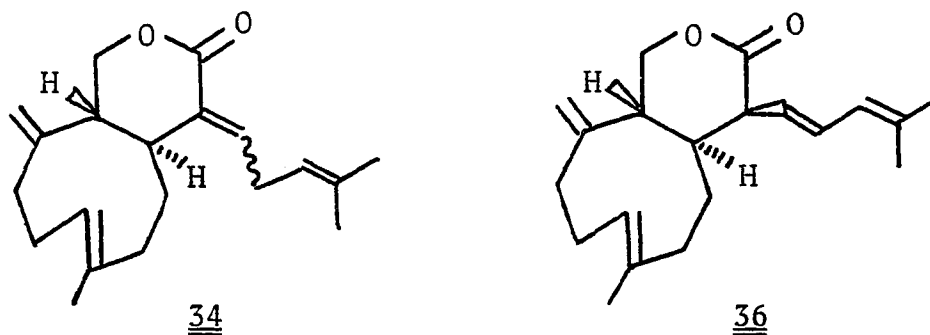


Figure 44. 100 MHz ^1H NMR spectrum of coraxeniolide-D (36) in CDCl_3 .

Several attempts were made to transform coraxeniolide-C (34) to hexacoraxeniolides 23 and 24 by hydrogenation, in order to prove that the ring juncture in coraxeniolide-C (34) is trans, as in coraxeniolide-A (22). However, in all cases the result was an inseparable mixture of two compounds with molecular weights 306 and 308. Since it was probably the C-4(12) double bond in 34 that was not being fully hydrogenated, hydrogenation of coraxeniolide-D (36), which contains no α,β -unsaturated lactone, should yield the same information.

Coraxeniolide-D (36) was hydrogenated by stirring with 10% Pd/C in methanol in a hydrogen atmosphere to give a 71% yield of a mixture of compounds identical to the hexacoraxeniolides 23 and 24 (^1H NMR, Fig. 45, MS, and IR). This proves that there is a trans ring juncture in 36 and, therefore, 34, and that the side chain bonded to C-4 in 36 has β -orientation.



An attempt was made to transform coraxeniolide-B (26) to coraxeniolide-D (36) with base in order to hydrogenate it and prove that 26 also contains a trans ring fusion.

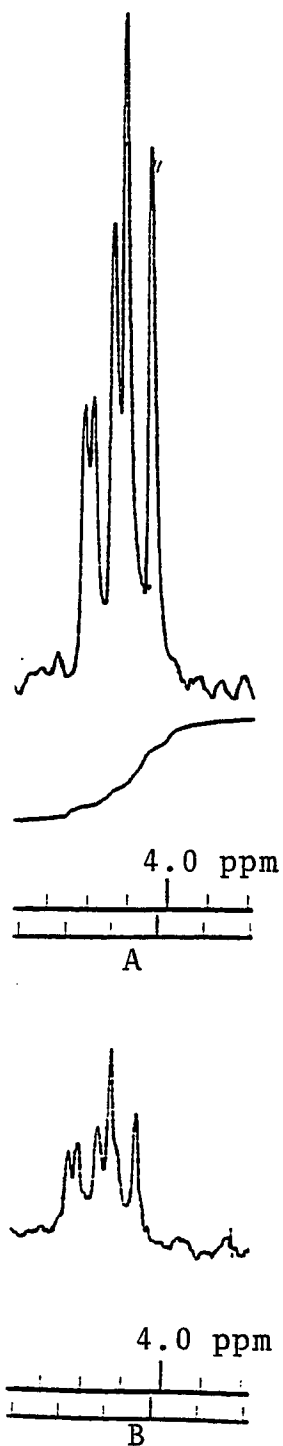


Figure 45. Comparison of the C-1 proton signals in the 100 MHz ¹H NMR spectrum (CDCl₃) of hexacoraxeniolide-A (23) and hexacoraxeniolide-A' (24) from coraxeniolide-A (22, spectrum A) and from coraxeniolide-D (36, spectrum B).

This attempt, however, was unsuccessful and resulted only in the recovery of unreacted starting material. The extreme similarity of the chemical shifts and coupling constants of the C-1 protons of 34 (δ 4.05 J = 12 Hz, J = 6 Hz; δ 3.56 J = 12 Hz, J = 12 Hz) and 26 (δ 4.05 J = 12 Hz, J = 6 Hz; δ 3.54 J = 12 Hz, J = 12 Hz) supports a trans ring fusion in coraxeniolide-B (26). On the other hand, examination of a model of 26 reveals that a cis ring fusion could generate similar coupling constants and, presumably, similar chemical shifts. The best argument for a trans ring fusion in coraxeniolide-B (26) is the extreme strain on the cyclononene ring in the conformation required for a cis ring fusion.

Coraxeniolide-D' (37), also from the reaction of coraxeniolide-C (34) with DBU, is a white, amorphous solid, mp 115-118°C. The mass spectrum of 37 (Fig. 46) has a molecular ion at m/z 300 with composition $C_{20}H_{28}O_2$, indicating that, like 36, it is isomeric with 34. The loss of C_6H_{11} (m/z 219, 12%) in the mass spectrum, along with a maximum at 237 nm in the UV spectrum (Fig. 47), strongly suggests that coraxeniolide-D' (37) is also a diene.

The 1H NMR spectrum (100 MHz, $CDCl_3$, Fig. 48, Table 4) confirms these conclusions and, moreover, suggests that coraxeniolide-D' (37) is simply the epimer of coraxeniolide-D (36) at C-4. The proton on C-4 is a doublet of doublets (J = 8 Hz, J = 8 Hz) at δ 2.89, coupled to a one-hydrogen doublet of doublets (J = 15 Hz, J = 8 Hz) at δ 5.52. The H-12

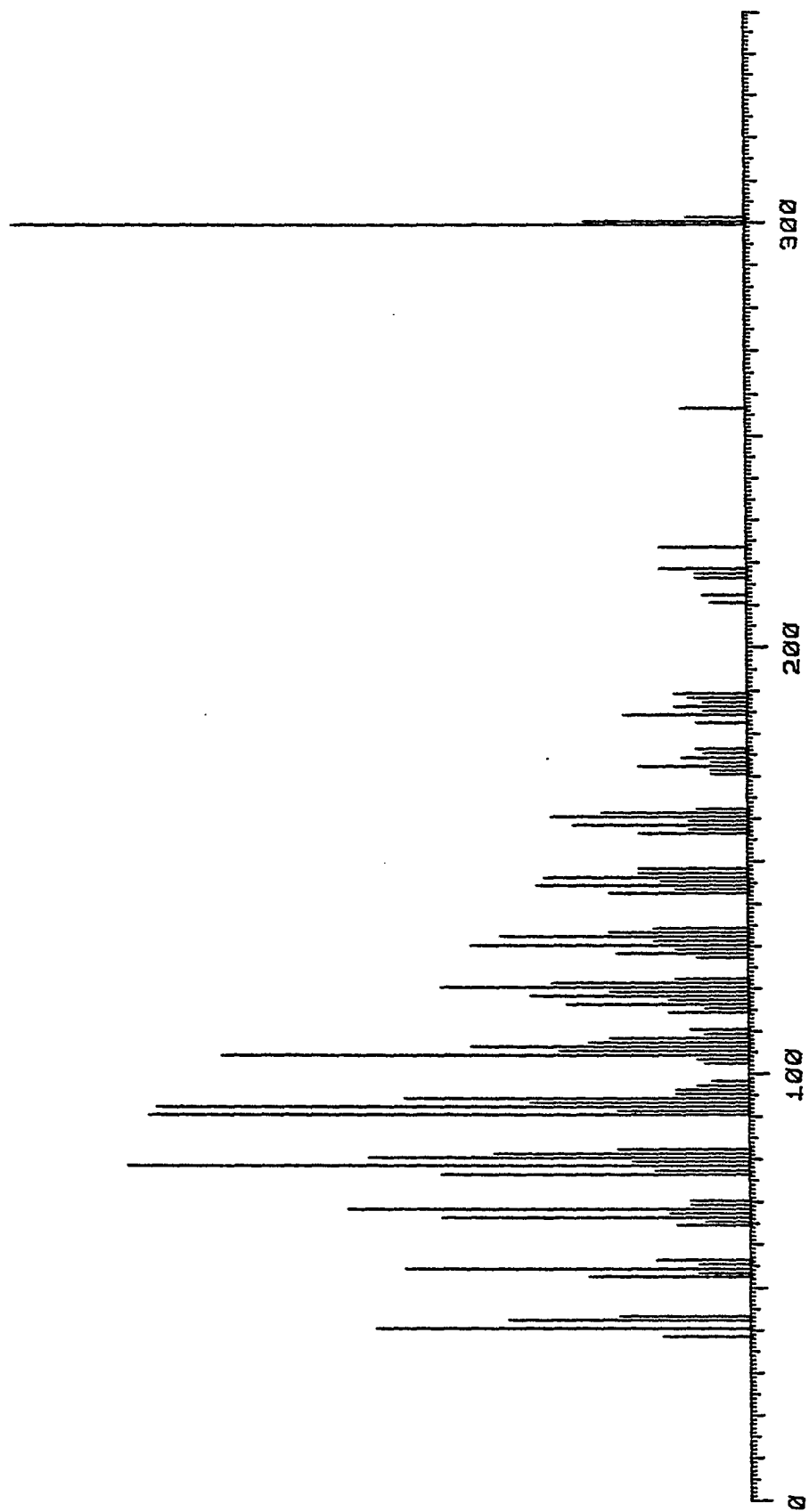


Figure 46. Mass spectrum of coraxeniolide-D' (37).

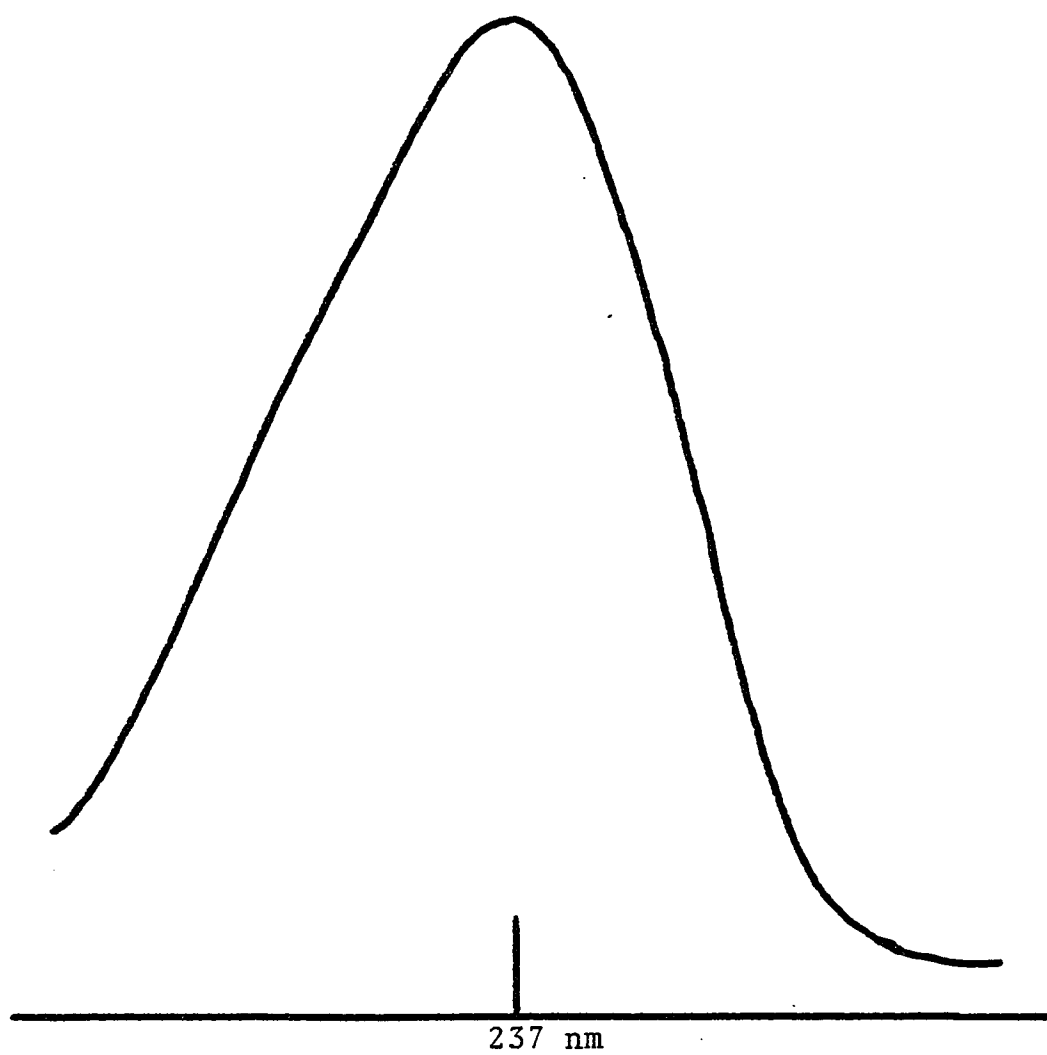


Figure 47. UV spectrum of coraxeniolide-D' (37).

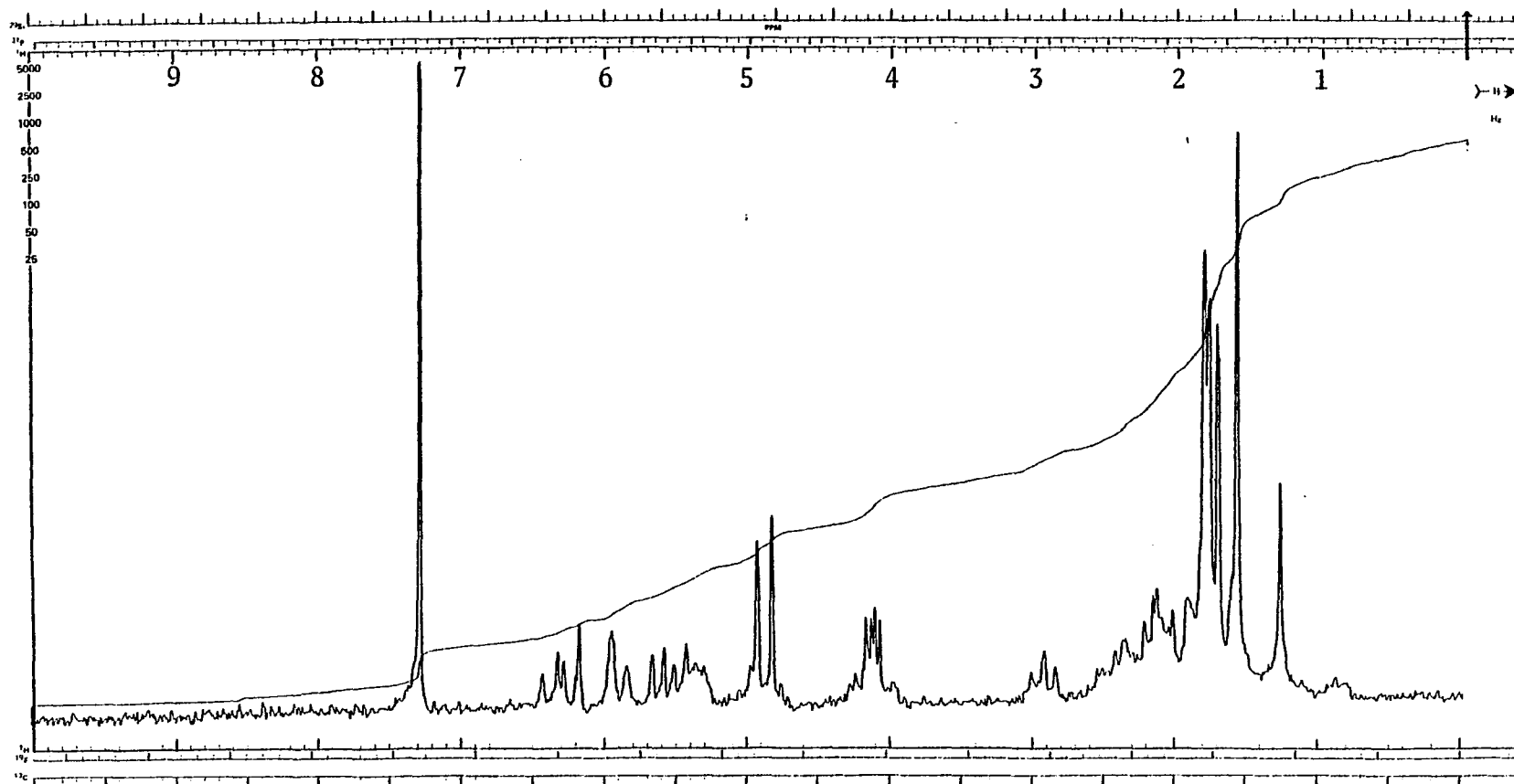


Figure 48. 100 MHz ^1H NMR spectrum of coraxeniolide-D' (37) in CDCl_3 .

proton at δ 5.52 is trans-coupled to H-13, which appears as a doublet of doublets ($J = 15$ Hz, $J = 10$ Hz) at δ 6.26. This proton is coupled to H-14 which appears as a broad doublet ($J = 10$ Hz) at δ 5.85. Three vinyl methyls are present at δ 1.76, δ 1.73, and δ 1.67. The olefinic proton on C-8 is seen as a multiplet at δ 5.34 and the exocyclic methylene protons appear as singlets at δ 4.89 and δ 4.79.

The C-1 protons of coraxeniolide-D' (37) appear as an AB system, which is difficult to interpret in the 100 MHz ^1H NMR spectrum (Fig. 48), but is well resolved in the 360 MHz ^1H NMR spectrum (CDCl_3 , Fig. 49). These protons appear at δ 4.15 and δ 4.01 and are both doublets of doublets with geminal coupling constants of 12 Hz and vicinal coupling constants of 4.5 Hz and 3.5 Hz, respectively. This radical change in the vicinal coupling of C-1 protons of coraxeniolide-D' (37) compared to coraxeniolide-D (36), can only be explained by a change in the conformation of the lactone ring (see Fig. 51).

In coraxeniolide-A (22) and coraxeniolide-D' (36) the conformation of the lactone ring is that of a boat with C-1 and C-4 down, as seen in Fig. 51. In this conformation the β -oriented side chain and C-11 of the nine-membered ring are in equatorial positions, while C-5 of the ring is axial. This conformation results in the 12 Hz and 6 Hz vicinal couplings of the protons on C-1, as well as the 7 Hz vicinal coupling observed for H-4 in 36 as illustrated in the Newman projections 1 and 2 (Fig. 51).

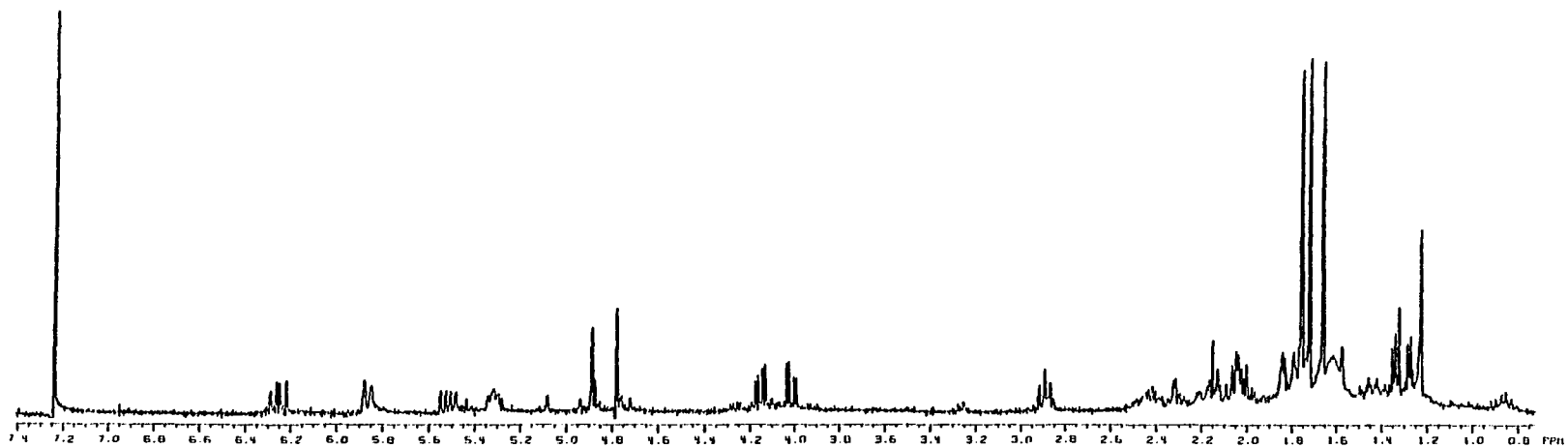


Figure 49. 360 MHz ^1H NMR spectrum of coraxeniolide-D' (37) in CDCl_3 .

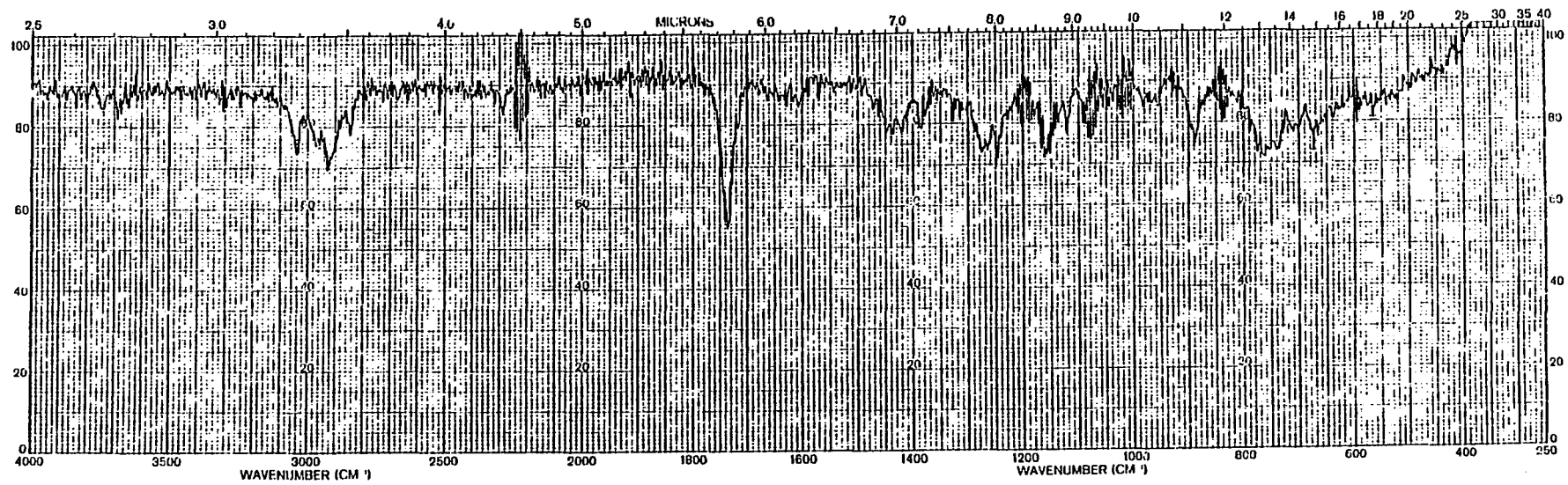


Figure 50. IR spectrum of coraxeniolide-D' (37).

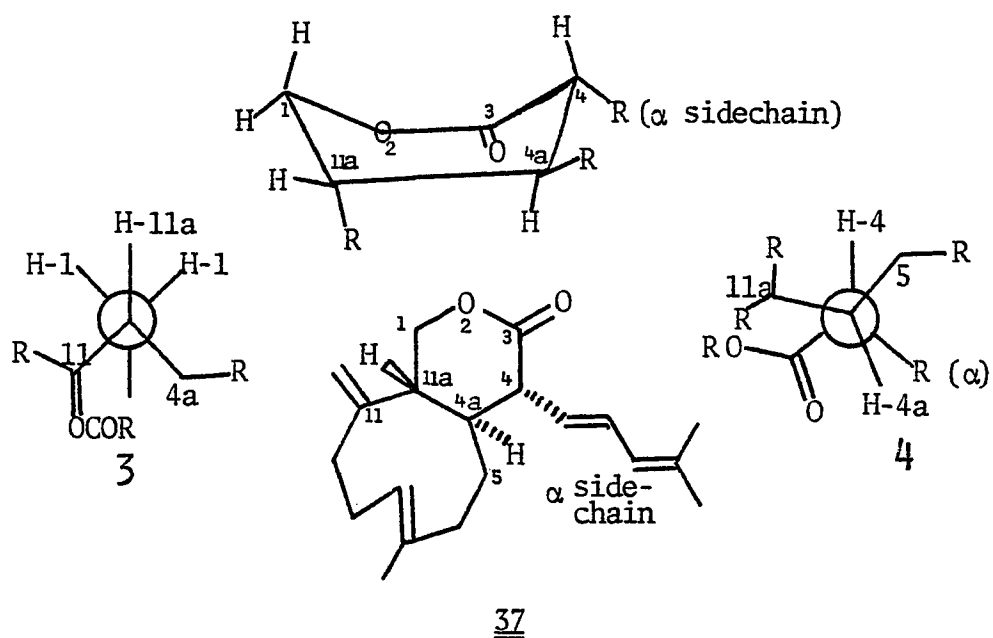
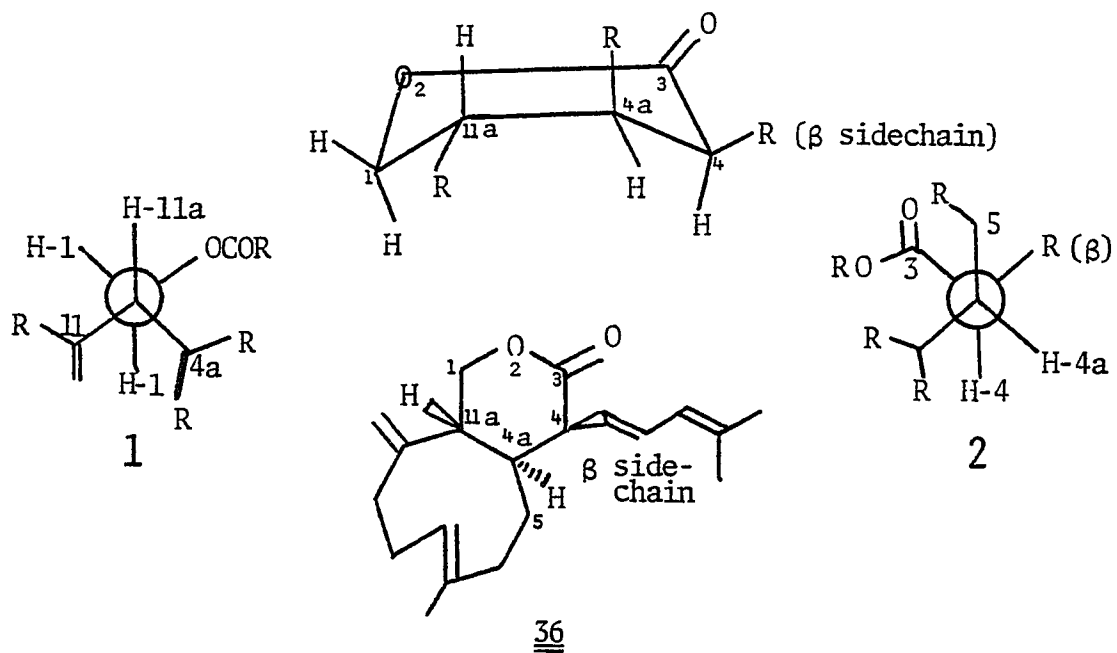
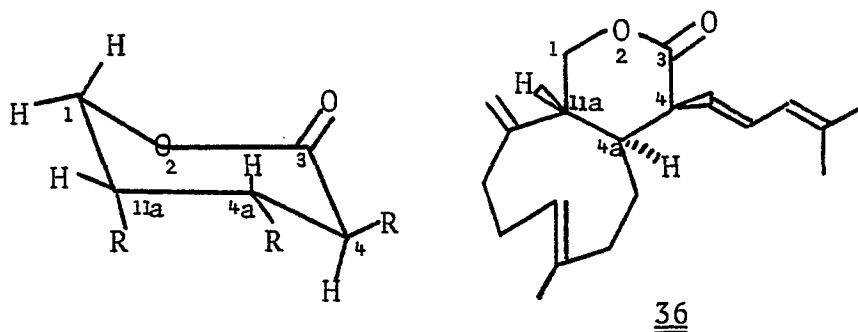


Figure 51. Conformation of coraxeniolide-D (36) and coraxeniolide-D' (37).

In compound coraxeniolide-D' (37), coupling constants of the C-1 and C-4 protons indicate another boat conformation, but with C-1 and C-4 up as seen in Fig. 51. The dihedral angle between H-11a and both C-1 protons is approximately 45° as illustrated in Newman projection 3 (Fig. 51). This explains the 3.5 Hz and 4.5 Hz vicinal coupling observed in these absorbances. Looking down the C-4a(4) bond, as seen in Newman projection 4 (Fig. 51), one observes that the dihedral angle between H-4a and H-4 is approximately 170° . This explains the 8 Hz coupling observed in the signal at δ 2.92 (H-4). In this conformation the α -side chain and C-5 of the cyclononene ring are equatorial, while C-11 is axial.

The possibility that coraxeniolide-D' (37) is a stable conformer (atropisomer) of coraxeniolide-D (36), while extremely unlikely, was considered. A chair conformation for 36 would be consistent with the data found for 37; how-



ever, hydrogenation of 37 leads to a mixture of compounds, none of which correspond to the hexacoraxeniolides 23 and 24 by thin-layer chromatography.

The configuration of the C-4(12) double bond of coraxeniolide-C (34), which still remains to be resolved, will be discussed in the next Section.

D. Structural Determination of Coraxeniolide-C' (38)

Coraxeniolide-C' (38) is another constituent (\approx 200 mg/kg) of pink coral. It is chromatographically very similar to coraxeniolide-B (26) and for this reason could never be rigorously purified. Although I was able to determine its structure, such data as the extinction coefficient of its UV maximum and its optical rotation may be slightly inaccurate.

Coraxeniolide-C' (38) is a colorless oil with composition $C_{20}H_{28}O_2$ (Fig. 52), again indicating seven unsaturations. Absorbances at 1730 and 892 cm^{-1} in the IR spectrum of 38 (Fig. 53) reveal the presence of a lactone, as well as the usual exocyclic methylene found in the coraxeniolides. The ^{13}C NMR spectrum confirms the presence of the lactone, with peaks at 171.29 and 71.07 ppm, and of the exocyclic methylene with an absorbance at 113.08 ppm. Seven other olefinic carbons appear at 152.44, 137.82, 135.53, 134.30, 133.77, 124.52, and 119.86 ppm indicating four double bonds in 38. This, as usual, leaves one additional ring besides the lactone in the structure of coraxeniolide-C' (38).

The maximum in the UV spectrum of coraxeniolide-C' (38) (Fig. 54) is found at 213 nm, which is indicative of an α,β -unsaturated lactone. These data, along with the ^1H NMR

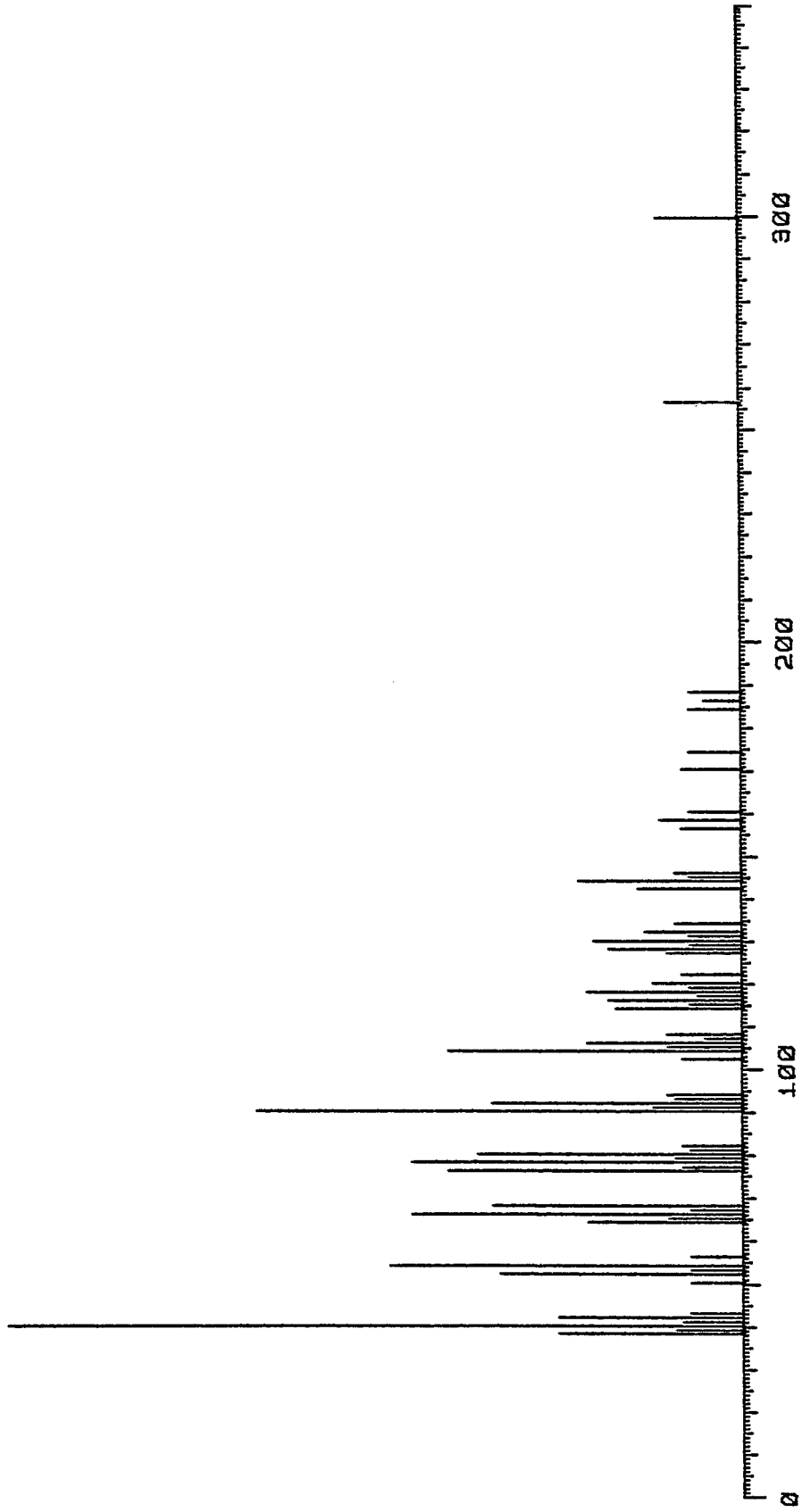


Figure 52. Mass spectrum of coraxeniolide-C' (38).

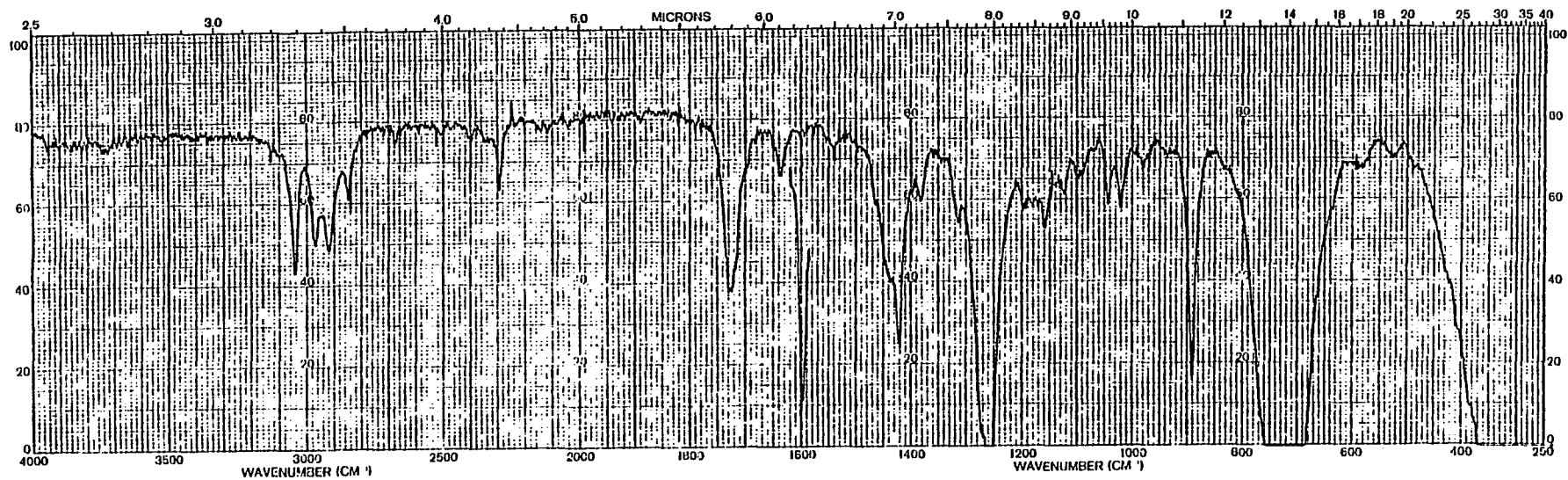


Figure 53. IR spectrum of coraxeniolide-C' (38).

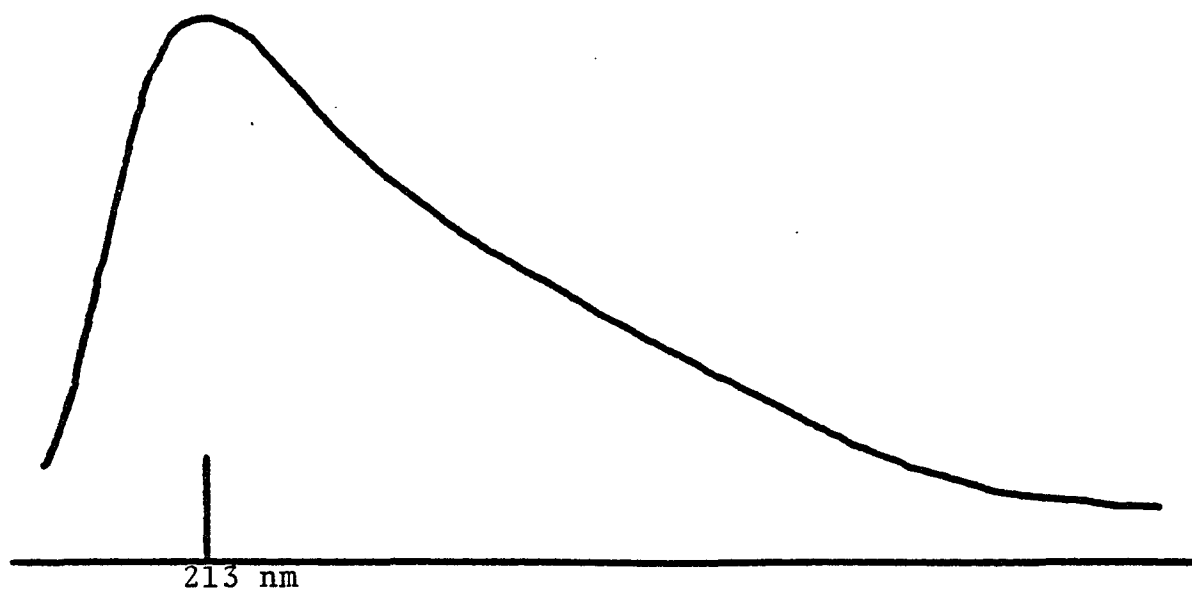
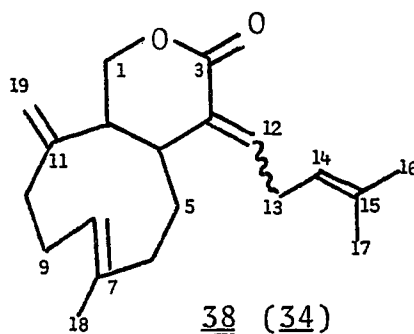


Figure 54. UV spectrum of coraxeniolide-C' (38).

spectrum (100 MHz, C_6D_6 , Fig. 55, Table 4) and decoupling experiments, suggest that coraxeniolide-C' (38) is epimeric with coraxeniolide-C at C-12.



The proton on C-12 is seen as a triplet at δ 6.57, coupled to a two-hydrogen broad doublet of doublets ($J = 8$ Hz, $J = 8$ Hz) at δ 2.72. The C-13 protons at δ 2.72 are in turn coupled to the proton on C-14, which is a triplet ($J = 8$ Hz) with fine coupling at δ 5.08. The exocyclic methylene protons are observed as singlets at δ 4.72 and δ 4.67, while the C-1 protons are seen as doublets of doublets at δ 3.84 and δ 3.38 with coupling constants of 12 Hz and 6 Hz, and 12 Hz and 12 Hz, respectively. Lastly, three vinyl methyls appear at δ 1.62, δ 1.50, and δ 1.42.

In the ^{13}C NMR spectrum of coraxeniolide-C' (38) the signal at 16.64 ppm is undoubtedly due to the methyl on C-7, although a sufficient amount of compound for an off-resonance spectrum could not be obtained due to the extreme difficulty of separating coraxeniolide-C' (38) from coraxeniolide-B (26). The chemical shift of this methyl again indicates E

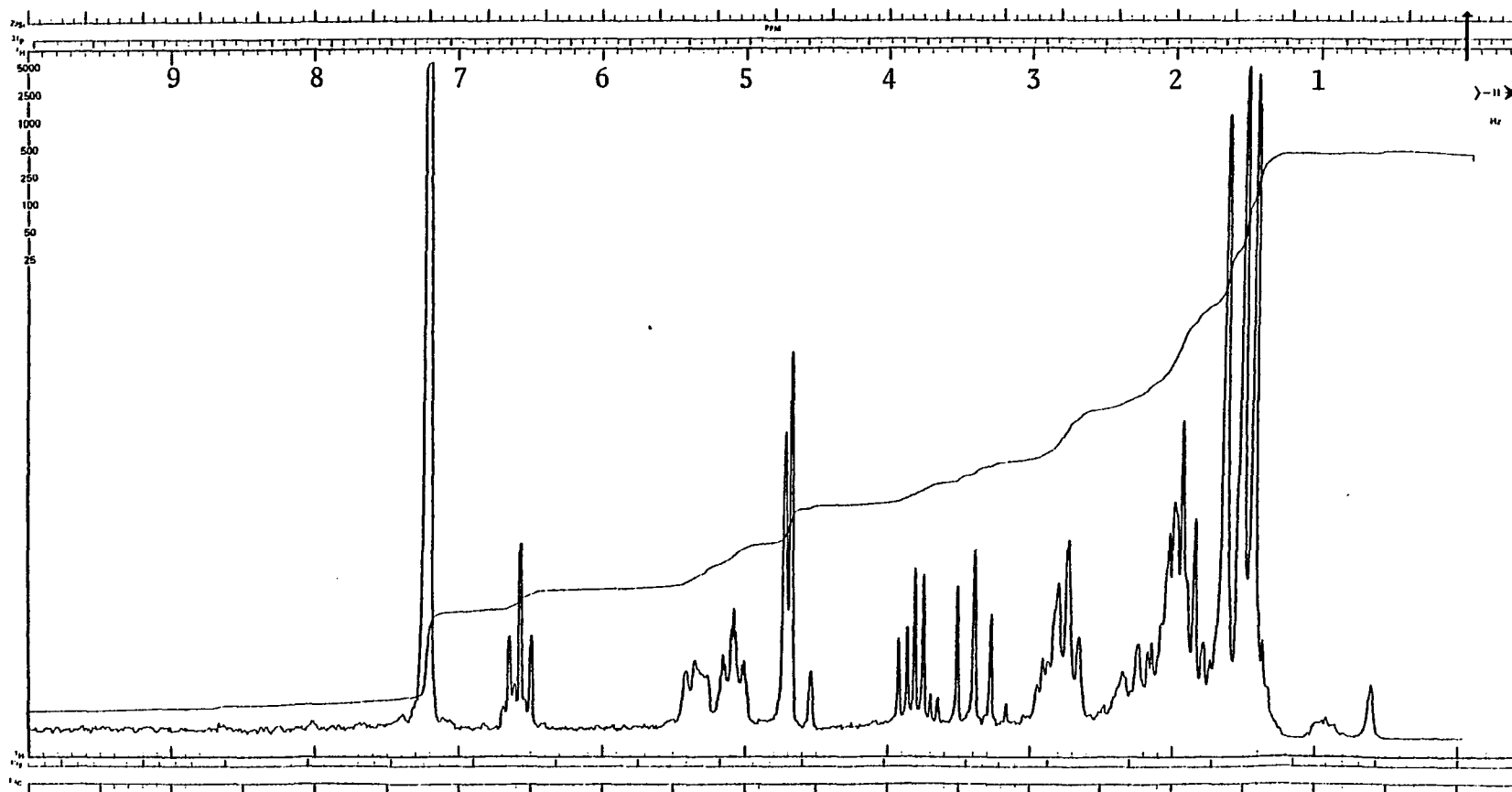


Figure 55. 100 MHz ^1H NMR spectrum of coraxeniolide-C' (38) in C_6D_6 .

configuration for the C-7(8) double bond, as discussed previously for coraxeniolide-B (26).²⁶

Coraxeniolide-C' (38) was also reacted with DBU to give a 29% yield of a compound identical with coraxeniolide-D (36) (¹H NMR, UV, IR, mp) and a 38% yield of a compound identical with coraxeniolide-D' (37) (¹H NMR, UV, IR, mp). This indicates a trans ring juncture in coraxeniolide-C' (38), as previously discussed for coraxeniolide-C (34).

Comparing the ¹H NMR spectral data (100 MHz, C₆D₆, Table 4) of coraxeniolide-C' (38) and coraxeniolide-C (34), one sees the only major differences in the chemical shifts of the protons on C-12 and C-13. The H-12 proton of 38 is found at δ 6.57, while in 34 it appears at δ 5.61. This large difference in the chemical shifts is undoubtedly due to the anisotropic effect of the lactone carbonyl. The question remains whether the carbonyl causes a shift to higher or lower field to the signal of the proton which is spatially closer, i.e., the E-isomer. An α -methylene- β -



lactone, in which the chemical shifts of the exocyclic methylene protons had been assigned, would make a good model system. I found a number of these systems, an example of

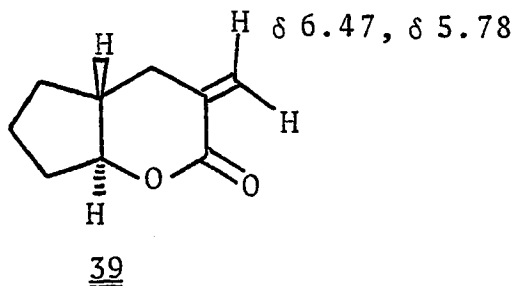
Table 4. 100 MHz ^1H NMR Spectral Data of Coraxeniolide-C (34), D (36), D' (37), and C' (38)

	<u>34</u> (C_6D_6)	<u>36</u> (CDCl_3) ^a	<u>37</u> (CDCl_3) ^a	<u>38</u> (C_6D_6)	<u>36</u> (CDCl_3) ^b	<u>37</u> (CDCl_3) ^b
H -1	3.81 1H dd (J=12,7 Hz) 3.48 1H dd (J=12,12 Hz)	4.21 1H dd (J=12,8 Hz) 3.96 1H dd (J=12,12 Hz)	4.19 1H dd (J=12,4 Hz) 4.03 1H dd (J=12,4 Hz)	3.84 1H dd (J=12,6 Hz) 3.38 1H dd (J=12,12 Hz)	4.20 1H dd (J=12,8 Hz) 3.95 1H dd (J=12,12 Hz)	4.19 1H dd (J=12,4 Hz) 4.03 1H dd (J=12,4 Hz)
H -4		3.58 1H bdd (J=7,7 Hz)	2.89 1H dd (J=8,8 Hz)		3.59 1H dd (J=7,7 Hz)	2.90 1H dd (J=8,8 Hz)
H -8		5.34 1H bt (J=7 Hz)	5.34 1H m	5.34 1H m	5.33 1H bt (J=7 Hz)	5.35 1H m
	5.28 2H m					
H -14		5.89 1H bd (J=10 Hz)	5.88 1H d (J=10 Hz)	5.08 1H mt (J=8 Hz)	5.89 1H bd (J=10 Hz)	5.89 1H bd (J=10 Hz)
H -13	3.25 2H bdd (J=8,8 Hz)	6.39 1H dd (J=15,10 Hz)	6.29 1H dd (J=15,10 Hz)	2.72 2H bdd (J=8,8 Hz)	6.39 1H dd (J=15,10 Hz)	6.30 1H dd (J=15,10 Hz)
H ₂ -13						
H -12	5.61 1H t (J=8 Hz)	5.90 1H dd (J=15,7 Hz)	5.55 1H dd (J=15,8 Hz)	6.57 1H t (J=8 Hz)	5.90 1H dd (J=15,7 Hz)	5.56 1H dd (J=15,8 Hz)
H ₃ -16	1.66 3H bs	1.78 6H bs	1.79 3H bs	1.62 3H bs	1.77 6H bs	1.80 3H bs
H ₃ -17	1.62 3H bs	1.68 3H d (J=2 Hz)	1.76 3H bs	1.50 3H bs	1.67 3H d (J=2 Hz)	1.77 3H bs
H ₃ -18	1.40 3H bd (J=1 Hz)		1.70 3H d (J=2 Hz)	1.42 3H d (J=1 Hz)		1.71 3H d (J=2 Hz)
H ₂ -19	4.73 1H s 4.69 1H s	5.04 1H s 5.01 1H s	4.92 1H s 4.82 1H s	4.72 1H s 4.67 1H s	5.04 1H s 5.00 1H s	4.90 1H s 4.81 1H s

^aFrom coraxeniolide-C (34).

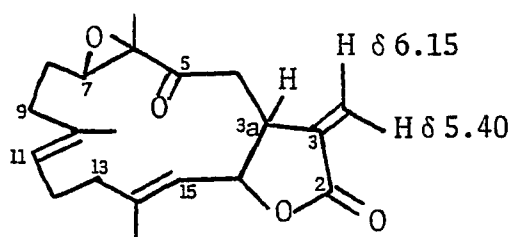
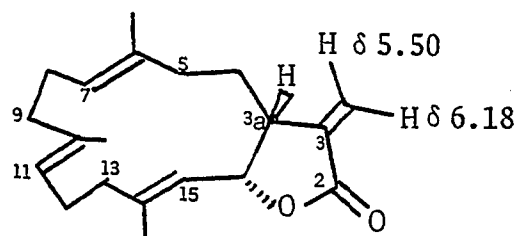
^bFrom coraxeniolide-C' (38).

which is compound 39 (100 MHz, CDCl_3).³¹ In all the examples I encountered the difference in chemical shifts of the two exocyclic methylene protons is dramatic, but the signals were never assigned.



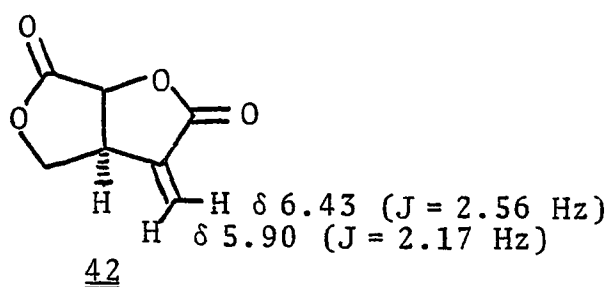
Since model δ -lactones failed to elucidate this point, I decided to look at α -methylene- γ -lactones, hoping that the exocyclic methylene protons would be assigned to particular absorbances in the ^1H NMR spectra of these compounds. A discussion of compounds 40³² and 41³³ will suffice to illustrate my experience with this line of reasoning, though the existing confusion was by no means limited to these two compounds.

In cembranolide 40 the higher field absorbance (δ 5.40, 100 MHz, CCl_4) was assigned to the proton cis to the carbonyl, while in cembranolide 41 the opposite assignment was made, with the lower field proton (δ 6.18, 100 MHz, CCl_4) cis to the carbonyl. An inquiry to the author who published the data for compounds 40 and 41 revealed that the proper assignment was made in compound 41, but not in 40. More importantly, he provided a rationale for this assignment.

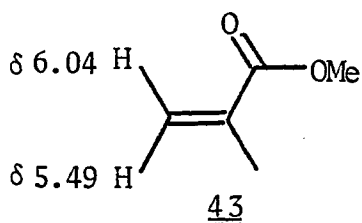
4041

The allylic coupling constant between the low-field proton and the hydrogen on C-3a was always larger than the corresponding coupling constant for the high-field proton.

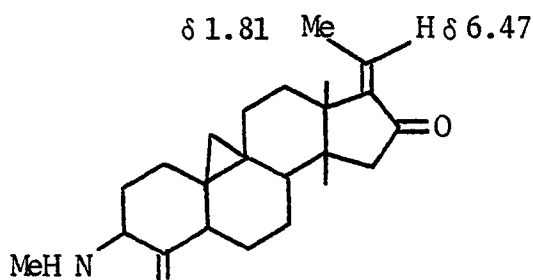
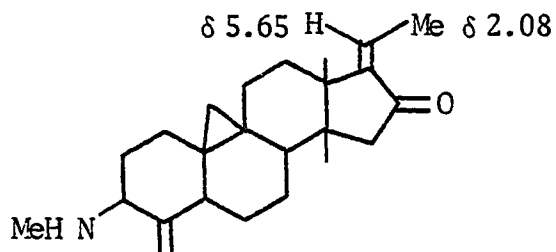
This appears to be the case as seen in the ^1H NMR spectrum (60 MHz, CDCl_3) of avenaciolide (42).³⁴ However,



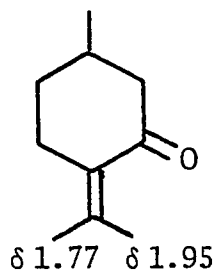
the observation that transoid allylic coupling in these systems is greater than cisoid coupling was based on the assignment of the δ 6.43 signal to the proton cis to the carbonyl. This assignment in avenaciolide (42) was made by analogy with methyl methacrylate (43), where assignments in the ^1H NMR spectrum (40 MHz, CCl_4) were based on a theoretical treatment of this system.³⁵



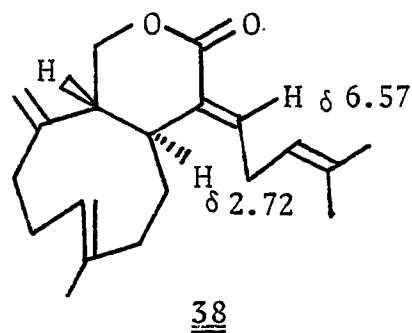
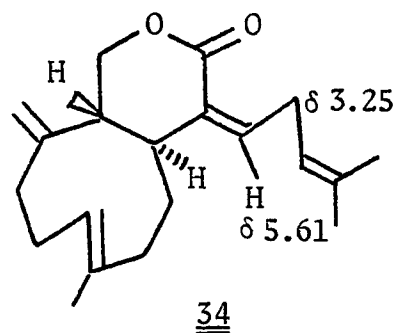
Eventually I discovered a more closely related set of model systems, two cyclopentanone derivatives of cyclobuxine (44 and 45).³⁶ From the spectral interpretations (60 MHz, CCl_4) of these compounds it appears that the anisotropic

4445

effect on β -methyls and β -protons, in an α,β -unsaturated carbonyl system is a shift to lower field. The anisotropic effect on the β -methyls of α -methylene cyclohexanones is also a shift to lower field as illustrated by pulegone (46) (60 MHz, neat).³⁷

46

The fact that the β -methyl in coraxeniolide-C (δ 3.25) is at lower field than in coraxeniolide-C' (δ 2.72), along with the observation that the β -proton in 38 (δ 6.57) is at lower field than in 34 (δ 5.61), proves that coraxeniolide-C (34) is the Z isomer and coraxeniolide-C' (38) is the E isomer.



E. Structural Determination of Corbohcin (47)

Corbohcin (47) is a trace (32 mg/kg) constituent of pink coral. A colorless oil with composition $C_{22}H_{34}O_2$, it contains six unsaturations. The mass spectrum of 47 (Fig. 56) shows a strong peak at m/z 270 ($M^+ - 60$), suggesting the presence of an acetate. The IR spectrum of corbohcin (47) (Fig. 57) is consistent with an acetate (1732 cm^{-1}) and further suggests the presence of an exocyclic methylene with an absorbance at 890 cm^{-1} . The UV spectrum shows only end absorption, implying that there are no conjugated systems in corbohcin (47).

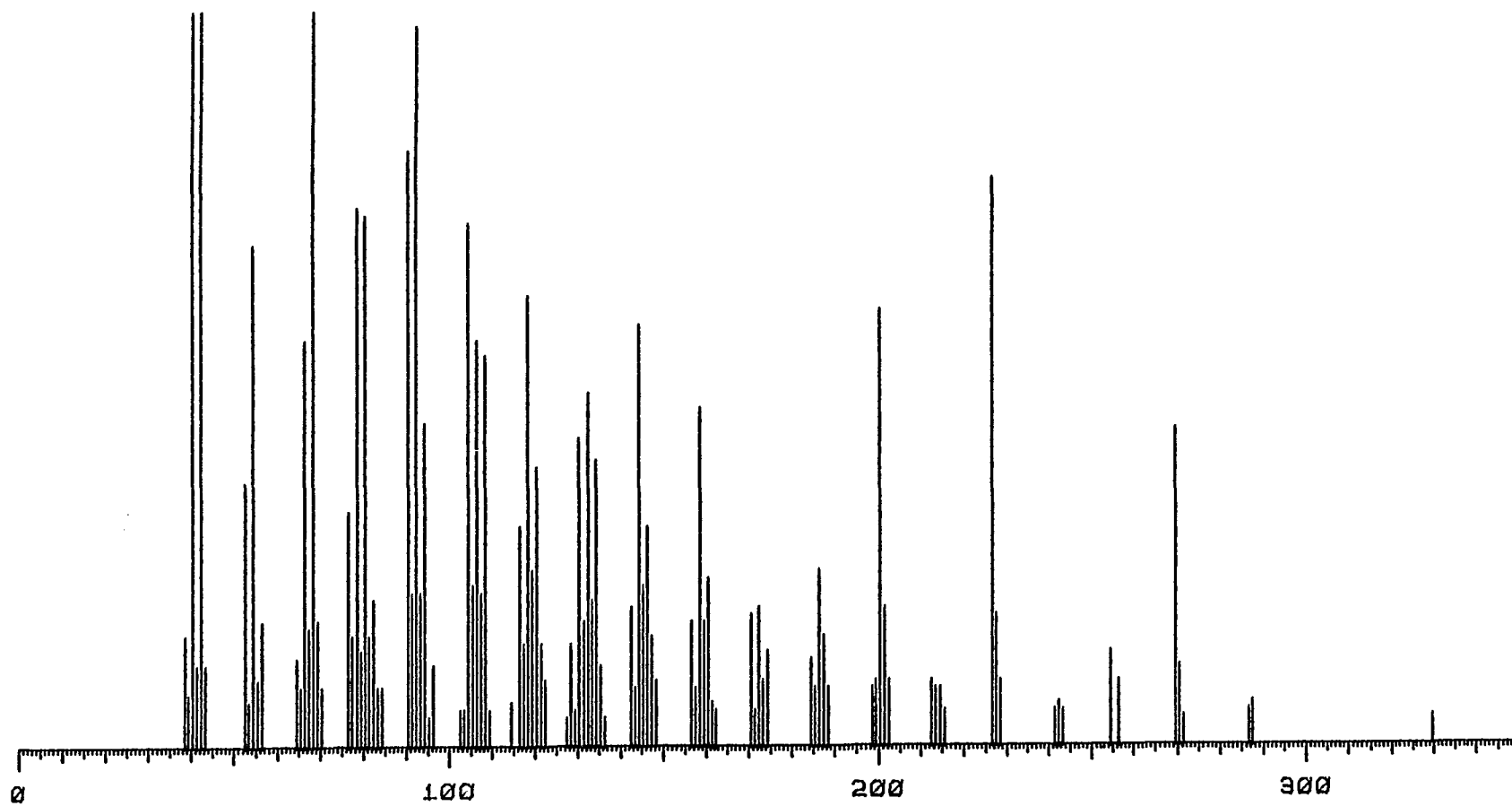


Figure 56. Mass spectrum of corbohcin (47).

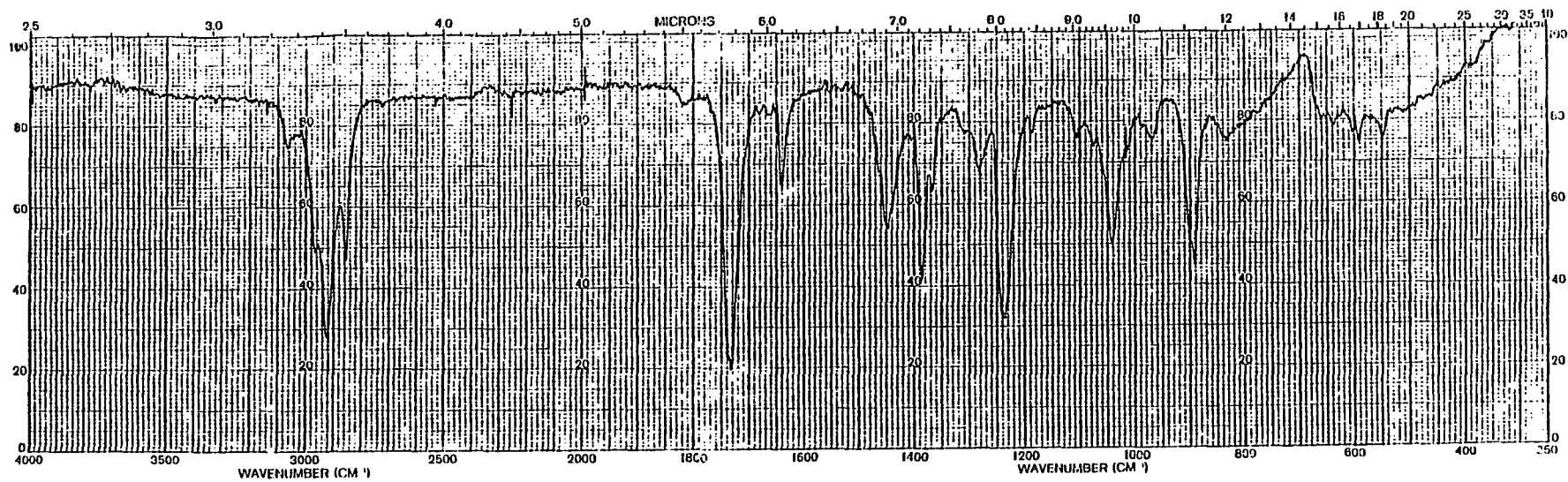
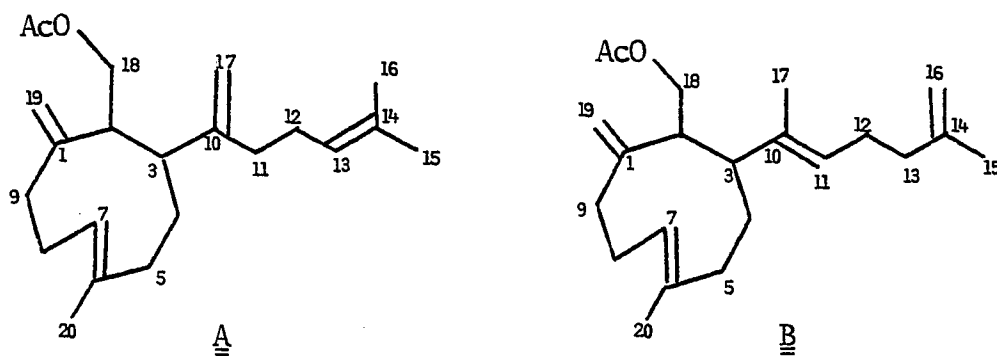


Figure 57. IR spectrum of corbohcin (47).

The ^{13}C NMR spectrum corroborates the existence of the acetate in corbohcin (47) with absorbances at 170.85 (s) and 65.52 (t). Additionally, it exhibits absorptions for four double bonds at 152.71 (s), 147.33 (s), 136.15 (s), 131.83 (s), 124.60 (d), 124.50 (d), 117.58 (t), and 109.03 (t) ppm, the last two signals of which correspond to exocyclic or terminal methylenes.

The ^1H NMR spectrum of corbohcin (47) (220 MHz, CDCl_3 , Fig. 58), along with the previously discussed characterization and biogenetic considerations, are consistent with two structures, A and B. Both proposed structures are unrearranged diterpenes containing a nine-membered carbocyclic ring, two exocyclic or terminal methylenes, and two additional olefins.



The most striking part of the ^1H NMR spectrum of corbohcin (47) (Fig. 58) is the three vinyl methyl singlets at δ 1.57, δ 1.63, and δ 1.69, as well as a sharp methyl singlet at δ 1.94, which unambiguously proves the existence of the acetate. The exocyclic and terminal methylenes are

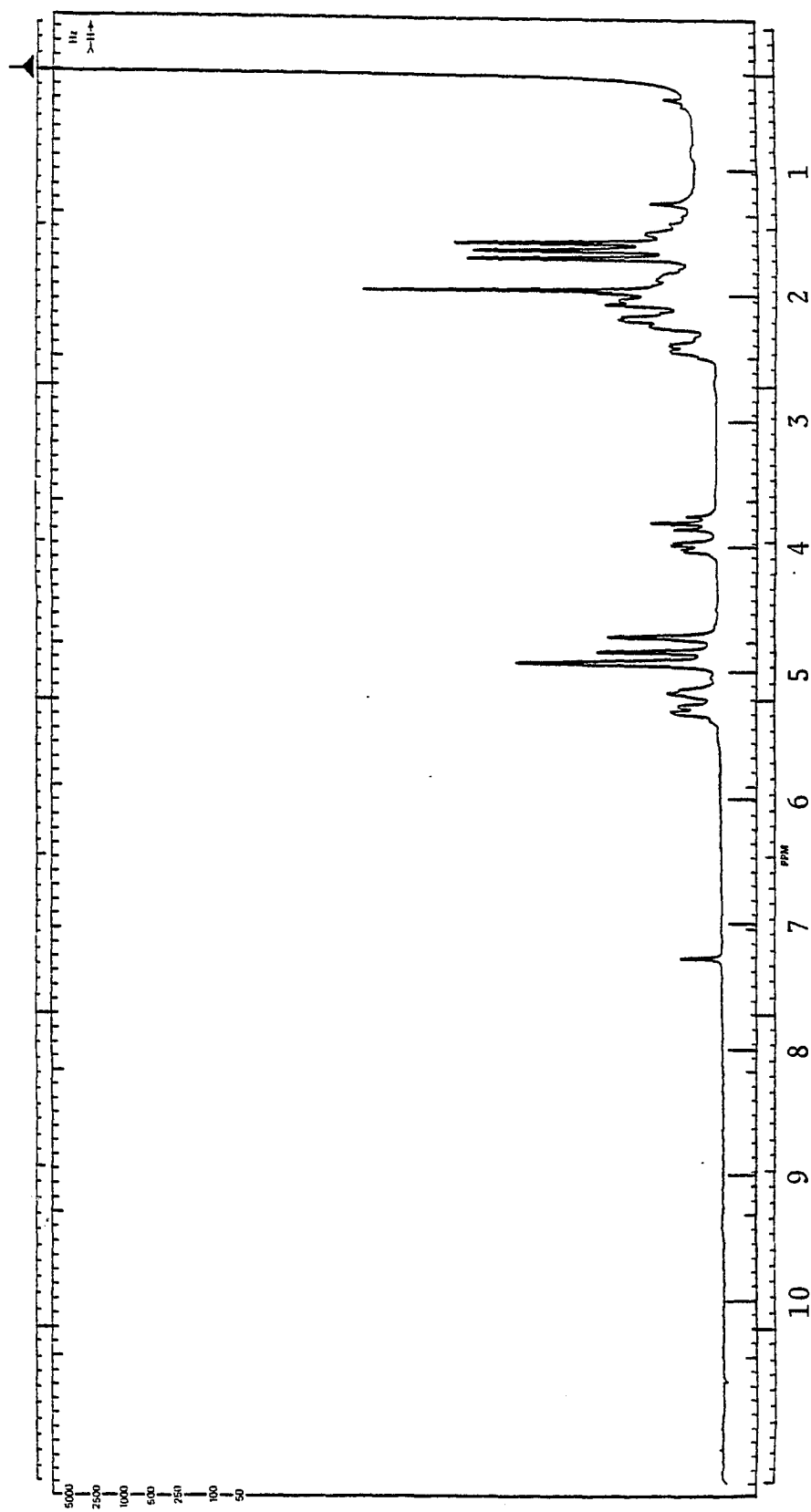
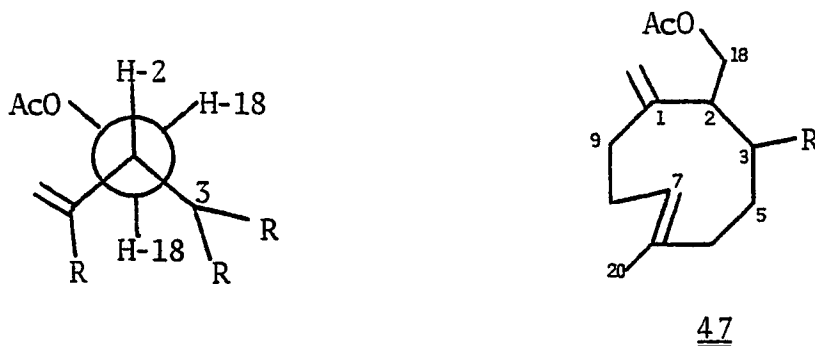


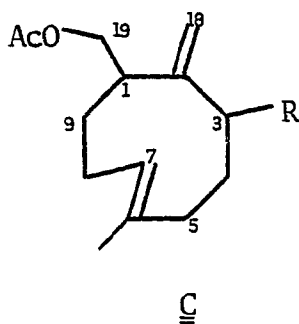
Figure 58. 220 MHz ^1H NMR spectrum of corbohcic acid (47) in CDCl_3 .

seen as two one-proton singlets at δ 4.71 and δ 4.82, and as a two-proton singlet at δ 4.91. Two other olefinic protons appear at δ 5.15 and δ 5.28.

The protons on C-18 appear as doublets of doublets ($J = 12$ Hz, $J = 6$ Hz and $J = 12$ Hz, $J = 12$ Hz) at δ 4.01 and δ 3.81, respectively. The bulky acetate group restricts rotation around the C-2(18) bond and must be placed as far away from the side chain on C-3 as possible, as represented in the Newman projection below. Another possible part



structure for compound corbohcin (47) is C, which was considered at one point. Examination of molecular models,

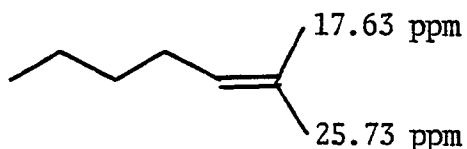


however, indicates that, in virtually any conformation, there is no restriction to rotation of the carbon bearing

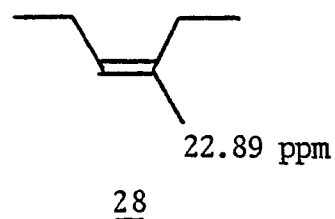
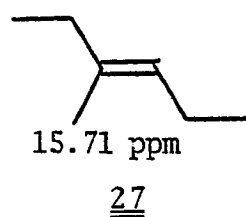
oxygen (C-19 in C) as is observed in compound 47. The difference in chemical shifts of the C-18 protons of corbohcin (47) is 20 Hz, less than three times the geminal coupling ($3 \times 12 = 36$ Hz), which results in a triplet for C-18 in the off-resonance ^{13}C spectrum.²⁵

Decoupling experiments were used to distinguish between structures A and B. Irradiation of the olefinic protons at δ 5.28 and δ 5.15 should cause enhancement of all three vinyl methyls in A (C-15, C-16, C-20) and only two vinyl methyls in B (C-17, C-20). When the experiment was performed, irradiation of the δ 5.28 signal caused enhancement of the methyl found at δ 1.57, while irradiation of the olefinic proton signal at δ 5.15 enhanced both the δ 1.69 and δ 1.63 vinyl methyls. This information indicates that A is the correct structure for corbohcin (47).

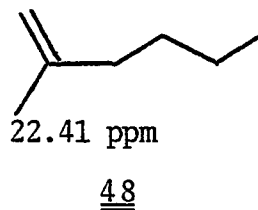
The ^{13}C NMR spectrum of corbohcin (47) also supports structure A. There are four methyl quartets in the off-resonance ^{13}C NMR spectrum of 47 at 26.33, 21.22, 18.14, and 17.97 ppm. The 26.33 ppm signal must be assigned to C-15 in A, as previously discussed for compound 35.²⁶



There is, however, no methyl in structure B that can correspond to the methyl signal found at 26.33 ppm. Methyls on trisubstituted double bonds (C-17 and C-20) are never found at lower field than about 23 ppm as seen in 27 and 28,²⁶ previously discussed for coraxeniolide-B (26).



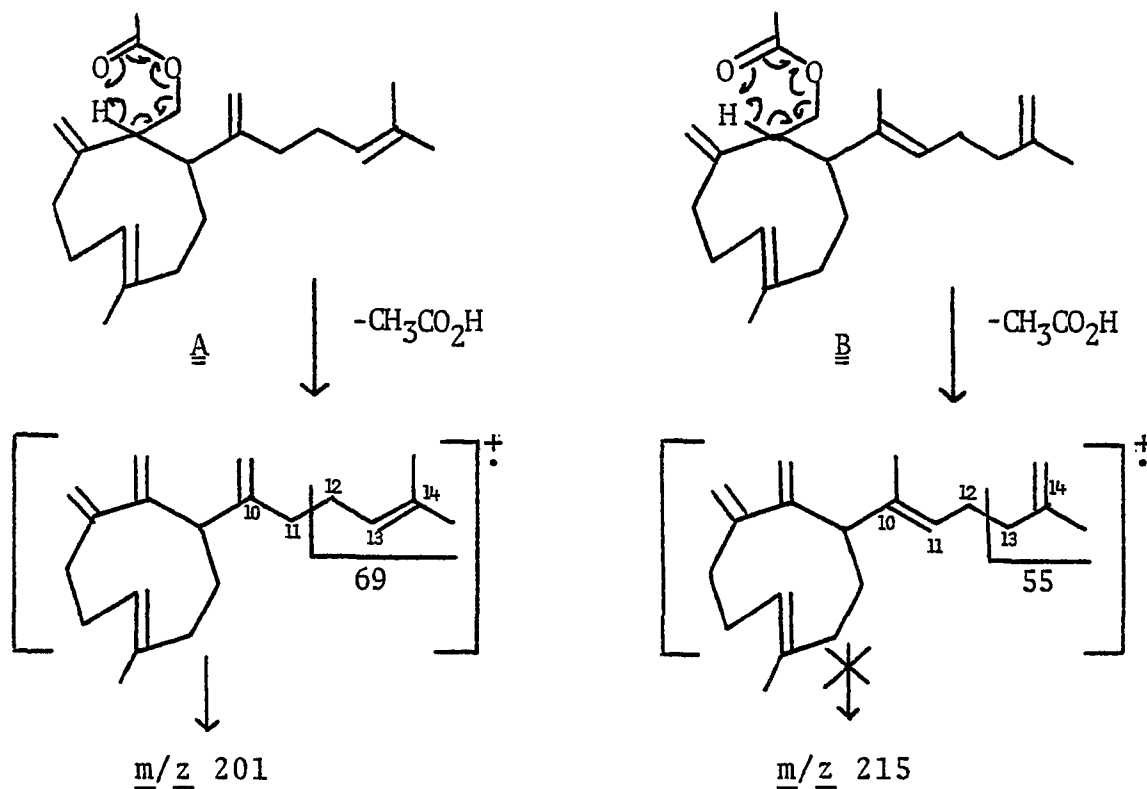
A model for C-15 in B is compound 48 with a vinyl methyl at 22.41 ppm.²⁶ In light of this, it seems unlikely that



C-15 could absorb at 26.33 ppm. And lastly, examination of the chemical shifts of more than 25 acetate methyls indicates that they fall in the range 20.4 to 21.5 ppm.³⁸

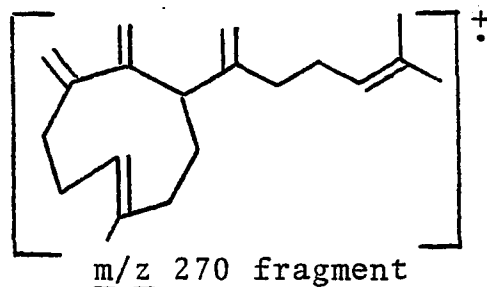
The vinyl methyls at 26.33, 21.22, 18.14, and 17.97 ppm are, therefore, assigned to C-15, the acetate methyl, C-16, and C-20, respectively, in structure A. The 17.97 ppm shift for C-20 in A again indicates E configuration for the C-6(7) double bond of the cyclononene ring.²⁶

The mass spectrum (Fig. 56) also confirms this structural assignment. Corbohcin (47) loses 60 mass units from its molecular ion as illustrated for A and B in Scheme 5. There is a doubly allylic bond between C-11 and



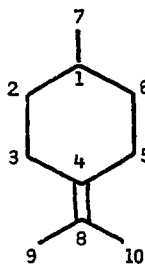
C-12 in A and between C-12 and C-13 in B. Loss of this piece should result in a strong peak at $\underline{m/z}$ 201 for A and $\underline{m/z}$ 215 for B. The intensity of the peak at $\underline{m/z}$ 215 in the mass spectrum of 47 is 8% of the base peak, while the peak at $\underline{m/z}$ 201 is 59% as intense as the base peak at $\underline{m/z}$ 69. Therefore, A is the correct structure for corbohcin (47).

One piece of data, however, still remains to be explained. One of the strongest peaks (77%) in the mass spectrum of corbohcicn (47) (Fig. 56) is found at m/z 227. High resolution mass measurement indicates that this fragment has composition $C_{17}H_{23}$, corresponding to the loss of CH_3CO_2H and C_3H_7 . This was very confusing--how can the m/z 270 ($M^+ - 60$) fragment lose C_3H_7 ? A C_3H_7 fragment can



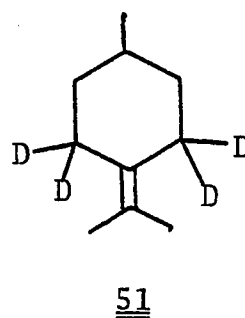
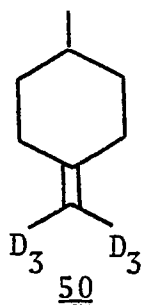
only be derived from an isopropyl group and there is simply no isopropyl group in 47 no matter how the data are interpreted. This peak, therefore, must be due to a highly favored rearrangement.

Weinberg and Djerassi³⁹ described such a rearrangement and proposed a mechanism for it on the basis of deuterium labeling studies. In the mass spectrum of $\Delta^{4(8)}$ -methene (49) the base peak is found at m/z 95, corresponding to a

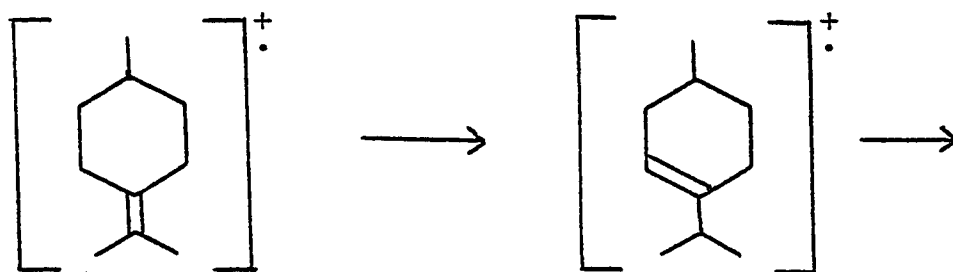


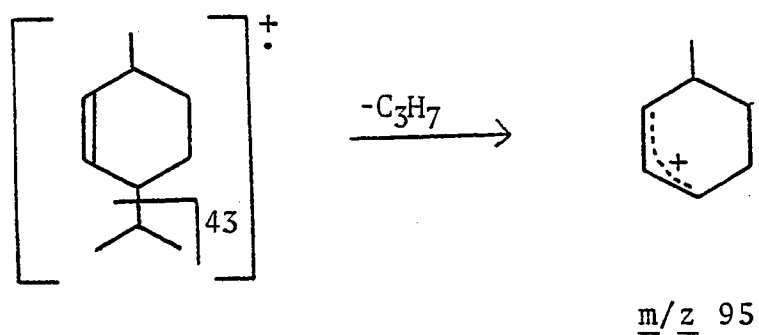
loss of C_3H_7 from the molecular ion. This is clearly due to a rearrangement since there is no isopropyl group in this hydrocarbon.

The mass spectrum of 50 shows that 80-90% of the m/z 95 ($M^+ - 43$) peak in 49 remains at m/z 95 in 50, indicating that the molecule is losing the hexadeuterioisopropylidene group



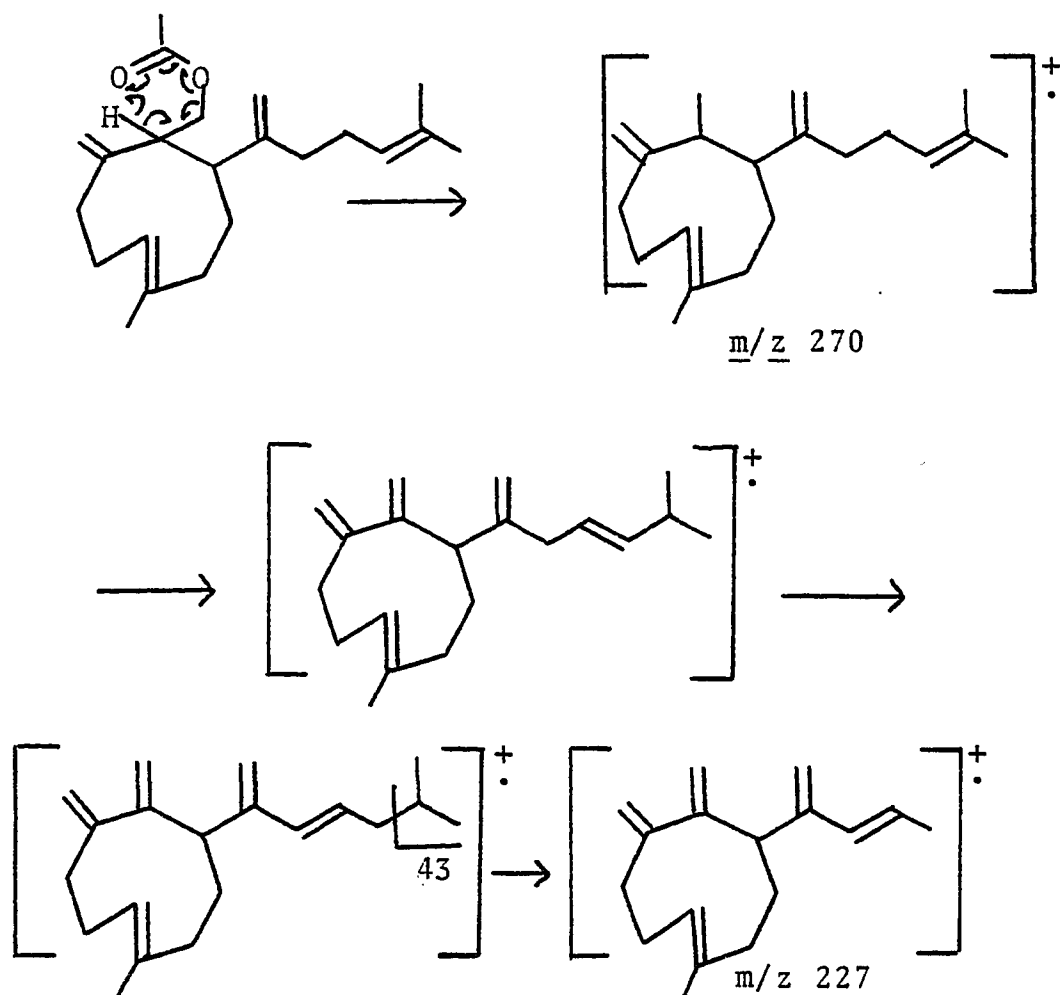
plus one hydrogen. In the mass spectrum of 51 the base peak is found at m/z 98 ($M^+ - 44$), which corresponds to a loss of C_3H_6D . This shows that the primary source of hydrogen in the rearrangement of 49 is the protons on C-3 or C-5. On the basis of these data Weinberg and Djerassi suggested a two-step rearrangement, followed by a highly favored allylic cleavage of the resulting isopropyl group as seen in Scheme 6.³⁹





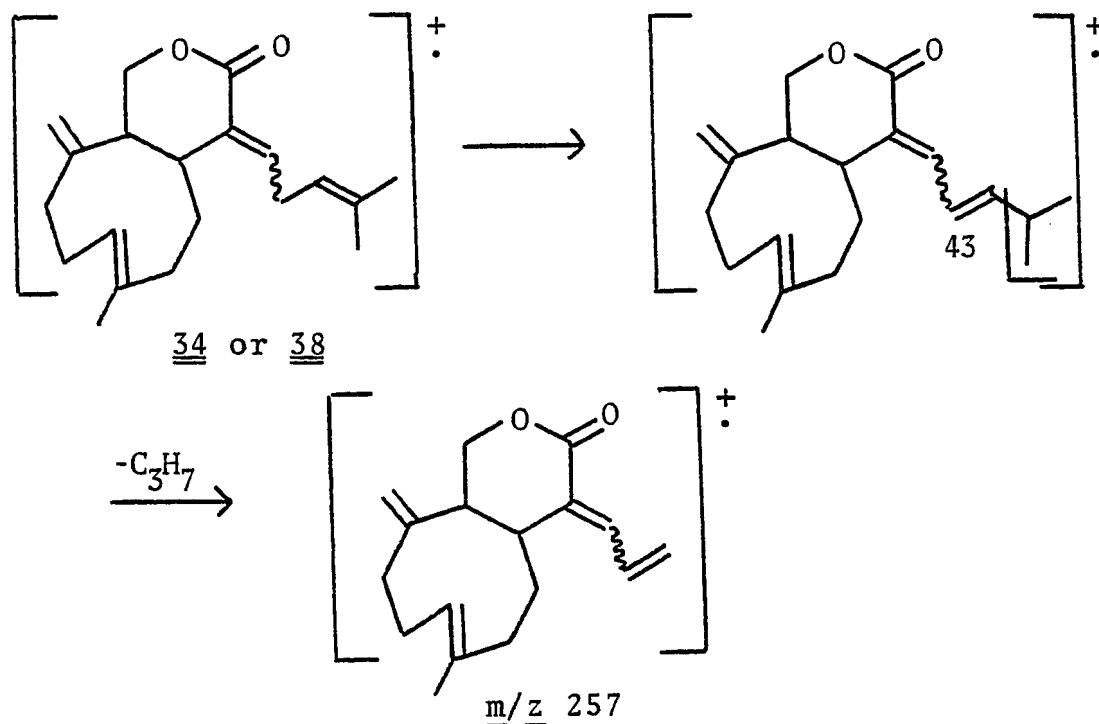
Scheme 6

Corbohcin (47) can undergo a similar rearrangement, followed by allylic cleavage of the isopropyl group, as illustrated in Scheme 7, which explains the intense peak at m/z 227.



Scheme 7

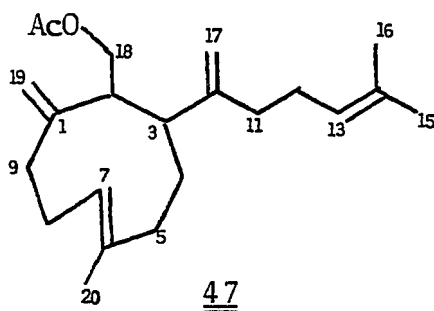
Both coraxeniolide-C (34) and coraxeniolide-C' (38) can undergo similar one-step rearrangements (Scheme 8); however, the cleavage is not allylic and, therefore, not favored as evidenced by the weak m/z 257 peaks in 34 (14%) and 38 (10%).



Scheme 8

The stereochemistry of C-2 and C-3 in corbohcin (47) could not be determined; however, it seems likely that the sidechain on C-2 has α -orientation and the sidechain on C-3 has β -orientation, by analogy with the coraxeniolides discussed previously.

I would like to suggest the name corbohcin for compound 47, derived from the name of the coral from which it is isolated, Corallium sp., and the name of the man who made this research possible, Boh Bartko.



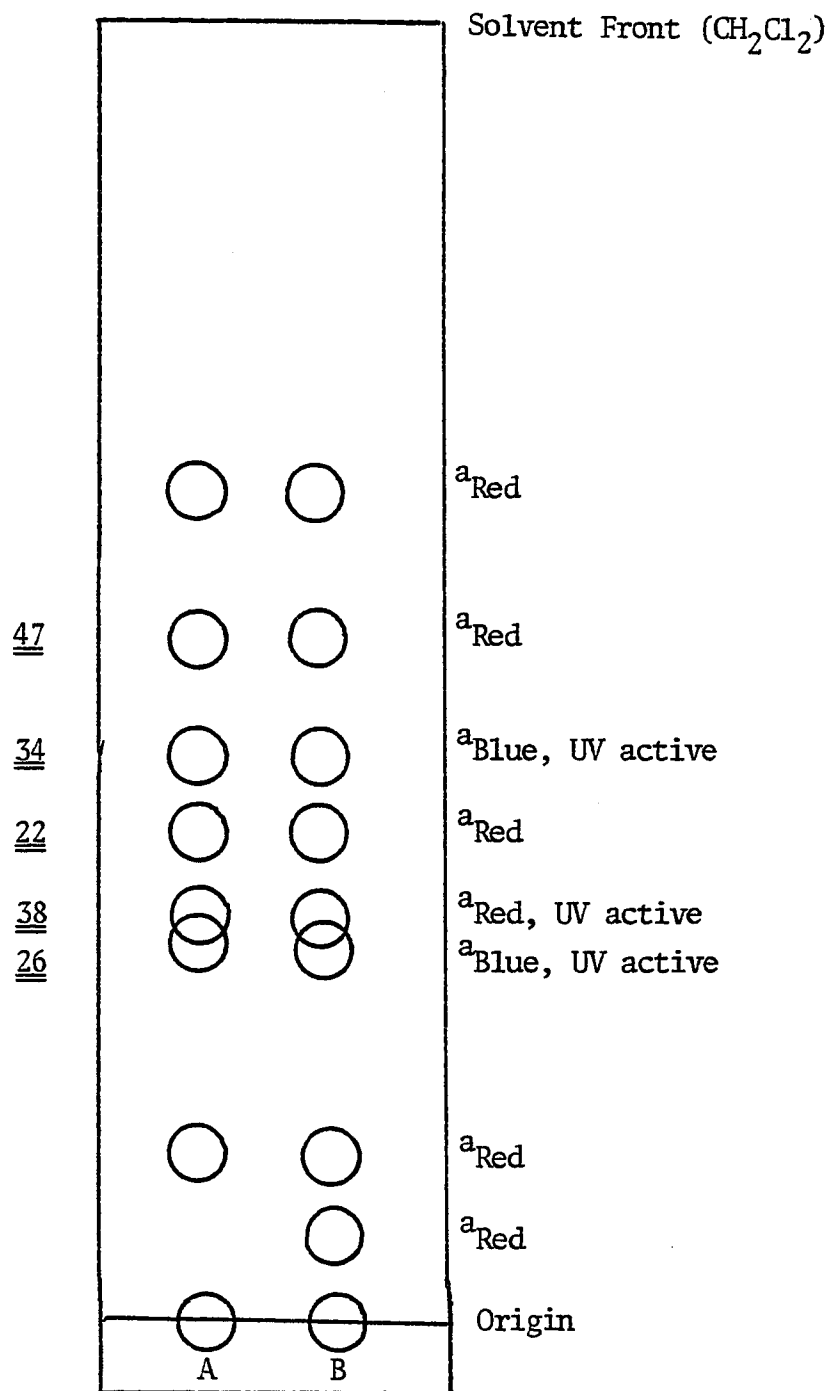
F. Constituents of *Paragorgia* sp.

While working on the constituents of *Corallium* sp. I had the chance to examine a number of other deep-sea corals. One coral in particular seemed interesting because of my work with *Corallium* sp.

This coral is an undescribed species belonging to the same order as *Corallium* sp. (Gorgonacea), but to a different family (Paragorgiidae) and genus (*Paragorgia*) (see Preface). It is a fan-shaped coral with yellow-colored polyps and a crumbly, chalky-textured endoskeleton.

Paragorgia sp. was extracted by soaking it in methanol, concentrating, and partitioning the residue between dichloromethane and water. The thin-layer chromatogram of the dichloromethane layer was compared with the corresponding extract from *Corallium* sp. and is shown schematically in Figure 59.

Except for an additional compound in *Paragorgia* sp. the compounds on the chromatogram of *Paragorgia* sp. and *Corallium* sp. appear to be identical with regard to R_f ,



^aRed and blue refer to the colors of the spots after charring with H_2SO_4 /vanillin.

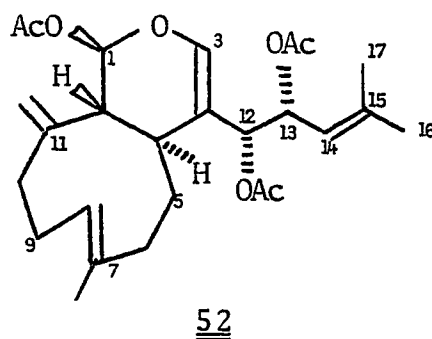
Figure 59. TLC comparison of the CH_2Cl_2 extracts from Corallium sp. (A) and Paragorgia sp. (B).

UV absorbance, and color upon charring with H_2SO_4 /vanillin. This is good evidence, although by no means proof, that coraxeniolides-A (22), B (26), C (34), C' (38), and corbohcin (47) isolated from Corallium sp. are also present in Paragorgia sp.

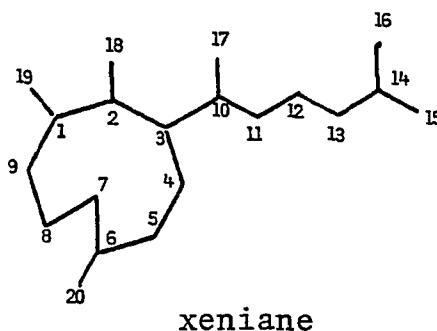
IV. RELATED RESEARCH BY OTHERS

A. Previously Isolated Xenianes

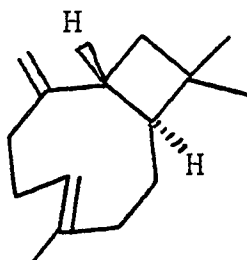
In 1977 Schmitz and coworkers isolated compound 52 from the soft coral Xenia elongata and determined its structure by single-crystal X-ray analysis.²⁴ They named



this compound xenicin and suggested the name xeniane, with numbering as shown, for this new carbon skeleton.

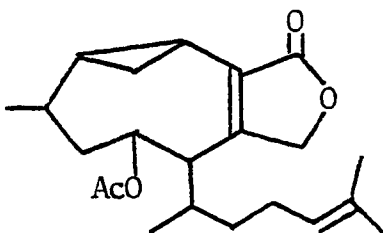


Very few cyclononenes were known before the discovery of xenicin, except for a number of sesquiterpenes related to caryophyllene. Caryophyllene is a constituent of some pine trees (Pinus sp.). It contains a nine-membered ring trans-fused to a cyclobutane ring.⁴⁰ It seems strange that

53

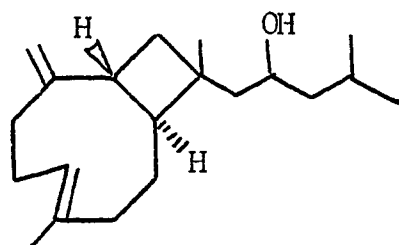
these two unusual, but closely related compounds (52 and 53), were isolated from such diverse sources. Related compounds, however, have since been isolated from a number of other sources.

Acetoxycrenulatin (54) was isolated from the brown alga

54

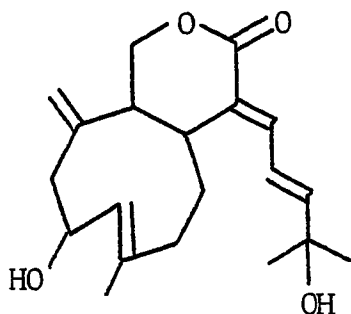
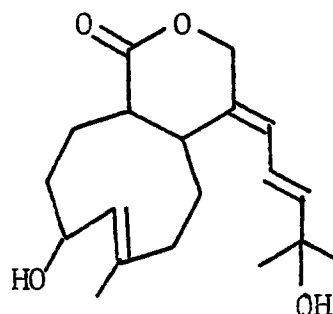
Dictyota crenulata by Fenical and coworkers; its structure was also published in 1977.⁴¹ In this compound, C-18 and C-19 (xeniane numbering system) are oxidized, rather than C-17 and C-18, as was observed in xenicin.

In the following year Kashman and coworkers published the structures of a plethora of related compounds isolated from the soft coral Xenia macrospiculata. Six compounds, of a new structural type represented by xeniaphyllenol (55), were isolated from this organism.^{29,42} These diterpenes

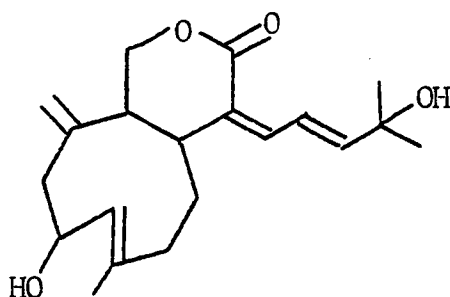
55

with a cyclononene ring trans-fused to a cyclobutane ring are, obviously, closely related to the sesquiterpene caryophyllene (53).

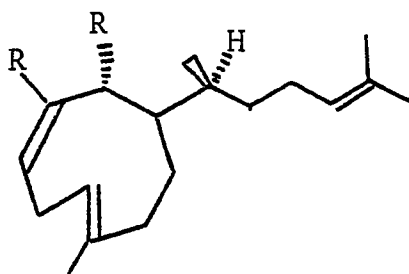
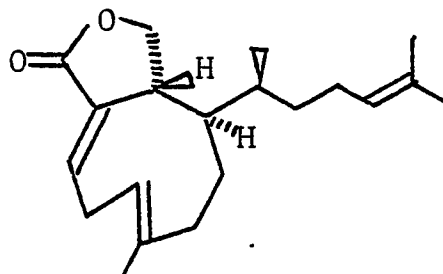
Two related δ -lactones were also isolated from Xenia macrospiculata. These compounds were named xeniolide-A (32), discussed previously, and xeniolide-B (56), and

3256

differ from each other only in the position of the lactone carbonyl.²⁹ In 1979 Tursch and coworkers isolated another closely related xenolide from Xenia novae-britanniae which they called isoxenolide-A (33),³⁰ as discussed previously.

33

Also in 1979, research groups in Hawaii, California, New York, and Italy collaborated in the publication of the structures of dictyodial (57a) and dictyolactone (58).⁴³

57a R=CHO57b R=CH₂OH58

Dictyodial was isolated from the brown algae Dictyota crenulata collected in Hawaii and Dictyota flabellata, from Mexico. The structure of dictyodial (57a) was determined by ¹³C and ¹H NMR spectroscopy, as well as single-crystal X-ray diffraction of dictyodiol (57b) from the reduction of dictyodial (57a) with LiAlH₄. Dictyodial shows antibiotic activity against Staphylococcus aureus and Bacillus subtilus and antifungal activity against Candida albicans.

Coraxeniolide-A was also tested. It showed no antibiotic activity against Escherichia coli.

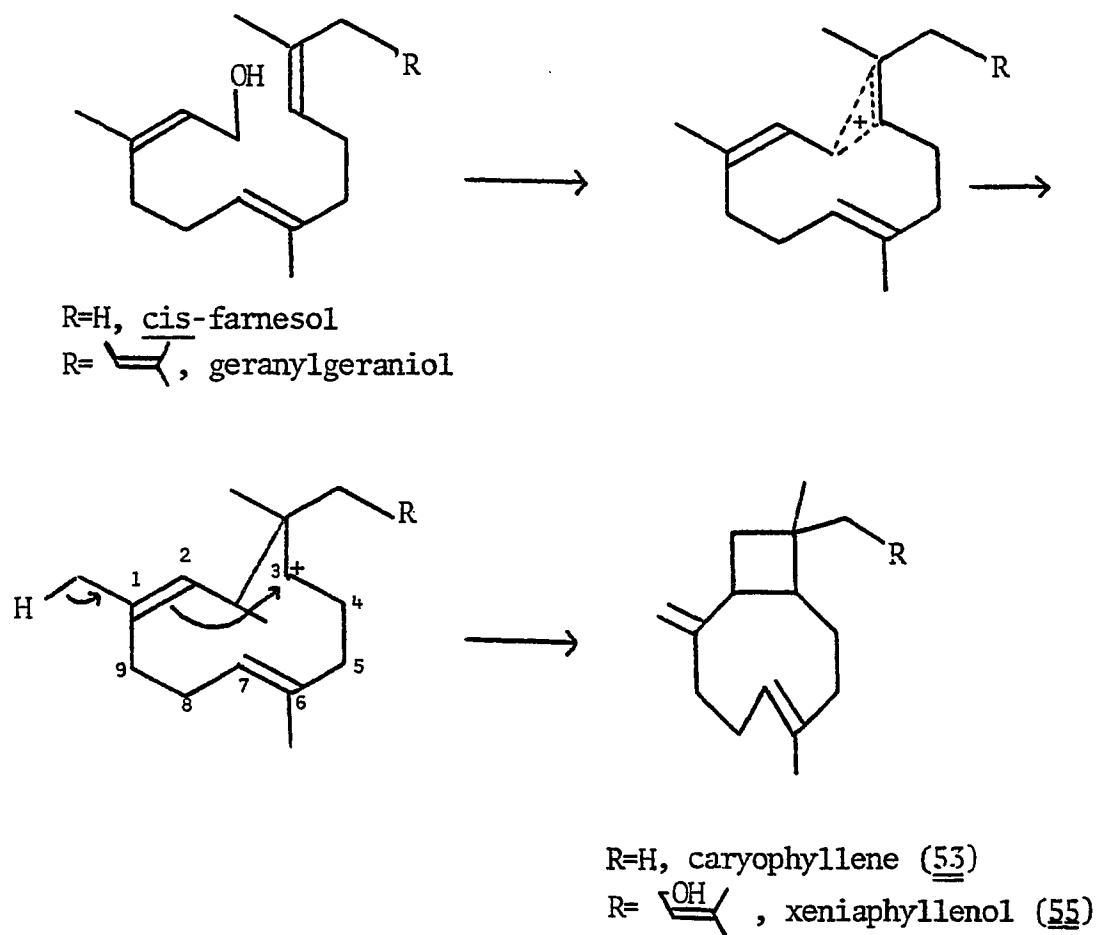
Dictyolactone (58) was isolated from Aplysia depilans, collected in the Bay of Naples, and its structure was elucidated via single-crystal X-ray analysis. This organism is known to feed on algae belonging to the genus Dictyota, and it is suspected that the algae are the source of this compound. Dictyodial and dictyolactone are closely related to acetoxycrenulatin (54); they are xenianes oxidized at C-18 and C-19, rather than C-17 and C-18, as is the case in the compounds isolated from Xenia.

A large number of xenianes have been isolated in a very short period of time, as they were unknown before 1977.

B. Biogenesis of Coraxeniolides

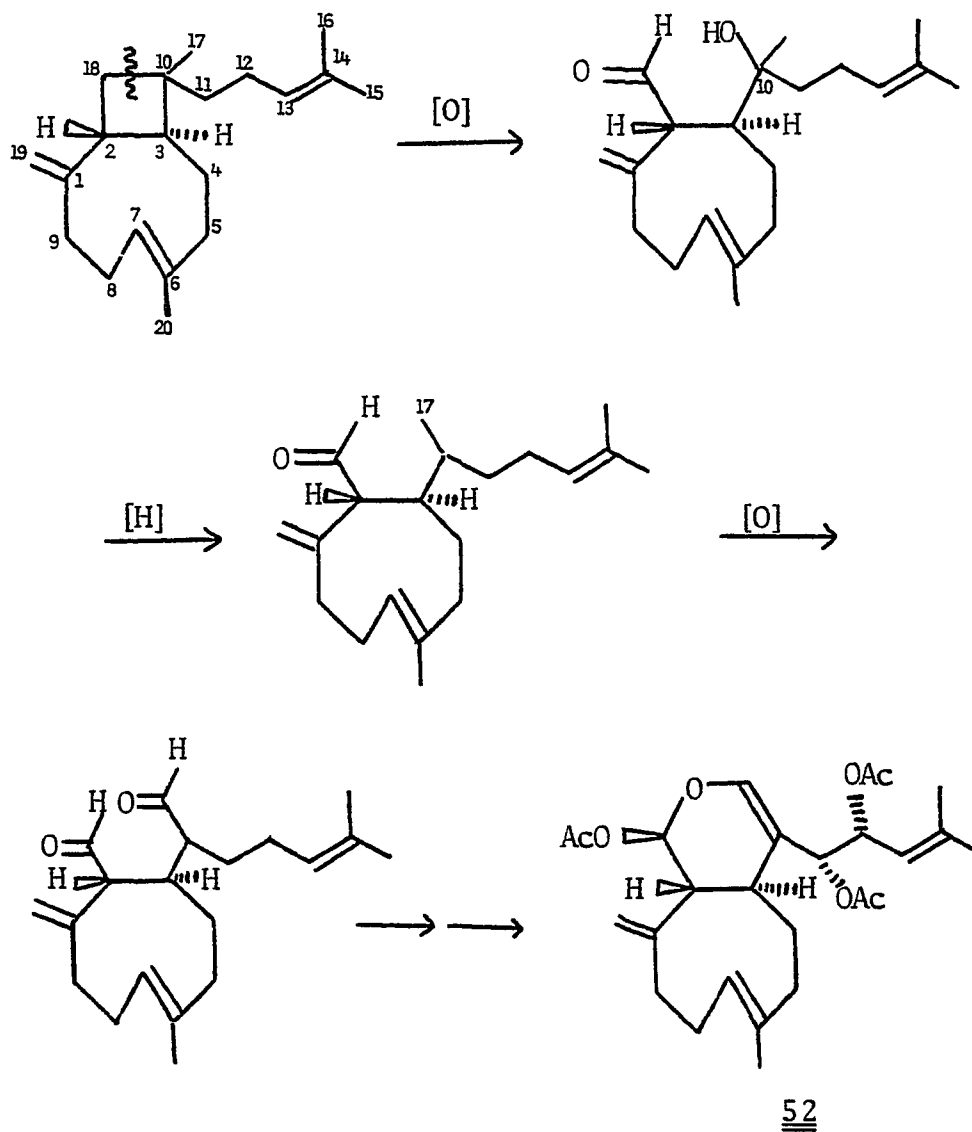
Hendrickson has proposed a biogenesis for caryophyllene (53) as outlined in Scheme 9.⁴⁰ The Z configuration of the C-1(2) double bond in the 11-membered ring intermediate explains the trans-nature of the ring juncture in caryophyllene. Assuming that this is correct, it seems likely that the xeniaphyllenols are synthesized in a similar fashion, starting with geranylgeraniol (Scheme 9).

Schmitz has suggested that xenicin (52) may result from the oxidative cleavage of the C-10(18) bond (xeniane numbering) of the cyclobutane ring in a xeniaphyllenol-type intermediate.²⁴ Kashman feels that the isolation of



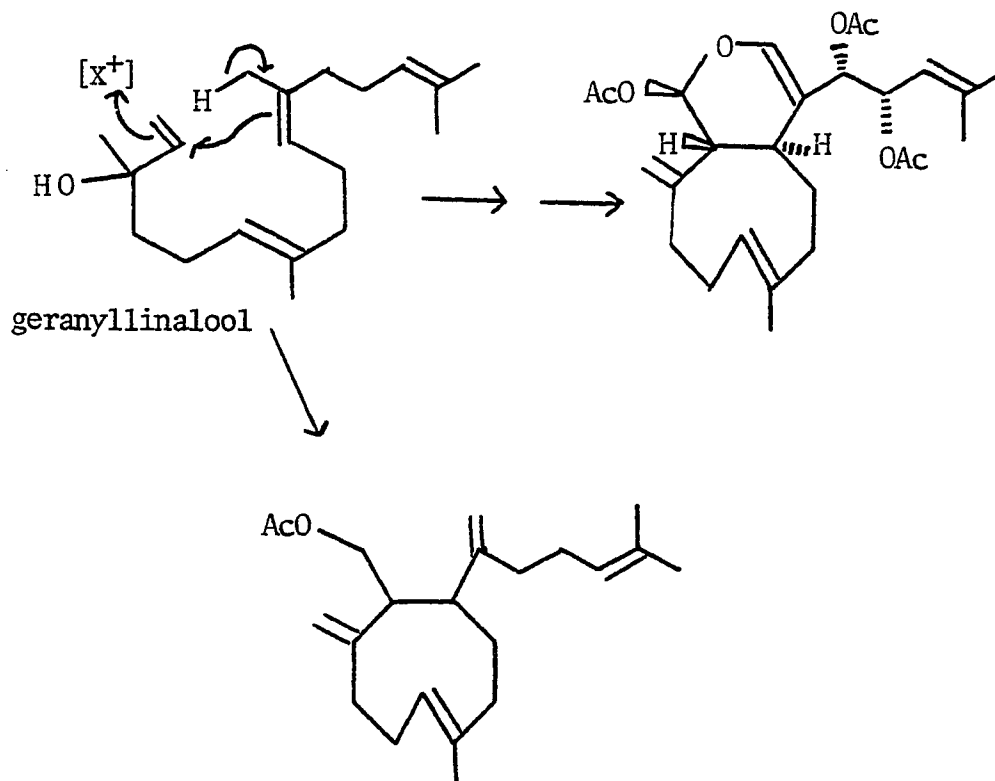
Scheme 9

xeniaphyllenols supports this postulated biogenesis.⁴² This proposed biogenesis requires the oxidative cleavage of the C-10(18) bond, followed by reduction of C-10, oxidation of C-17, ring closure, and acetylation as seen in Scheme 10. This seems to be unnecessarily complex; however, it does explain the origin of the trans-ring juncture in xenicin (52).



Scheme 10

Alternately, Schmitz has suggested that the biogenesis of xenicin (52) may involve the oxidative cyclization of geranylgeranyl pyrophosphate as illustrated in Scheme 11.²⁴ This is perhaps a plausible explanation for the formation of corbohcic acid (47); however, further oxidation of an olefinic carbon (C-17) is required to generate xeniolides

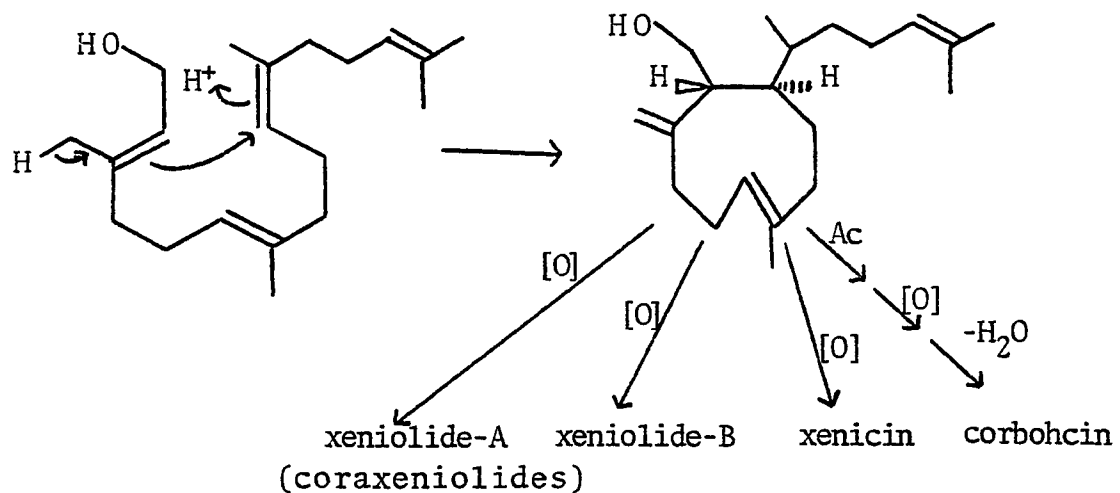


47

Scheme 11

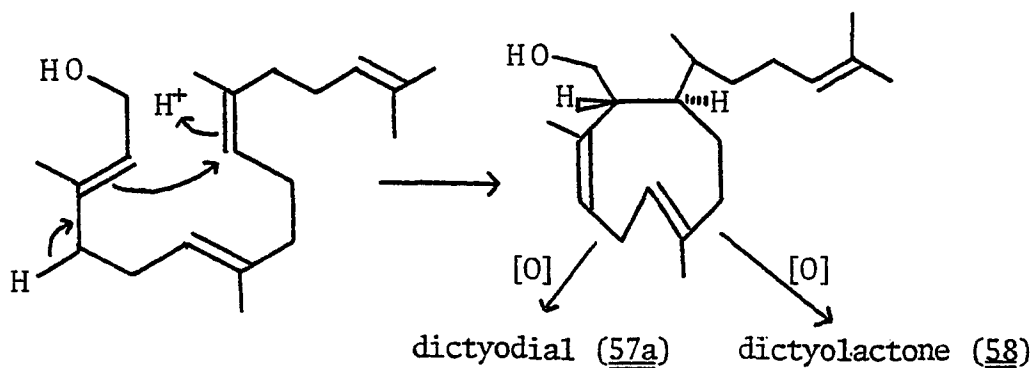
(coraxeniolides) and xenicin. Also, this proposed biogenesis does not explain the trans-ring juncture found in the bicyclic xenianes, although the nature of the enzymes may be responsible for the observed stereochemistry.

A simpler explanation, however, is the direct cyclization of geranylgeraniol followed by selective oxidation to give xeniolide-A (coraxeniolides), xeniolide-B, xenicin, and corbohcin as seen in Scheme 12.



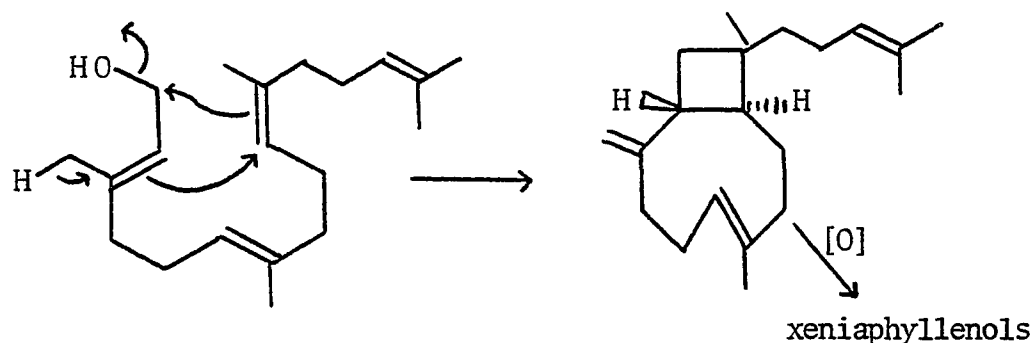
Scheme 12

The biogenesis of dictyodial (57a) and dictyolactone (58) can be explained by a similar cyclization of geranylgeraniol, followed by selective oxidation as illustrated in Scheme 13.



Scheme 13

Even the xeniaphyllenols could originate from geranylgeraniol via a concerted cyclization followed by oxidation (Scheme 14).



Scheme 14

The biogenesis of the xenianes from a common source (geranylgeraniol), by a series of closely related cyclizations, is certainly the simplest explanation; however, until labeling studies are performed, it is only a conjecture.

The next question I would like to consider is the biogenetic source of these compounds. Isolation of diterpenes from brown algae, in the case of dictyodial, does not seem unusual; plant biosynthesis of terpenes is well established. Xeniane diterpenes, however, have been isolated from three different genera of corals: Xenia is a genus of alcyonacean (soft coral), while Corallium and Paragorgia belong to the order Gorgonacea (see Preface).

The genera Xenia and Corallium represent extremes with respect to the relationship between corals and symbiotic zooxanthellae. Gohar⁴⁴ investigated this relationship in xeniid corals with a series of feeding experiments.

His research indicated that this genus of coral does not appear to be equipped for external feeding. When the animal is presented with food, a frantic waving of the tentacles occurs; however, this movement only serves to drive the food away from their mouths. Also, the tentacles of xeniid corals do not appear to have nematocysts (stinging cells). Food coming in contact with the tentacles does not stick to them and, in Gohar's words, live organisms "literally promenaded on the tentacles and on the peristomial disk, as well as on the borders of the mouth."⁴⁴

Another set of feeding experiments was performed. Four different tanks, containing all available Xenia species, were prepared. The first tank was kept in the dark and had unfiltered seawater; the second tank was also dark but had filtered seawater. The third and fourth tanks were set in the sunlight and had unfiltered and filtered seawater, respectively. Presumably, the lack of light eliminates zooxanthellae as a nutritional source, while filtering of the seawater should eliminate zooplankton as a source of nutrition.

The results of this experiment were simple and conclusive. All xeniid species that were kept in the dark were dead after three weeks, and all xeniids exposed to sunlight survived in good health for three months, at which time the experiment was discontinued. Gohar concluded that corals belonging to the genus Xenia are almost completely

dependent on their symbiotic zooxanthellae for nutrition.⁴⁴

And, of course, xenianes isolated from xeniids may be biosynthesized by their zooxanthellae, another example of plant biosynthesis of terpenes.

Deep-sea corals, on the other hand, would not be expected to have viable zooxanthellae because of the lack of light. There have been isolated reports of deep-sea corals (as deep as -400 m) which contain large amounts of zooxanthellae.^{45,46} However, these organisms have been brought up by trawls and dredges, and the reported depths of their habitats should, therefore, be viewed critically until those depths can be confirmed by direct observation.

Corallium sp., in particular, does not contain symbiotic zooxanthellae.⁴⁷ This means that the presence of coraxeniolides and corbohcin in pink coral may be due to animal biosynthesis of terpenes, although the possibility that the animals obtain these compounds from their diet cannot be eliminated.

V. CONCLUSION

The constituents of deep-sea corals do not appear to be radically different from the constituents of shallow-water corals. The zoanthoxanthins and xenianes isolated from gold coral (Gerardia sp.) and pink coral (Corallium sp.), respectively, both have closely related counterparts previously isolated from shallow-water organisms. The significance of this research, however, may simply be that these compounds are present in organisms growing in this unusual environment.

On the other hand, I have only scratched the surface. In the order Gorgonacea alone there are still more than 80 species of Hawaiian deep-sea corals, which have not been examined. The chemistry of these deep-sea organisms may still prove to be as unique as the environment in which they grow.

Specifically, the bioluminescence of deep-sea organisms warrants further investigation. Although virtually no sunlight penetrates to a depth of -350 m, a large number of deep-sea organisms generate their own light.¹ The nature and purpose of this bioluminescence remains a mystery.

The union of science and industry in the investigation and utilization of deep-sea corals has been a delicate, but profitable, enterprise. Industry has supplied the funding and science has provided guidelines for the rational use of

Hawaii's coral resources. As a result of rising costs, however, this relationship has been terminated. Hopefully it will soon be reinstated, as there is still much to be learned about the ocean floor, and there is no substitute for first-hand observation of this environment.

LITERATURE CITED

1. Muzik, K. Bull. Mar. Sci. 1978, 28, 735-741.
2. Grigg, R. W.; Opresko, D. In "Reef and Shore Fauna of Hawaii, Section I: Protozoa through Ctenophora"; Devaney, D., Eldredge, L., Eds.; Bishop Museum Press: Hawaii, 1977; pp. 242-269.
3. Grigg, R. W.; Bayer, F. M. Pac. Sci. 1976, 30, 167-175.
4. Muzik, K., U.S. National Museum, personal communication, 1977.
5. Gieskes, J. M. In "The Sea: Marine Chemistry"; Goldberg, E., Ed.; Wiley: New York, London, Sydney and Toronto, 1974; Vol. 5, Chapter 3.
6. Young, D. In "Experimental Coelenterate Biology"; Lenhoff, H.; Muscatine, L.; Davis, L., Eds.; University of Hawaii Press, Honolulu, 1971; Chapter 25.
7. Hyman, L. H. "The Invertebrates: Protozoa through Ctenophora" American Museum of Natural History: New York; McGraw-Hill: New York and London, 1940; Vol. 1, pp. 538-628.
8. Bartko, B., personal communication, 1977.
9. Grigg, R. W., University of Hawaii, personal communication, 1979.
10. Cariello, L.; Crescenzi, S.; Prota, G. Comp. Biochem. Physiol. 1979, 63B, 77-82.

11. Cariello, L.; Crescenzi, S.; Prota, G.; Giordano, F.; Mazzarella, L. J. Chem. Soc. Chem. Commun. 1973, 99-100.
12. Cariello, L.; Crescenzi, S.; Prota, G.; Zanetti, L. Tetrahedron 1974, 30, 3281-3287.
13. Cariello, L.; Crescenzi, S.; Prota, G.; Zanetti, L. Tetrahedron 1974, 30, 4191-4196.
14. Schwartz, R. E.; Yunker, M. B.; Scheuer, P. J.; Ottersen, T. Tetrahedron Lett. 1978, 2235-2238.
15. Schwartz, R. E.; Yunker, M. B.; Scheuer, P. J.; Ottersen, T. Can. J. Chem. 1979, 57, 1701-1711.
16. Cariello, L.; Crescenzi, L.; Prota, G.; Zanetti, L. Experientia 1974, 30, 849-850.
17. Komoda, Y.; Kaneko, S.; Yamamoto, M.; Ishikawa, M.; Itai, A.; Iitaka, Y. Chem. Pharm. Bull. 1975, 23, 2464-2465.
18. Komoda, Y.; Kaneko, S.; Yamamoto, M.; Ishikawa, M.; Itai, A.; Iitaka, Y. "Symposium Papers", 19th Symposium of the Chemistry of Natural Products, Hiroshima, Japan, Oct. 1975; Chemical Society of Japan, Japanese Society of Pharmaceutical Sciences, Japanese Society of Agricultural Chemistry, Tokyo, Japan.
19. Braun, M.; Büchi, G. J. Am. Chem. Soc. 1976, 98, 3049-3050.
20. Braun, M.; Büchi, G.; Bushey, D. F. J. Am. Chem. Soc. 1978, 100, 4208-4213.

21. Cariello, L.; Crescenzi, S.; Prota, G.; Zanetti, L. Tetrahedron 1974, 30, 3611-3614.
22. Grigg, R. W. "Hawaii's Precious Corals"; Island Heritage Limited: Hawaii, 1977; Chapter 4.
23. Grigg, R. W. "Fishery Management of Precious and Stony Corals in Hawaii"; Sea Grant Technical Report, Sept. 1976.
24. Vanderah, D. J.; Steudler, P. A.; Ciereszko, L. S.; Schmitz, F. J.; Ekstrand, J. D.; van der Helm, D. J. Am. Chem. Soc. 1977, 99, 5870-5874.
25. Hagaman, E. W. Org. Magn. Res. 1976, 8, 389-398.
26. Couperus, P. A.; Clague, A. D. H.; van Dongen, J. P. C. M. Org. Magn. Res. 1976, 8, 426-431.
27. Patel, D. J. Nature 1969, 221, 825-828.
28. Watt, D. S.; Corey, E. J. Tetrahedron Lett. 1972, 4651-4654.
29. Kashman, Y.; Groweiss, A. Tetrahedron Lett. 1978, 4833-4836.
30. Braekman, J. C.; Dalozze, D.; Tursch, B.; Declercq, J. P.; Germain, G.; van Meerssche, M. Bull. Soc. Chim. Belg. 1979, 88, 71-77.
31. Marschall, H.; Vogel, F.; Weyerstahl, P. Chem. Ber. 1974, 107, 2852-2859.
32. Bowden, B. F.; Coll, J. C.; Mitchell, S. J.; Stokie, G. J. Aust. J. Chem. 1978, 31, 1303-1312.

33. Coll, J. C.; Mitchell, S. J.; Stokie, G. J. Aust. J. Chem. 1977, 30, 1859-1863.
34. Brookes, D.; Sternhell, S.; Tidd, B. K.; Turner, W. B. Aust. J. Chem. 1965, 18, 373-377.
35. Jackman, L. M.; Wiley, R. H. J. Chem. Soc. 1960, 2881-2886.
36. Brown, K. S.; Kupchan, S. M. J. Am. Chem. Soc. 1962, 84, 4590-4591.
37. Williams, D.; Flemings, I. "Spectroscopic Methods in Organic Chemistry," 2nd ed.; McGraw-Hill: London and New York, 1973; Chapter 3.
38. Wehrli, F. W. In "Progress in the Chemistry of Organic Natural Products"; Herz, W., Griesbach, H., Kirby, G., Eds.; Springer-Verlag: Vienna, 1979; Vol. 36, Chapter 1.
39. Weinberg, D. S.; Djerassi, C. J. J. Org. Chem. 1966, 31, 115-119.
40. Hendrickson, J. B. Tetrahedron 1959, 7, 82-89.
41. McEnroe, F.; Robertson, K.; Fenical, W. In "Marine Natural Products Chemistry"; Faulkner, J. D., Fenical, W., Eds.; Plenum Press: New York, 1977; 179-190.
42. Groweiss, A.; Kashman, Y. Tetrahedron Lett. 1978, 2205-2208.
43. Finer, J.; Clardy, J.; Fenical, W.; Minale, L.; Riccio, R.; Battaile, J.; Kirkup, M.; Moore, R. E. J. Org. Chem. 1979, 44, 2044-2047.

44. Gohar, H. A. F. Publ. Mar. Biol. Sta. Ghardaqa, Red Sea, Egypt 1940, 2, 25-118.
45. Zahl, P. A.; McLaughlin, J. A. J. Protozool. 1959, 6, 344-352.
46. Stephenson, T. A. In "British Antarctic (Terra Nova) Expedition, 1910: Zoology, Coelenterata. Part I-- Actinaria"; Vol. V, pp. 1-68.
47. Muzik, K., U. S. National Museum, personal communication, 1979.